WP 6: OFFSHORE & ONSHORE GAS LOADING/UNLOADING SYSTEMS

Task 6.3: THE LIMITING WEATHER ANALYSIS DURING LOADING/UNLOADING OPERATION

Sub-task: Sea State limit during loading/unloading operativity in various onshore/offshore operations

Project:	GASVESSEL
Project No.:	723030
Deliverable No.:	D6.3
Deliverable Name:	Sea State limit during loading/unloading operativity in various onshore/offshore operations
WP n.	06
Document Version:	02
Document Preparation Date:	2020-05-27
Responsability:	SINTEF Ocean

Type of Deliverable		
R	Document, Report	Report
DEM	Demonstrator, pilot, prototype	
DEC	Websites, patent fillings, videos, etc.	
OTHER		
ETHICS	Ethics requirements	
ORDP	Open Research Data Pilot	

Dissemination Level		
PU	Public	[X]
CO	Confidential, only for Members of the Consortium (including the EU Commission Services)	

Version Management

Software used		Microsoft Word
Company Internal Doc. n.		[D 6.3 - Report on the offshore loading/unloading operation analyses
Author(s)		Decao Yin, Halvor Lie, Ivar Fylling, Halgeir Ludvigsen
Reviewed by		Halvor Lie
Approved by		The Coordinator
Authorized by		The Coordinator
Revision No.	**Date**	**Modification description**
RV 1	2020-05-25	
RV 2	2020-05-27	Merged two parts into one document
RV 3		

EC Grant Agreement	No.723030
Project Acronym	GASVESSEL
Project Title	Compressed Natural Gas Transport System
Instrument	HORIZON 2020
Programme	Smart, green and integrated Transport
Start Date of Project	2017-06-01
Duration	48 months
Organisation Name of Lead Contractor for this Deliverable	SINTEF Ocean

Financial/Administrative Coordinator	
Project Coordinator Name	Mr. Loris COK
Project Coordinator Organization Name	NAVALPROGETTI Srl
Address	Via dei Papaveri, 21 34151 TRIESTE (Italy)
Phone Numbers	0039 040 212918,
Email	loris.cok@navalprogetti.net; gasvessel@navalprogetti.net;
Project web-sites & other Access Points	www.gassvessel.eu

The GASVESSEL Project has received funding from the European Union's Horizon 2020 Research and Innovation Programme under Grant Agreement no. 723030

Contents

List of Figures

List of Tables

Glossary, abbreviations and acronyms

CNG	Compressed natural gas
Crossflex®	Registered trademarks of TechnipFMC
DP	Dynamic positioning
ERS	Emergency release system
ESD	Emergency shut down
FE	Finite element
FEM	Finite element method
FLIP	FLow Induced Pulsations
FPSO	Floating production storage and offloading
FSO	Floating storage and offloading
JONSWAP	Joint North Sea Wave Project
LF	Low frequency
MBR	Minimum Bending Radii
NG	Natural gas
NP	Navalprogetti Srl – Trieste – Italy – The Coordinator – Partner -Lead Beneficiary of WP1 and WP5
OLS	Offshore Loading System
RAO	Amplitude ratio of motion transfer functions
RPM	Revolutions per minute
SO	SINTEF Ocean AS – Trondheim – Norway – Partner – Lead Beneficiary WP7
UKOLS	Ugland-Kongsberg Offshore Loading System
WF	Wave frequency
α	Utilization factor
κ	Curvature
θ_c	Current direction
θ_h	Hose direction
θ_v	CNG vessel heading
θ_w	Wave propagation direction
B	Vessel breadth
b	Stiffness/load parameter, $b = (EI/w)^{1/3}$
C_d	Drag coefficient
C_m	Added mass coefficient
D_h	Hose distance
EI	Bending stiffness of loading hose
H_s	Significant wave height
L_h	Hose length
L_{OA}	Length over all
L_{PP}	Length between perpendiculars
R	Radius of hose curvature
r	Non-dimensional radius
R_0	Radius of hose curvature with zero tension
R_b	Non-dimensional radius of bending-dominated hose
R_c	Radius of catenary curve
r_c	Non-dimensional radius of catenary curve
T	Tension, support force, axial force, also called 'effective tension', not including effects of internal and external hydrostatic pressure
T_p	Peak wave period
T_{AP}	Draught at aft perpendicular, m (basic hull)
T_M	Midship draught, m (basic hull)

T_{FP}	Draught at fore perpendicular, m (basic hull)
U_c	Current velocity
U_z	Vessel heave velocity
V_{CG}	Z-coordinate of CG taking into account free-surface effects, m
w	Weight/length in water
Δ	Displacement
r_{44}	Mass radius of gyration around X-axis at COG (dry)
r_{55}	Mass radius of gyration around Y-axis at COG (dry)
r_{66}	Mass radius of gyration around Z-axis at COG (dry)

1. Introduction

1.1 Executive Summary

As a part of European Commission Horizon 2020, GASVESSEL project develops offshore transport and distribution technologies for natural gas. In the present study, the feasibility of an offshore loading/unloading system of CNG transportation system in the Barents Sea is investigated.

Offloading hoses/flexible pipes are used to transfer compressed natural gas (CNG) from an intermediate floating storage and offloading unit (FSO) to CNG vessel (GASVESSEL). The floating hoses are subjected to environmental loads that are mainly waves, current, and vessel motions from both the FSO and the CNG vessel.

The present study investigates the CNG loading/unloading system in the Barents Sea, especially the loading hose, mooring and DP systems of the FSO. Based on an earlier study [1], we have chosen as a zone (ESD1) where the hose can be safely operated. The ESD1 zone is 100±15 m, with ±30 deg behind the stern of FSO. The operational extreme sea-state has significant wave height Hs=6 m.

The present study has been divided into two activities.

1. Dynamic hose study. The CNG loading/unloading system (including FSO and CNG vessels, loading hoses) should be designed so that it is able to operate safely under the sea-state Hs=6 m within the ESD1 zone. The work from this activity is presented in the first part of this report.

2. Positioning analyses of the FSO and GASVESSEL. The positioning system of the two vessels (FSO and GASVESSEL) should give motions under the sea-state Hs=6 m so the ESD1 zone is not exceeded. The work from this activity is presented in the second part of this report.

In the first part, un-bonded flexible pipe was identified as a suitable alternative for the present study which requires high pressure (240 bar) and large diameter (Internal diameter 14''). Numerical simulations are performed by using the software RIFLEX under SIMA workbench. Critical responses such as curvature and axial forces are checked. For the new offloading hose, it is important to have a combined bending-tension loading capacity check. The results show that the specified hoses/flexible pipes of the loading/unloading system have ample capacity for the considered operating conditions.

In the second part, station keeping analysis (SIMO calculation) of a turret-moored FSO with DP system under critical sea-states (100 years return period) in the Barents Sea has been carried out. A turret mooring system and DP system are proposed to the FSO. Critical sea-states are identified.

Numerical simulations with the chosen mooring system and DP system, the loading/unloading operations including both vessels in significant wave height up to Hs=6 m is investigated. The motions are found generally to be within the ESD1 zone and therefore to be feasible.

1.2 Purpose and Scope

The work carried out in the present report is defined under following work package and task of the GASVESSEL project [2]:

- WP6 - Offshore/Onshore Gas Loading/Unloading Systems
    - Task 6.3 - The limiting weather analysis during loading/unloading operation
        - Sea-state limit during loading/unloading operativity in various onshore/offshore operations

Following tasks are identified within Task 6.3:

1. Offshore loading/unloading analysis of the CNG transport system in the Barents Sea under the operating conditions with significant wave height Hs=6 m.

2. Station keeping analysis of the turret-moored FSO under critical (e.g. 100 years return period) sea-states in the Barents Sea
    a. Propose a turret mooring system to the FSO
    b. Identify the critical sea-states
3. Loading/offloading station keeping analysis of the turret-moored FSO and CNG vessel in the Barents Sea under maximum operational sea-states.
    a. Identify the critical sea-states
    b. Check that the large motions are within the capability of the loading hose

The present study focuses on the offshore loading/unloading analysis of the CNG transport system in the Barents Sea. The report presents results from a feasibility study of the loading/unloading system. For further development of the system more detailed analyses are recommended.

1.3 Relations with other deliverables

This report is divided into two parts which cover the three sub-tasks listed in Section 1.2.

- The first part documents the results of the first sub-task (Offloading analysis using RIFLEX), giving inputs to the other two subtasks.
- The second part will document the results of the second and third sub-tasks.

2. Research Methodology and Procedures

2.1 Part 1 – Dynamic hose analysis

A RIFLEX analysis model has been prepared, which involves a finite element (FE) model of the hose and motion transfer functions of the two support vessels: CNG vessel and FSO [1]. Numerical analysis has been carried out on loading/unloading hoses under various weather conditions.

2.2 Part 2 – Positioning analysis of FSO and GASVESSEL

Following sub-tasks and corresponding numerical tools are listed:

1. Check the mooring line tension has enough safety margin, and that the vessel offset for the suggested turret mooring is within reasonable range under extreme condition (100 years return period sea-state). (Mimosa frequency-domain/ SIMO time-domain).
2. Tune a SIMO DP-system for thruster assisted mooring (heading control only) of the FSO, that has an acceptable performance under operational conditions (Hs=6 m).
3. Tune a SIMO DP-system for the CNG that has an acceptable performance under operational condition (Hs=6 m)
4. Time-domain (SIMO) calculation on the tandem arrangement of FSO and CNG vessel, with simplified spring in between two vessels, FSO with mooring and DP system, CNG vessel with DP system, under operational condition (Hs=6 m), check the near and far position, identify the worst condition (varying Tp, wind direction and heading)

PART 1 – DYNAMIC HOSE ANALYSIS

3. Conceptual Design of Loading/Unloading System

3.1 General

Figure 1 summarizes the loading of gas from offshore and transporting it using the GASVESSEL concept to the gas unloading location. [3]

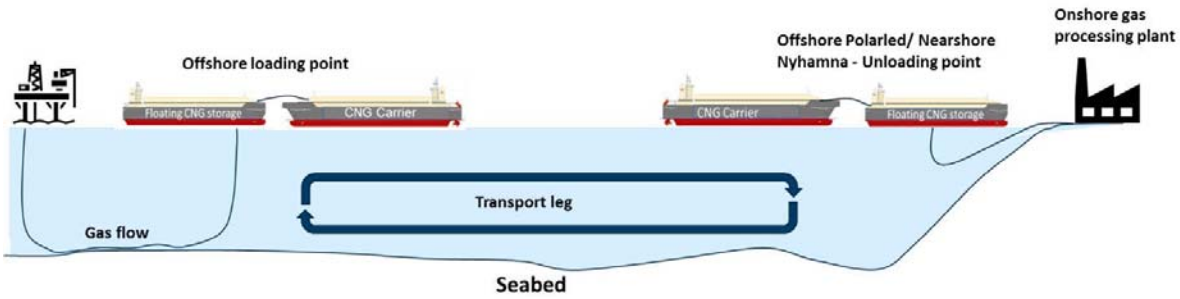

Figure 1 Main value chain aspects of Barents Sea scenarios [3].

The system consists of

1. Turret moored floating storage and offloading unit (FSO)
2. Shuttle tanker – compressed natural gas vessel, denoted GASVESSEL
3. Loading hose

The loads in the loading hose consist of

1. Static loads due to gravitation. The magnitude is governed by mass, buoyancy, hose length, distance between end supports and height of support points.
2. Dynamic loads due to acceleration and hydrodynamic drag- and inertia forces on submerged part of the hose.

The dynamic excitation sources are

1. Motions of FSO stern and tanker bow, wave frequency (WF) motions only. The low frequency (LF) motions are not included explicitly. The mean distance variation covers typical range of relative surge motions (mean offset and low frequency motions).
2. Water wave motion. Most important are velocity and acceleration normal to the local longitudinal hose axis.

3.2 Barents Sea scenario

In the present study, the area on focus is indicated by the red quadrant in Figure 2. Since all the potential oil and gas fields for GASVESSEL are in the South West area of the Barents Sea, the area indicated is Barents Sea South West [3].

The reason for focusing on the Barents Sea is that it presents clear potential for monetizing stranded and associated gas due to lack of infrastructure and small volumes of gas discovered. The North Sea has not been considered, mainly since it is a well-established region served by an extensive network of pipelines.

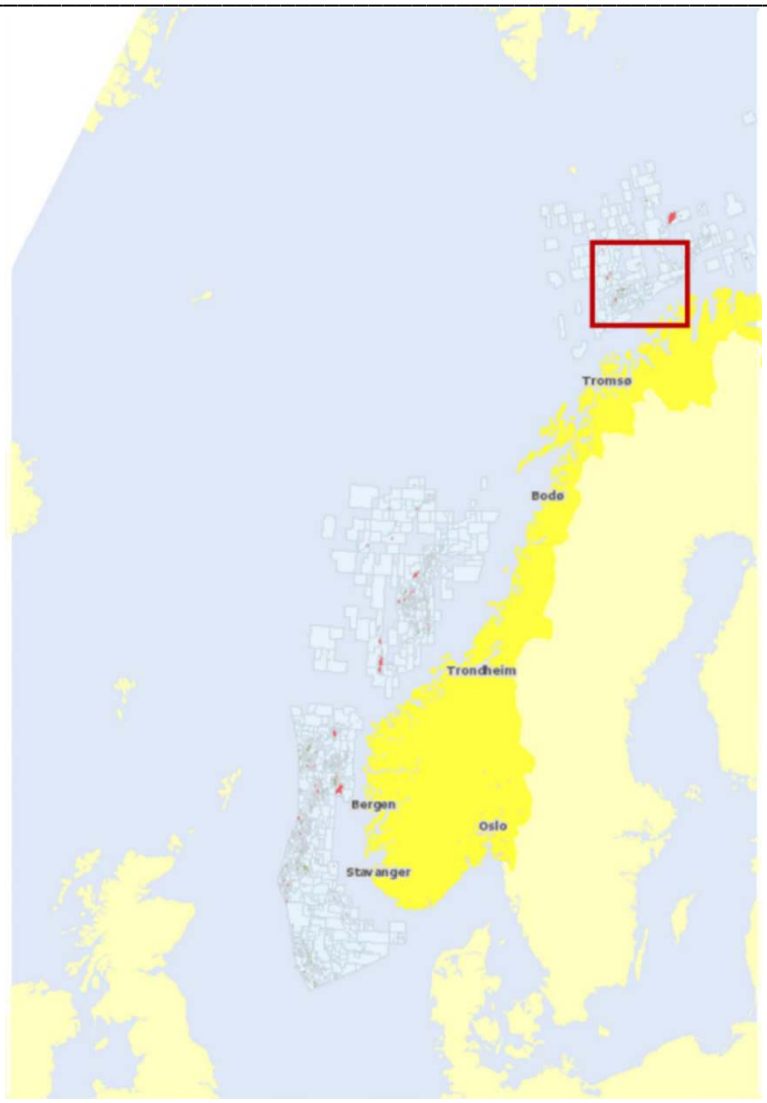

Figure 2 Barents Sea south west [3].

It is shallow water in the focus area, the water depth is 300 to 400 m.

The area characterized by cold climate, challenging conditions during winter including darkness, severe wind and waves, and fog during summer season. The flow of Atlantic (Gulf Stream) and Coastal waters is responsible for absence of ice formation and relatively middle temperatures. Information for the Goliat FPSO indicates that average air temperature varies from -2 °C to 6 °C, with min/max of approximately -15 °C to +25 °C. Sea water temperature lies in the range of 5-8 degrees at seabed and in the range of 1-10 degrees at sea level [3].

Average significant wave height in Southwest Barents Sea varies from 1.5 m to 3.3 m. It should be noted that the significant wave height is generally higher in the Norwegian Sea compared to the Barents Sea, see Figure 3.

The average wind speed varies from 5 to 10 m/s in the Barents Sea southwest. With peaks at, for instance 28 m/s registered at GOLIAT FPSO (corresponding wind direct 260 degrees), see Figure 4.

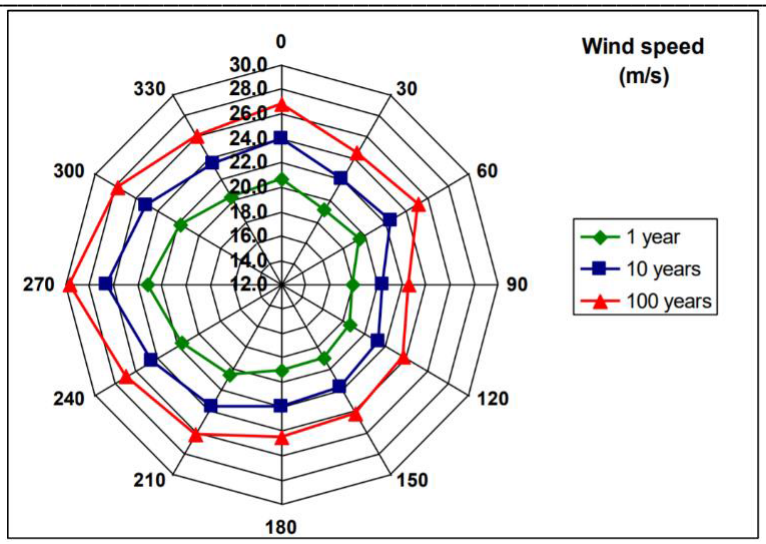

Figure 3 Significant wave height, Goliat FPSO [3].

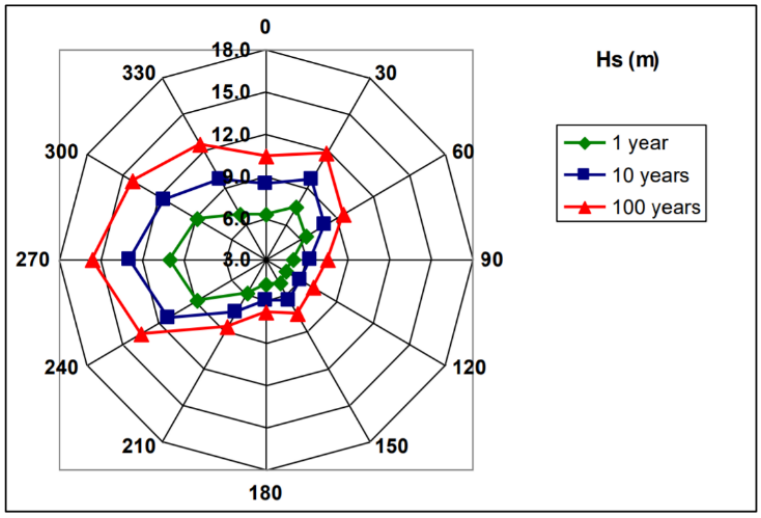

Figure 4 Wind speed, Goliat FPSO [3].

Based on technical data about offshore loading locations, and in accordance with the project partners, the following two gas fields have been selected as offshore gas loading locations for GASVESSEL, see Figure 5.

- ALKE – gas field
- JOHAN CASTBERG - Oil & Gas field with Associated gas

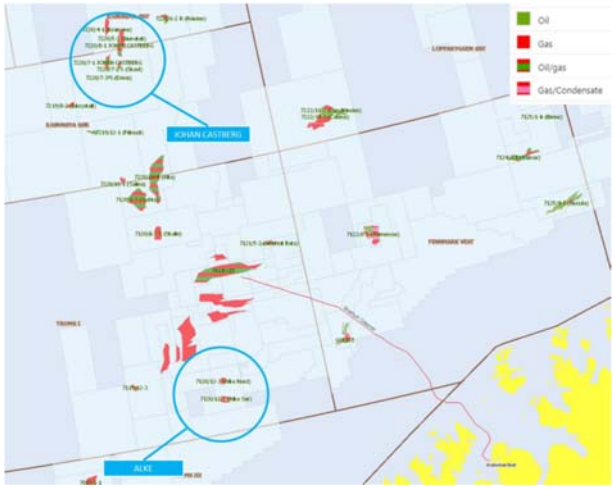

Figure 5 Map of the two suggested loading fields: JOHAN CASTBERG and ALKE [3].

3.2.1 Environment data

Key environment data are:

- Significant wave height, H_s
- Peak wave period, T_p
- Wave direction, θ_w
- Current speed, U_c
- Current direction, θ_c

3.3 Offloading method

There exist several methods to loading/unloading oil/gas offshore, as shown in Figure 6:

1. FPSO side by side
2. FPSO tandem
3. Submerged turret
4. Calm buoy
5. Spar
6. Fixed tower
7. Ugland-Kongsberg Offshore Loading System (UKOLS)

Figure 6 Sketch of different offshore loading methods. [4]

FPSO tandem loading is selected for the present study, as a result by considering several factors such as environmental loads, costs etc.

3.4 Vessels

Two versions of CNG vessels have been designed [5, 6], the dimensions of the two vessels are shown in Table 1.

Table 1 Dimensions of CNG vessels. [5, 6]

Property	**Unit**	**Old version** [5]	**New version** [6]
Length over all, L_{OA}	m	205.0	205.0
Length between perpendiculars, L_{PP}	m	190.9	190.9
Max breadth	m	36.0	36.0
Height main deck	m	22.0	15.5
Design draft	m	7.5	7.5
Capacity – NG @ 300 bar, 20 ˚C	Nm^3	$15{\cdot}10^6$	$12{\cdot}10^6$
TYPE A gas cylinder length	m	22.5	17.0
TYPE A gas cylinder outer diameter	m	3.4	3.4
TYPE A gas cylinder quantity	pcs	256	256
TYPE B gas cylinder length	m	20.5	15.0
TYPE B gas cylinder outer diameter	m	3.4	3.4
TYPE B gas cylinder quantity	pcs	12	16
TYPE C gas cylinder length	m	18.5	13.0
TYPE C gas cylinder outer diameter	m	3.4	3.4
TYPE C gas cylinder quantity	pcs	4	4

In the offshore loading system (OLS) of present study, the 'Old' version CNG vessel is taken as FSO, and the 'New' version CNG vessel is taken as GASVESSEL.

3.4.1 FSO

'Old' version GASVESSEL (big): [5]

DP system [7-9]:

Table 2 Propeller and thrusters of old version CNG vessel.

Main propellers performance	
Type	2x Steerprop SP90 CRP ECO LM, 6500 kW/445RPM
Propeller diameter	4300 mm
Input speed	445 mm
Input power	6500 kW
Propeller speed	135 RPM
Azimuth capacity	1.5 RPM
Bow thruster performance	
Type	Wartsila WTT-14
Max power	1450 kW
Propeller diameter	2000 mm

3.4.2 CNG vessel - GASVESSEL

'New' version (small): [6]

DP system: '*two bow thrusters will be installed on the small GASVESSEL ship, so their total capacity will be twice as on big ship. The astern thrusters will be the same in quantity and in capacity.*' [10] Confer Table 2.

3.4.3 Loading conditions

The summer draft is at 7.0 m above the base line.

DESIGNATION	UNIT	FSO ("Big one")			GASVESSEL ("Small one")		
		Ballast	Medium	Loaded	Ballast	Medium	Loaded
T_{AP}	m	7.23	7.01	7.50	6.48	6.85	7.00
T_{M}	m	7.17	6.97	7.50	6.47	6.84	7.00
T_{FP}	m	7.10	6.87	7.50	6.46	6.83	7.00
V_{CG}	m	11.74	13.43	13.63	10.23	11.16	11.66
Δ	ton	38765	37360	40863	34473	36756	37723
r_{44}	m	13.68	12.26	12.34	13.75	13.34	13.09
r_{55}	m	47.27	49.28	47.34	48.67	48.92	49.00
r_{66}	m	47.90	49.51	47.23	49.31	49.35	49.28

The main deck (Deck 7) above base line (B.L.):

FSO: 22 m

CNG vessel: 15.5 m

The design water line (DWL) for both vessels are 7.5 m

The connectors are located above the mean water line:

FSO: 22 - 7.5 = 14.5 m

CNG vessel: 15.5 – 7.5 = 8 m

3.5 Loading/Unloading hose

3.5.1 Specifications

Loading hose or flexible pipe is considered for loading/unloading system.

Following specifications/requirements of the pipe are desired:

Table 3 Required specification of loading hose/flexible pipe. [11]

SPECIFICATION	VALUE
Maximum loading pressure	240 bar
Inner pipe diameter ('single line')	14 inch
Inner pipe diameter ('3 lines')	14 inch
Length	≈200m
Working temperature range	Extreme values we have considered so far are -50°C (min) and +70°C (max)… but it is possible to adapt

Table 4 shows the properties of the flexible pipe for loading/unloading in the present study [12].

Table 4 Properties of the flexible pipe for loading/unloading. [12]

GASVESSEL - Compressed gas loading hose		
Supplier	**TechnipFMC**	
Property	**Unit**	**Value**
Weight in air full of sea water	t/m	0.359
Diameter outside	M	0.467
Diameter inside	M	0.355
Area of external cross section, AE	m^2	0.172
Area of internal cross section, AI	m^2	0.099
Gyration radius, rgyr	M	0.206
Axial stiffness, EA	kN	
Bending stiffness, EI	kNm^2/rad	399.300
Torsion stiffness, GT	kNm^2/rad	
Density of sea water	t/m^3	1.025
Density of gas	t/m^3	0.190
Submerged weight, empty, (kN/m)	kN/m	1.798
Submerged weight, water filled, (kN/m)	kN/m	2.796
Submerged weight, gas filled, (kN/m)	kN/m	1.983
Drag coefficient, C_d	-	1.2
Free fall speed, water filled (m/s)	m/s	3.12
Free fall speed, gas filled (m/s)	m/s	2.63
Added mass coefficient, C_m		1
Free fall acceleration, water filled	m/s^2	4.39
Free fall acceleration, gas filled	m/s^2	3.11
With zero tension		
Radius of curvature, water filled	M	4.60
Radius of curvature, gas filled	M	5.16
Curvature utilization, Rstorage/Rstatic		0.60

Table 5 Tension - curvature capacity parameters in operational condition.

	Capacity
$T_{\kappa=0}$	**5405.14 (kN)**
$\kappa_{T=0}$	**1/5.16 (m^{-1})**

At the present the minimum tension/compression capacity of the hose is not known. However, based on previous work of flexible pipes the capacity is limited and should preferably be above zero. We have assumed that it should be not lower than the order of 10 kN.

3.5.2 Boundary conditions

Free-to-rotate in bending behaviour of the couplings used on-board both GASVESSEL and FSO. These coupling will be quick connect/disconnect type [10, 13, 14].

3.5.3 Temperature

The working temperature considered ranges from -50 °C (min) to +70 °C (max) [11].

Refer to [12, 15]:

"*In terms of use down to -50 °C in dynamic service I can confirm the following:*

In terms of the end fittings our steel is chirpy tested to -50 °C by default as part of its procurement process.

For Crossflex® pressure sheath material this is suitable for -50 °C in static application we did further qualification work on that for a static flowline down to -45 °C to demonstrate that the end fitting crimping could take repeated thermal cycles.

Even in dynamic service the EF's would never generally be 'dynamic' at the crimping location as we would always have some sort of support or control fitted (small bend stiffener, etc).

Crossflex® has a glass transition temperature down to -125.7 °C however dynamic bending tests have only been conducted down to -30 °C @ MBR (7.7% strain).

For this new CNG application – depending on the eventual operating conditions and configuration – we would suggest that a dynamic bending test be conducted as part of the development / procurement program to the minimum required temperature."

3.5.4 Gas flow

Refer to [11]:

- peak velocity at (free) unloading phase: 22 m/s
- peak velocity at (free) loading phase: 6.5 m/s

Refer to [12]:

"*Note that with a high offloading velocity of up to 22m/s it is possible that FLIP (FLow Induced Pulsations) may occur. In order to overcome this issue we could adapt the inner carcass to our new FLIP resistant S-Carcass – this would add approximately 10 kg/m to the weight of the product. Alternatively, if the design of the surrounding pipework is such that it will not be effected by FLIP (as the FLIP generally does not cause any issue with the flexible product itself) we could just live with the FLIP. Otherwise we could revert to a smooth bore pipe design subject to further clarification on configuration the end fittings (for venting of the diffused gas).*"

3.6 Operation limit

Figure 7 illustrates the emergency shut down (ESD) sectors behind FSO.

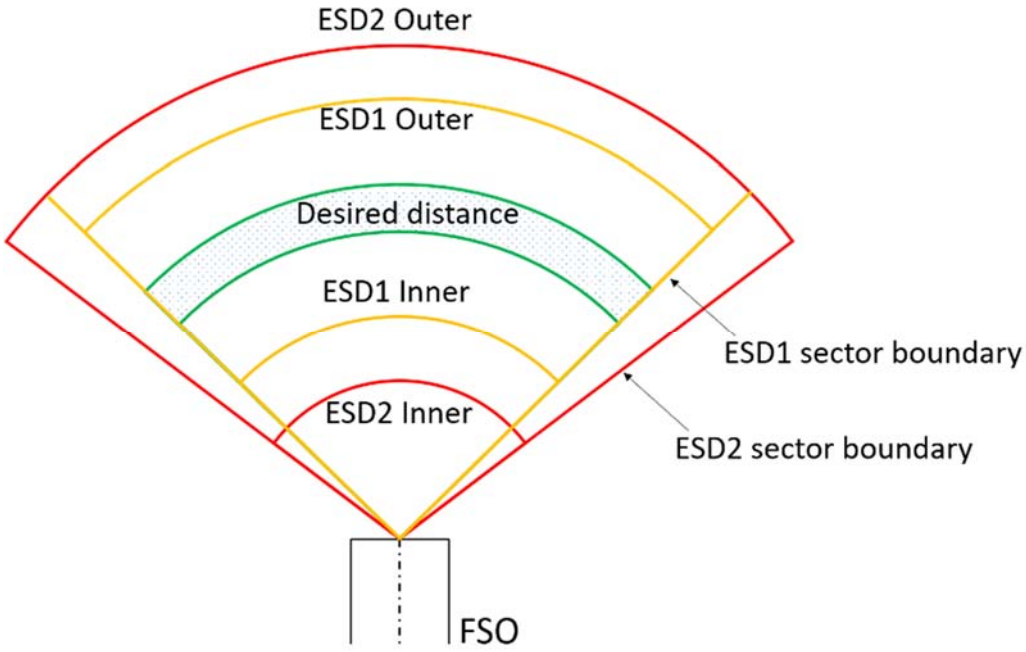

Figure 7 Illustration of offloading sectors behind FSO.

4. Numerical Analysis of Loading/Unloading Operation Under Various Sea-states

4.1 Softwares and version control

Table 6 Softwares and version control.

SOFTWARE	VERSION
SIMA	3.7.1
RIFLEX	4.16.1.BIWR-21
WAMIT	7.062

4.2 Numerical model

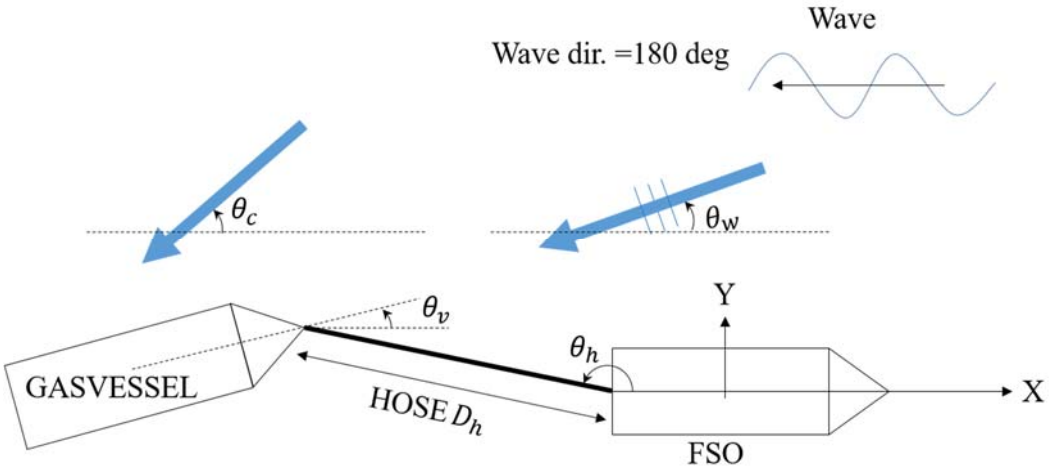

Figure 8 Coordinate system and operational parameters of a tandem loading/unloading system.

Table 7 Boundary conditions of two supernodes of the loading hose.

	X	Y	Z	RX	RY	RZ
Fso_stern	Fixed	Fixed	Fixed	Free	Free	Fixed
Gasvessel_bow	Fixed	Fixed	Fixed	Free	Free	Free

4.3 Environmental loads

The loading hose is subject to combined wave and current loads, the basic load condition is shown in Table 8 .

Table 8 Environmental conditions and input parameters for sensitivity study on hose distances.

H_s [m]	T_p [s]	θ_w [deg]	U_c [m/s]	θ_c [deg]	θ_h [deg]	θ_v [deg]
6	13.5	210	0.89	225	180	0

4.4 Loading conditions

Table 9 Loading conditions of FSO and CNG vessel.

Condition	FSO	CNG vessel
1	Medium	Medium
2	Loaded	Ballast
3	Medium	Loaded

5. Dynamic analysis – sensitivity study

Sensitivity studies on hose distance, hose length, wave height and wave period under different loading conditions are carried out through non-linear time domain dynamic analysis using software RIFLEX and SIMA. The key results are presented in this section.

Two rounds of sensitivity study have been performed:

- Preliminary sensitivity study under medium loaded conditions on FSO and CNG vessel.
- Detail sensitivity study

5.1 Preliminary sensitivity study – (ISOPE 2020-5PC-0704)

5.1.1 Hose distance (D_h)

To investigate the hose dynamic response with regard to varying hose distance D_h, other environmental basis and input parameters are fixed, as shown in Table 8.

The hose distance D_h has been varied from 50 m to 90 m with 10 m increment, while the hose length L_h is kept as 115 m, see the list of cases in Table 10.

Table 10 Definition of cases for sensitivity study on hose distance.

Case #	D_h [m]
1	50
2	60
3	70
4	80
5	90

5.1.2 Hose distance (L_h)

To investigate the hose dynamic response with regard to varying hose length L_h, other environmental basis and input parameters are fixed, as shown in Table 8.

The hose length L_h has been varied from 165 m to 212 m, while the hose length D_h is kept as 100 m, see the list of cases in Table 11.

Table 11 Definition of cases for sensitivity study on hose length.

Case #	L_h [m]
1	165
2	182
3	192
4	202
5	212

5.1.3 Significant wave height (Hs)

To investigate the hose dynamic response under irregular wave and current with varying significant wave height H_s, other environmental basis and input parameters are fixed, as shown in Table 8.

The hose distance $D_h = 100\ m$, the hose length $L_h = 192\ m$. The significant wave height H_s has been varied from 3.5 m to 6.0 m with 0.5 m increment, see the list of cases in Table 12.

Table 12 Definition of cases for sensitivity study on significant wave height.

Case #	H_s [m]
1	3.5
2	4.0

3	4.5
4	5.0
5	5.5
6	6.0

5.1.4 Peak wave period (Tp)

To investigate the hose dynamic response under irregular wave and current with varying peak wave period T_p, other environmental basis and input parameters are fixed, as shown in Table 8.

The hose distance $D_h = 100\ m$, the hose length $L_h = 192\ m$. The peak wave period T_p has been varied from 8.0 s to 17.6 s, see the list of cases in Table 13.

Table 13 Definition of cases for sensitivity study on peak wave period.

Case #	T_p [s]
1	8.0
2	10.0
3	13.6
4	15.6
5	17.6

5.1.4 Results and discussions

The results and discussions are published in the 30th International Ocean and Polar Engineering Conference (ISOPE 2020-TPC-0704), and the paper is attached in the appendix.

From the preliminary sensitivity study in this section, the supplied unbounded flexible pipe was selected to be used as the loading/unloading hose. Under the loading condition 1 in Table 9 (medium loaded on both FSO and CNG vessel), $L_h = 192$ m and $D_h = 100$ m were found to be feasible for the operational sea-states in Table 12 and Table 13.

5.2 Detail sensitivity study

The emergency shut-down (ESD) zones for loading/unloading is illustrated in Figure 9. ESD1 crossing indicates preparation for closing and disconnecting, while ESD2 indicates immediate disconnect. By considering the size of the FSO and CNG vessels, and refer to previous offloading study in [1], the inner and outer distance limits are defined in Table 14, and sensitivity studies has been performed.

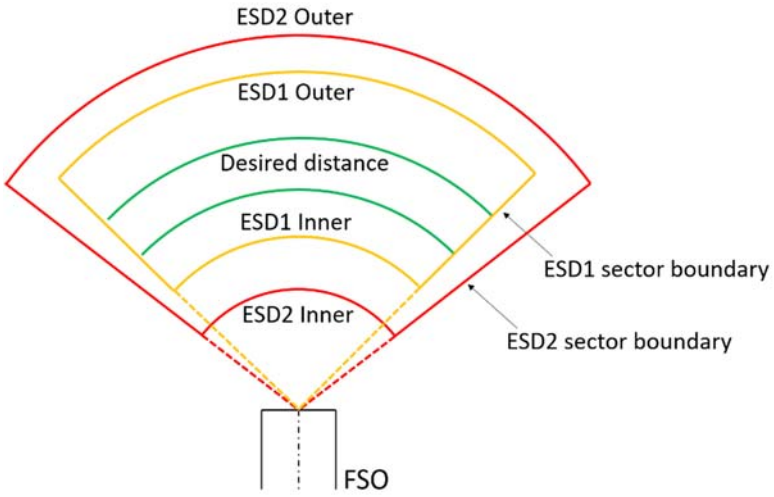

Figure 9 Illustration of offloading sectors behind FSO.

Table 14 Definition of ESD1 zone.

	Near	Preferred	Far
D_h [m]	85	100	115

In this section, sensitivity study has been performed for several rounds on the operational sea-states (Table 12 and Table 13) with both 'near' and 'far' distance (D_h).

5.2.1 Round 1 – position check

In this round, the hose with the same properties as in Section 5.1 are applied in the analysis, which are:

- Mass/length=253 kg/m
- $L_h = 192$ m

Table 15 Condition set of the 1st round sensitivity study.

							Condition set
D_h (m)	85	100	115			Lh=192 m, Hs=6 m, Tp=13.6 s	Distance_ESD1
H_s (m)	3.5	4	4.5	5	5.5	Lh=192 m, Dh=85 m, Tp=13.6 s	Wave_Hs_ESD1_near
H_s (m)	3.5	4	4.5	5	5.5	Lh=192 m, Dh=115 m, Tp=13.6 s	Wave_Hs_ESD1_far
T_p (s)	8	10	13.6	15.6	17.6	Lh=192 m, Dh=85 m, Hs=6 m	Wave_Tp_ESD1_near
T_p (s)	8	10	13.6	15.6	17.6	Lh=192 m, Dh=115 m, Hs=6 m	Wave_Tp_ESD1_far

Dynamic analysis has been performed on the defined conditions in Table 15. The maximum curvature, minimum and maximum axial forces of the loading hose have been checked and summarized in Table 16. Envelop curves of corresponding curvature and axial force of these conditions are presented in Figure 25 Maximum curvature envelope curves of the cases in Condition set - Distance_ESD1 (Table 15).Figure 25 to Figure 39 in Appendix A.

Table 16 Summary of the peak values of dynamic curvatures and tension forces of 1st round sensitivity study.

Condition set	Curvature κ (1/m)			Tension F (N)	
	FSO	Mid	CNG	Min	Max
Distance_ESD1	0.08	0.067	0.086	-4.00E+04	3.10E+05
Wave_Hs_ESD1_near	0.037	0.067	0.08	-3.40E+04	2.60E+05
Wave_Hs_ESD1_far	0.071	0.0425	0.137	-4.00E+04	3.00E+05
Wave_Tp_ESD1_near	0.115	0.067	0.111	-4.00E+04	3.20E+05
Wave_Tp_ESD1_far	0.012	0.042	0.014	-4.20E+04	3.30E+05

The curvature and maximum axial force are well within the hose capacity. However, we observe negative minimum axial force, which indicates compression. In the following studies, we try to find a solution to solve the 'compression' problem.

5.2.2 Round 2 – hose properties

'Compression' (negative axial forces) is observed in some conditions in Section 5.2.1. In order to avoid such compression, the mass/length of the flexible pipe has been increased from 253 kg/m to 450 kg/m, and varying lengths were checked. The length of 232 m is found to be suitable.

The sensitivity study has been carried out:

- $m/l = 450$ kg/m
- $L_h = 232$ m

Table 17 Condition set of the 2nd round sensitivity study.

								Condition set
L_h (m)	182	192	202	212	**232**	252	Dh=100 m, $H_s = 6$ m, Tp=13.6 s	Wave_Tp_Heavy
H_s (m)	3.5	4	4.5	5	5.5	6	Lh=232 m, Dh=85 m, Tp=13.6 s	Wave_Hs_ESD1_near_Heavy
H_s (m)	3.5	4	4.5	5	5.5	6	Lh=232 m, Dh=115 m, Tp=13.6 s	Wave_Hs_ESD1_far_Heavy
T_p (s)	8	10	13.6	15.6	17.6		Lh=232 m, Dh=85 m, Hs=6 m	Wave_Tp_ESD1_near_Heavy
T_p (s)	8	10	13.6	15.6	17.6		Lh=232 m, Dh=115 m, Hs=6 m	Wave_Tp_ESD1_far_Heavy

Dynamic analysis has been performed on the defined conditions in Table 17. The maximum curvature, minimum and maximum axial forces of the loading hose have been checked and summarized in Table 18. Envelop curves of corresponding curvature and axial force of these conditions are presented in Figure 25 Maximum curvature envelope curves of the cases in Condition set - Distance_ESD1 (Table 15).Figure 40 to Figure 54 in Appendix A.

Table 18 Summary of the peak values of dynamic curvatures and tension forces of 2nd round sensitivity study.

Condition set	Curvature κ (1/m)			Tension F (N)	
	FSO	Mid	CNG	Min	Max
Wave_Tp_Heavy	0.023	0.06	0.032	-1.00E+04	5.90E+05
Wave_Hs_ESD1_near_Heavy	0.023	0.073	0.021	1.10E+04	5.50E+05
Wave_Hs_ESD1_far_Heavy	0.021	0.045	0.025	400	5.60E+05
Wave_Tp_ESD1_near_Heavy	0.033	0.073	0.052	-5.00E+03	6.00E+05
Wave_Tp_ESD1_far_Heavy	0.0325	0.045	0.04	400	6.00E+05

The curvature and maximum axial force are well within the capacity of the hose. By increasing the mass/length and length of the hose, we avoid 'compression' for most of the cases, negative axial force is only observed at 'near' position, when the wave peak period is 10 s.

5.2.3 Round 3 –

After the second round sensitivity study in Section 5.2.2 with increased mass/length and length of the flexible pipe, 'compression' occurs under only one 'near' condition with $H_s = 6$ m, $T_p = 10$ s (see Table 17). A sensitivity study on this condition has been performed by further varying the length and mass/length of the hose, the matrix is presented in Figure 34Table 19:

Table 19 Condition set of the 3rd round sensitivity study on condition $H_s = 6\ m,\ T_p = 10\ s$.

					Condition set
L_h (m)	262	282	302	m/l=450 kg/m, Dh=100 m	Wave_Tp10_Heavy5
m/l (kg/m)	470	490	510	Lh=232 m, Dh=100 m	Wave_Tp10_Heavy5
L_h (m)	262	282	302	m/l=450 kg/m, Dh=85 m	Wave_Tp10_Heavy_near
m/l (kg/m)	470	490	510	Lh=232 m, Dh=85 m	Wave_Tp10_Heavy_near

Dynamic analysis has been performed on the defined conditions in Table 19. The maximum curvature, minimum and maximum axial forces of the loading hose have been checked and summarized in Table 20. Envelop curves of corresponding curvature and axial force of these conditions are presented in Figure 25 Maximum curvature envelope curves of the cases in Condition set - Distance_ESD1 (Table 15).Figure 55 to Figure 66 in Appendix A.

Table 20 Summary of the peak values of dynamic curvatures and tension forces of 3rd round sensitivity study.

Condition set	**Curvature κ (1/m)**			**Tension F (N)**	
	FSO	Mid	CNG	Min	Max
Wave_Tp10_Heavy5	0.03	0.063	0.03	-2.00E+03	7.30E+05
Wave_Tp10_Heavy5	0.03	0.057	0.027	2.50E+03	6.80E+05
Wave_Tp10_Heavy_near	0.03	0.078	0.032	-4.00E+03	7.50E+05
Wave_Tp10_Heavy_near	0.03	0.072	0.035	-2.00E+03	6.80E+05

From this sensitivity study, a combination of $m/l = 510$ kg/m, $L_h = 232$ m can avoid compression problem for the condition $H_s = 6$ m, $T_p = 10$ s.

5.2.4 Round 4 – updated hose property

As concluded from the 3rd round in Section 5.2.3, sensitivity study has been carried out in ESD1 boundary distances with updated input parameters:

- $m/l = 510$ kg/m
- $L_h = 232$ m

Table 21 Condition set of the 4thround sensitivity study with $m/l = 510\ kg/m$, $L_h = 232\ m$.

								Condition set
H_s (m)	3.5	4	4.5	5	5.5	6	Dh=85 m, Tp=13.6 s	Wave_Hs_ESD1_near_m510l232
H_s (m)	3.5	4	4.5	5	5.5	6	Dh=115 m, Tp=13.6 s	Wave_Hs_ESD1_far_m510l232
T_p (s)	8	10	13.6	15.6	17.6		Dh=85 m, Hs=6 m	Wave_Tp_ESD1_near_m510l232
T_p (s)	8	10	13.6	15.6	17.6		Dh=115 m, Hs=6 m	Wave_Tp_ESD1_far_m510l232

Dynamic analysis has been performed on the defined conditions in Table 21. The maximum curvature, minimum and maximum axial forces of the loading hose have been checked and summarized in Table 22. Envelop curves of corresponding curvature and axial force of these conditions are presented in Figure 25 Maximum curvature envelope curves of the cases in Condition set - Distance_ESD1 (Table 15).Figure 67 to Figure 78 in Appendix A.

Table 22 Summary of the peak values of dynamic curvatures and tension forces of 4th round sensitivity study.

Condition set	Curvature κ (1/m)			Tension F (N)	
	FSO	Mid	CNG	Min	Max
Wave_Hs_ESD1_near_m510l232	0.022	0.074	0.02	1.90E+04	6.30E+05
Wave_Hs_ESD1_far_m510l232	0.02	0.046	0.023	1.35E+04	6.40E+05
Wave_Tp_ESD1_near_m510l232	0.03	0.074	0.048	2.65E+03	6.70E+05
Wave_Tp_ESD1_far_m510l232	0.03	0.046	0.042	1.30E+04	6.80E+05

5.2.5 Round 5 – other loading conditions

It is discovered from WAMIT calculations, that the pitch response is largest at $T_p = 12$ s. A sensitivity study has been performed at $H_s = 6$ m with different distances, as shown in Table 23.

Sensitivity study has been carried out on other two loading conditions (see Table 9) with updated input parameters:

- $m/l = 510$ kg/m
- $L_h = 232$ m

Table 23 Condition set of the 5th round sensitivity study with $m/l = 510$ kg/m, $L_h = 232$ m.

							Condition set
D_h (m)	85	100	115			Hs=6 m, Tp=12 s	Distance_Tp12
T_p (s)	8	12	13.6	15.6	17.6	Dh=85 m, Hs=6 m, FSO loaded	Wave_Tp_ESD1_near_CNGballast
T_p (s)	8	12	13.6	15.6	17.6	Dh=115 m, Hs=6 m, FSO loaded	Wave_Tp_ESD1_far_CNGballast
T_p (s)	8	12	13.6	15.6	17.6	Dh=85 m, Hs=6 m, FSO medium	Wave_Tp_ESD1_near_CNGloaded
T_p (s)	8	12	13.6	15.6	17.6	Dh=115 m, Hs=6 m, FSO medium	Wave_Tp_ESD1_far_CNGloaded

Dynamic analysis has been performed on the defined conditions in Table 23. The maximum curvature, minimum and maximum axial forces of the loading hose have been checked and summarized in Table 24. Envelop curves of corresponding curvature and axial force of these conditions are presented in Figure 25 Maximum curvature envelope curves of the cases in Condition set - Distance_ESD1 (Table 15).Figure 79 to Figure 93 in Appendix A.

Table 24 Summary of the peak values of dynamic curvatures and tension forces of 5th round sensitivity study.

Condition set	Curvature κ (1/m)			Tension F (N)	
	FSO	Mid	CNG	Min	Max
Distance_Tp12	0.021	0.075	0.025	-5000	7.00E+05
Wave_Tp_ESD1_near_CNGballast	0.03	0.075	0.048	-700	6.70E+05
Wave_Tp_ESD1_far_CNGballast	0.03	0.046	0.036	-5000	7.00E+05
Wave_Tp_ESD1_near_CNGloaded	0.03	0.075	0.048	-700	6.70E+05
Wave_Tp_ESD1_far_CNGloaded	0.03	0.046	0.036	-5300	7.00E+05

The curvature and maximum axial force are well within the hose capacity. But we observe negative minimum axial force, which indicates compression. But since the magnitude of 'compression' is relative small, in addition, the present study is not detail design of the loading hose, no effort has been made to further investigation.

PART 2 – POSITIONING ANALYSES OF FSO AND GASVESSEL

6. Simulation set-up

6.1 General

For the set-up in SIMA we need to configure two vessels: FSO and GASVESSEL.

Two versions of the CNG vessel have been designed [5, 6]. The old version is used as FSO, and the new as GASVESSEL. The vessels have the same hull, but different superstructure. For the simulations, the FSO is assumed to be in loaded and the GASVESSEL in ballasted condition. The main dimensions of the two vessels are shown in Table 25. Another difference is the bridge that is assumed located fore on the FSO and aft on the GASVESSEL, changing the wind coefficients see section 6.2.2.

Table 25 Dimensions of CNG vessels. [5, 6]

Property	**Unit**	**FSO** [5]	**GASVESSEL** [6]
Length over all, L_{OA}	m	205.0	205.0
Length between perpendiculars, L_{PP}	m	190.9	190.9
Max breadth	m	36.0	36.0
Height main deck	m	22.0	15.5
Simulation draft	m	7.5	6.47
T_{AP}	m	7.50	6.48
T_M	m	7.50	6.47
T_{FP}	m	7.50	6.46
V_{CG}	m	13.63	10.23
Δ	ton	40863	34473
r_{44}	m	12.34	13.75
r_{55}	m	47.34	48.67
r_{66}	m	47.23	49.31

In the simulations, the GASVESSEL is positioned 100m behind the FSO as shown in Figure 10.

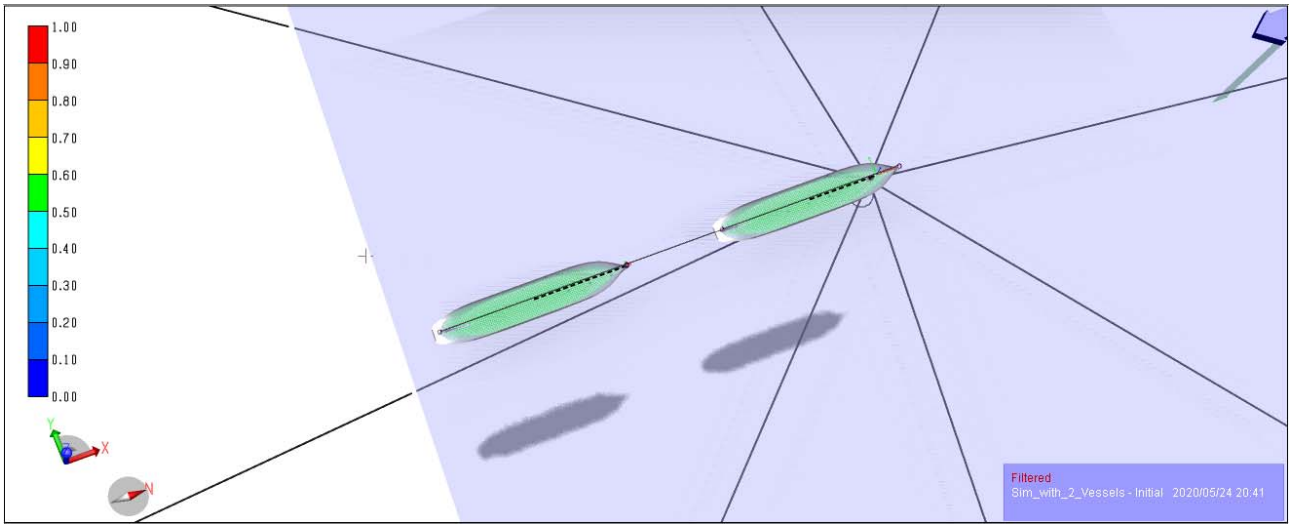

Figure 10 The hulls of the FSO with turret mooring, and the GASVESSEL as visualized in SIMA.

6.2 Hydrodynamic parameters

6.2.1 Wamit data

WAMIT was used in WP5 to generate kinetics for the hull for 6 different loading conditions. Most results have been reported in [16]. Wave drift data has been added to Appendix A.

SIMA imported the vessel mass data, hydrostatic stiffness, motion transfer functions and wave drift forces for the two drafts 6.47m and 7.5m.

6.2.2 Wind coefficients

The wind coefficients have been scaled from the dimensionless coefficients listed in [17].

The wind tunnel test was performed on the FSO with 7m draft, so only a minor change in surface area was needed for the scaling back to full size.

The GASVESSEL has a 6.5m lower main deck, so the surface area is much smaller than the FSO. We have assumed that the dimensionless coefficients are still valid, and scaled with the smaller side and front areas.

The bridge is moved from bow to stern on the GASVESSEL, so the full-scale parameters for the moment CN/CZ/C6 had to be adjusted. The side area of the bridge is approximately A = 6x12m, the moment arm approximated by $l = L_{pp}/2*\sin(\text{heading})$, and the air density ρ = 1.21 kg/m^3. The additional wind force due to a bridge at the stern is given the following moment, $M = \rho * A * l * v^2$.

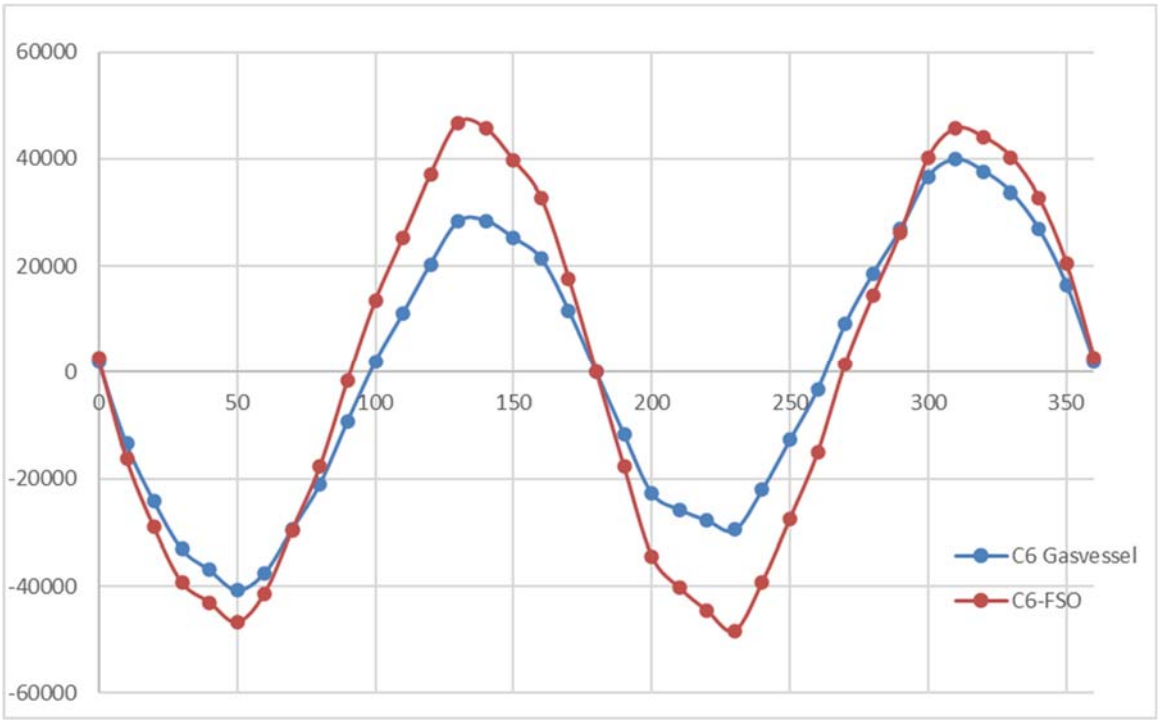

Figure 11 Wind coefficients [Ns^2/m] for yaw-moment as function of SIMO heading for FSO and GASVESSEL. The GASVESSEL is less directionally unstable than the FSO for head wind (180 deg).

6.2.3 Current coefficients

The current coefficients have been scaled from the dimensionless coefficients listed in [18]

The coefficients have been calculated by the GHS General HydroStatics - stability software for the 7.5m draft of the hull. This corresponds to the FSO in loaded condition, that could be scaled right back to full scale. The GASVESSEL was scaled with a draft of 6.47m.

These have also been reported in [16].

6.3 Thrusters

The thruster specification is according to [7-9]:

Table 26 Propeller and thrusters of CNG vessels.

Main propellers performance	
Type	2x Steerprop SP90 CRP ECO LM, 6500 kW/445RPM
Propeller diameter	4300 mm
Input speed	445 mm
Input power	6500 kW = 1027kN
Propeller speed	135 RPM
Azimuth capacity	1.5 RPM = 9 deg/s
Bow thruster performance	
Type	Wartsila WTT-14
Max power	1450 kW in Manouvre mode/1300kW in DP-mode
Propeller diameter	2000 mm

The GASVESSEL has 2 identical bow thrusters, see [10].

The positions of the thrusters are set according to the GA [5-6]. The extra bow thruster has been placed immediately aft of the one positioned in the GA.

The power conversion factor to be used is 0.158kN/kW according to DNVGL-ES-E301. No additional loss has been used.

6.4 FSO Mooring

A mooring system with 8 equal lines was designed to keep the vessel offset within 10% of the water depth in a 100 years environment condition and have a safety factor of at least 3.5 when the tension is calculated with SIMO, which gives qusa-static mooring line tension. The required safety factor when using SIMO is therefore higher than when using RIFLEX which gives slightly higher dynamic mooring line tension.

The system was designed for a water depth of 300m.

The definition of each mooring line is given in Table 27. The LineBuoy gives 50kN buoyancy, and the buoy2 elements gives -0.5kN buoyancy. The breaking strength is 12 000 kN.

Table 27 Line definition in SIMO

No	Num Elements	Buoy	Length	Bottom Friction	Diameter	E Mod	Em Fac	Uwia	Watfac	Transverse Drag	Longitudinal Drag
1	90		600.0	0.0	0.09	5.0e+10	2.0	1590.0	0.87	2.7	0.1
2	36	buoy2	360.0	0.0	0.1	7.5e+10	1.0	281.0	0.81	1.0	0.0
3	13	LineBuoy	13.0	0.0	0.1	7.5e+10	1.0	281.0	0.81	1.0	0.0
4	10	buoy2	70.0	0.0	0.1	7.5e+10	1.0	281.0	0.81	1.0	0.0

The location of the turret is in the simulations assumed to be behind the bridge, around frame 170. All lines are connected to the same point at baseline.

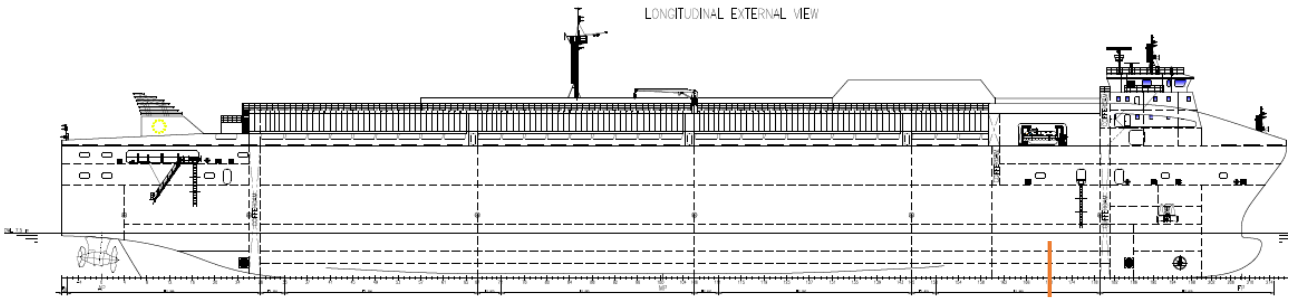

Figure 12 The GA showing the assumed location of the middle of the turret as a red line.

6.5 FSO DP

For the simulations, it was tuned a DP-controller for the vessel. The FSO is turret moored, and a standard heading + surge control was tuned using the internal SIMO DP. The tuning consists of setting the parameters for a Kalman filter to get a good representation of the low frequency motions with as little wave frequency noise as possible, and then setting the controller gains high enough to get acceptable performance without saturating the thrusters. A step response for the used heading controller is shown in Figure 13.

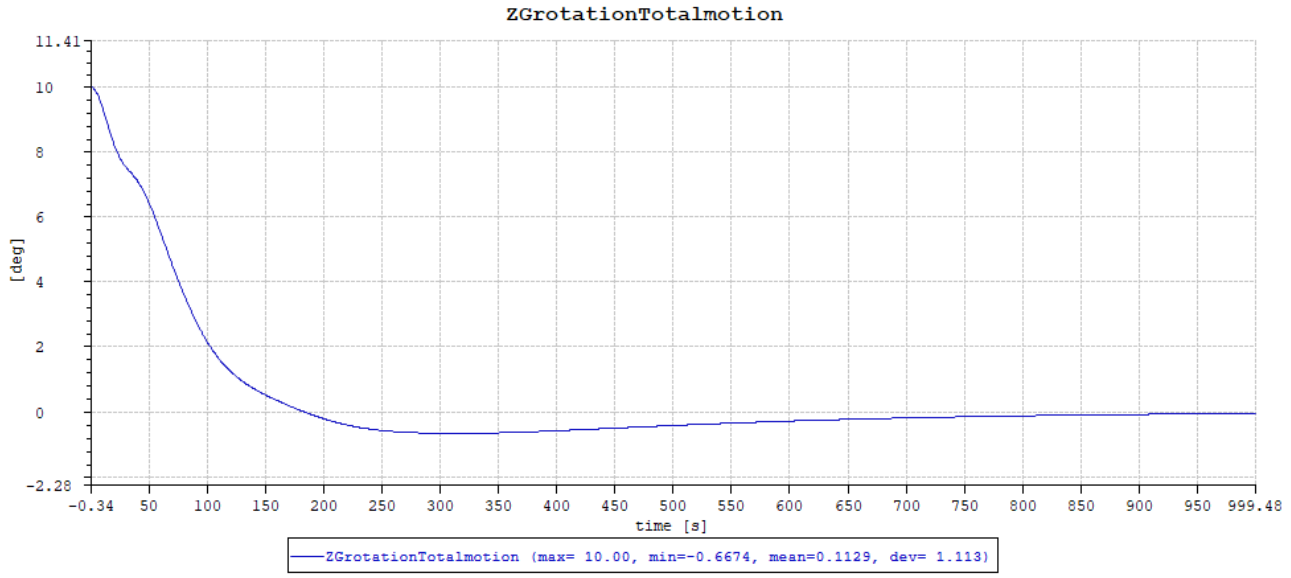

Figure 13 The step response for the heading with SIMO internal DP with gain corresponding to a natural period of 145 sec.

For the turret moored FSO, the aft azimuth thrusters give the best heading response, but they are limited to rotating 9 deg/s. It will then take 40 s to do a full turn, and the cut off for the filter must be at least 45 s due to that. For some environment conditions this will cause some fishtailing with the SIMO DP. The amount of fishtailing depends on the position of the turret, and the chosen Kalman filter cut off period.

In commercial DP-systems, it is possible to use a spread/star configuration to avoid this for most operational environment conditions. If the thrusters must operate close to max, due to waves, swell, current and wind coming from unfavourable directions, this might cause problems also for commercial systems.

6.6 GASVESSEL DP

A position and heading DP is necessary to keep the GASVESSEL in position relative to the FSO. Using a DP with measurements giving relative position is possible in commercial systems, but for the SIMO DP it was decided to tune the DP to a fixed point that gave an average gap of 100 m between the two vessels.

6.7 Loading hose

In the simulations, the hose was represented by a soft spring modelled by a Fixed Elongation Coupling SIMA element. This gives a small force in the straight line between the two connection points and an easy way to calculate the distance between the two vessels.

The actual forces from and on the hose was calculated using RIFLEX and is reported in part 1. These simulations will only verify whether that the vessels motions keep the hose within the ESD limits.

The connection points were above AP on the FSO and FP on the GASVESSEL. The connectors are located on the main deck, relative to the BL that is:

- FSO: 22 m
- GASVESSEL: 15.5 m

6.8 Environment conditions

For the simulations we specify these key environment data:

- Significant wave height, H_s
- Peak wave period, T_p
- Wave direction, θ_{wave}
- Current speed, U_c
- Current direction, θ_c
- Wind speed,
- Wind direction, θ_{wind}

The wind wave uses a Jonswap spectrum with parameters Gamma = 3.3, Ncos = 2 and 11 directions. Swell is not considered in this study.

The following conditions have been used to test the mooring system (corresponds to 100 years conditions for Johan Castberg and Goliat field):

Table 28 List of 100 years environment conditions.

#	H_s	T_p	θ_{wave}	U_c	θ_c	U_{wind}	θ_{wind}
1	15.6	18.2	180.0	1.23	180.0	33.0	180.0
2	15.0	16.3	180.0	1.23	180.0	33.0	180.0
3	14.0	15.0	180.0	1.23	180.0	33.0	180.0
4	15.0	19.0	180.0	1.23	180.0	33.0	180.0
5	14.0	20.0	180.0	1.23	180.0	33.0	180.0

For operational conditions, the following combinations have been simulated:

Table 29 List of environment conditions for test of operational limit.

#	H_s	T_p	θ_{wave}	U_c	θ_c	U_{wind}	θ_{wind}
1	6.0	6-12	180.0	0.89	180.0	20.0	180.0
2	6.0	6-12	180.0	0.89	180.0	20.0	165.0
3	6.0	6-12	180.0	0.89	180.0	20.0	150.0
4	6.0	6-12	180.0	0.89	165.0	20.0	165.0
5	6.0	6-12	180.0	0.89	150.0	20.0	150.0

DP-heading is against the waves for both vessels.

6.9 Operation limit

Figure 7 illustrates the emergency shut down (ESD) sectors behind the FSO. Part 1 has shown that the selected hose can operate with vessel distance 85-115m. The sector is ±30deg wide.

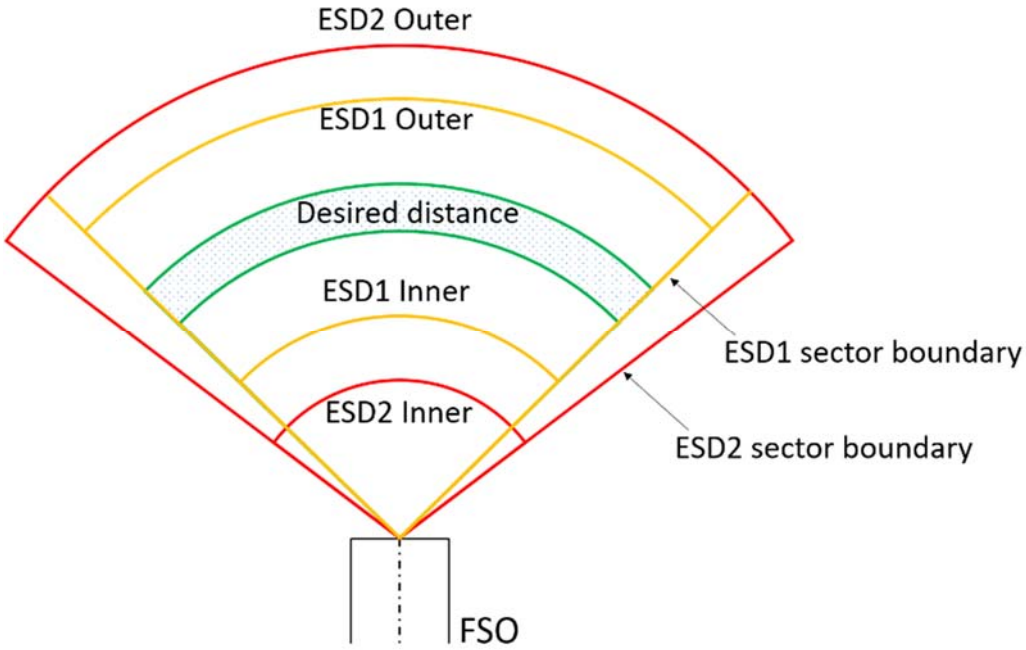

Figure 14 Illustration of offloading sectors behind FSO.

7. Simulation results

7.1 Software and version control

Table 30 Software and version control.

SOFTWARE	VERSION
SIMA	3.7.1
RIFLEX	4.16.1.BIWR-21
WAMIT	7.062

7.2 Mooring

Figure 15 shows how much the turret moves from its initial position when using only DP heading assist for the 5 cases listed in Table 28. The maximum offset is 24.89m ≈ 8% of the water depth. Figure 16 shows the corresponding tension in the line towards the incoming weather. This is the line with the highest tension, and it peaks at 2295kN, giving a safety factor of 5.3 based on the quasi-static line tension calculation in SIMO.

We have tested some additional cases were the wind is at 30 deg. and current at 45 deg., resulting in the DP losing control of the heading, and the vessel gets more of the ship side against the weather, resulting in higher offsets. Offsets up to 31m has been observed, with tension up to 3000kN. There exist more combinations of wind waves, swell, wind and current that may give larger offsets, but for this study we only needed a mooring system that will manage collinear 100 years conditions and have a reasonable response for the operational conditions, and this seems to be the case for the present system.

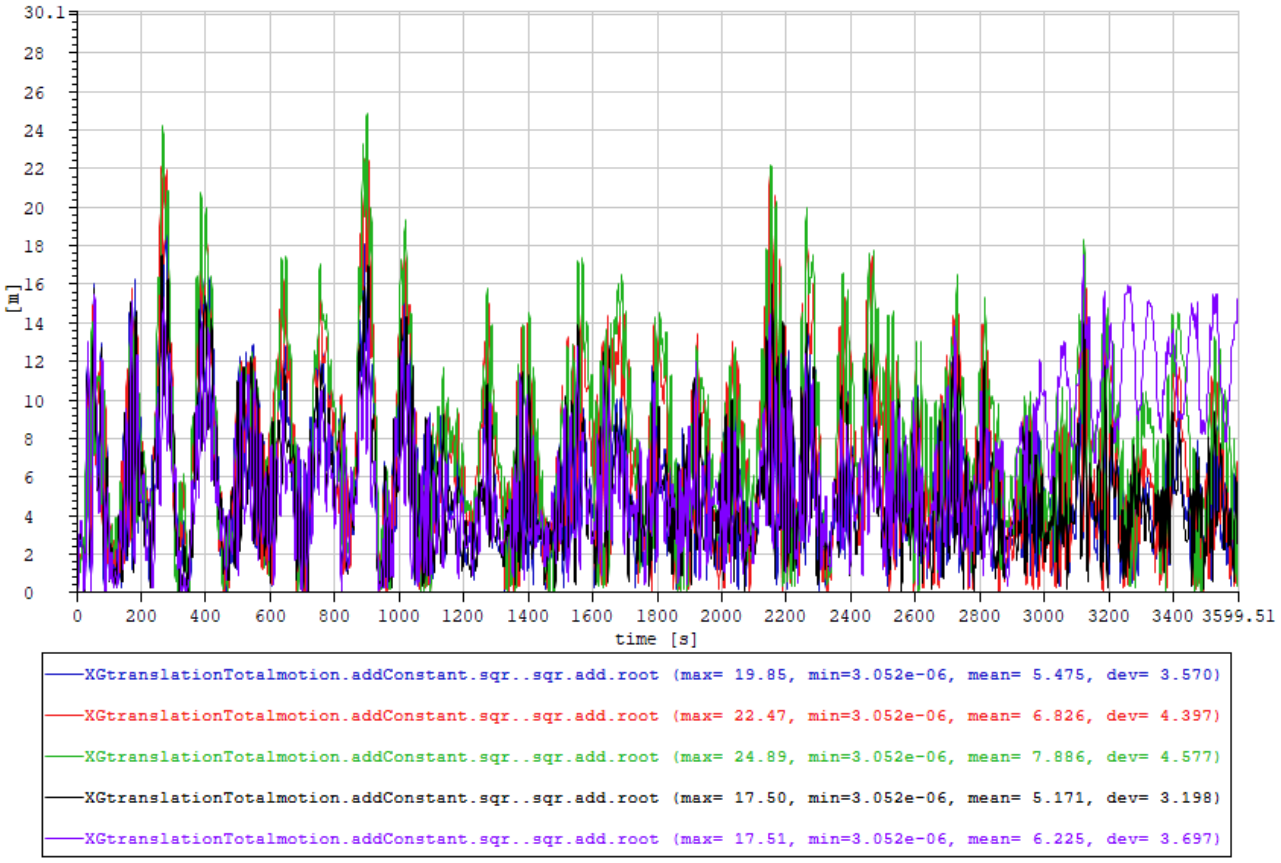

Figure 15 The turret offset for the 5 collinear 100 years environment cases.

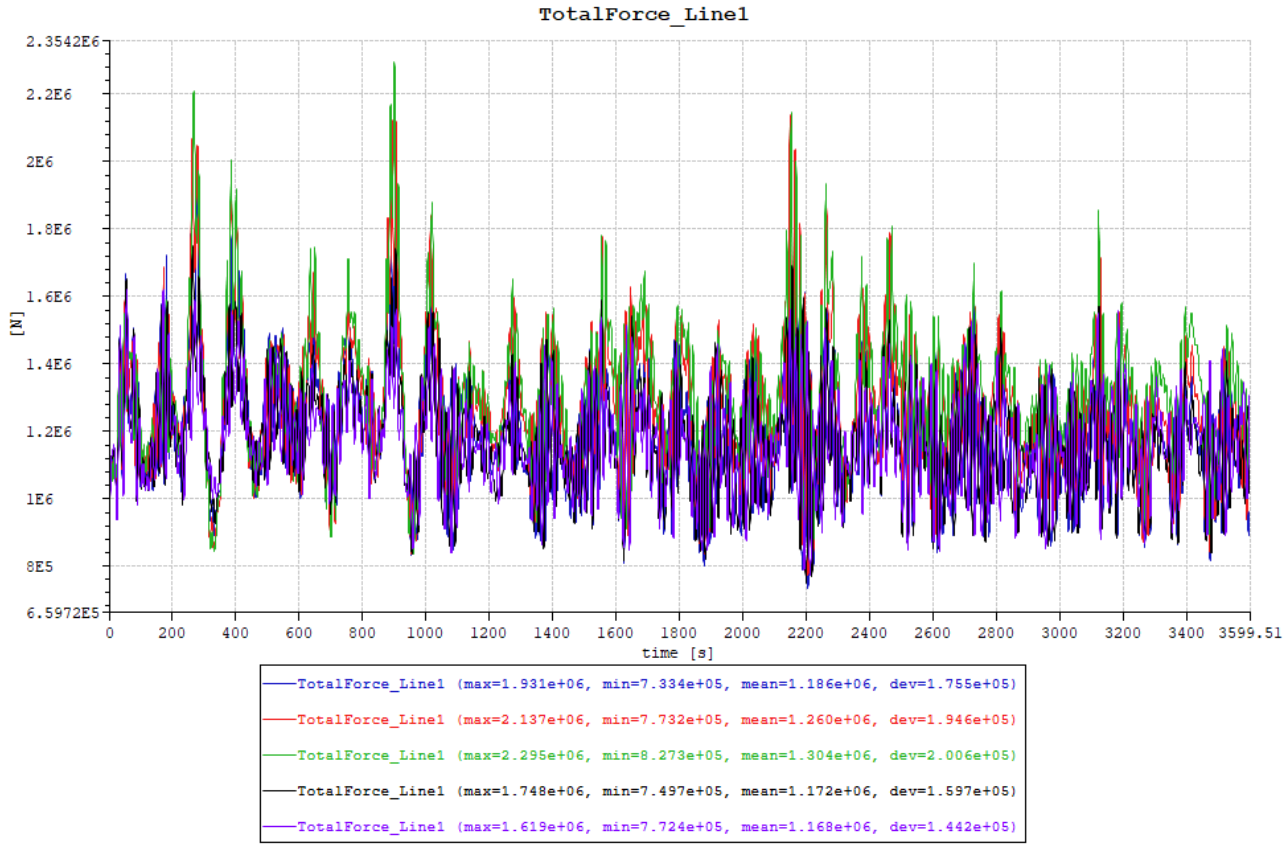

Figure 16 Line tension in the most exposed line for the 5 collinear 100 years environment cases.

7.3 FSO DP footprint in Hs 6m

With the DP operating in both heading, surge and sway, the motion around the mean position can be seen in Figure 17. The largest motions are for case 3 in Table 29 (wind coming 30 deg. to the side of the waves), with offset of ±10m in the surge direction.

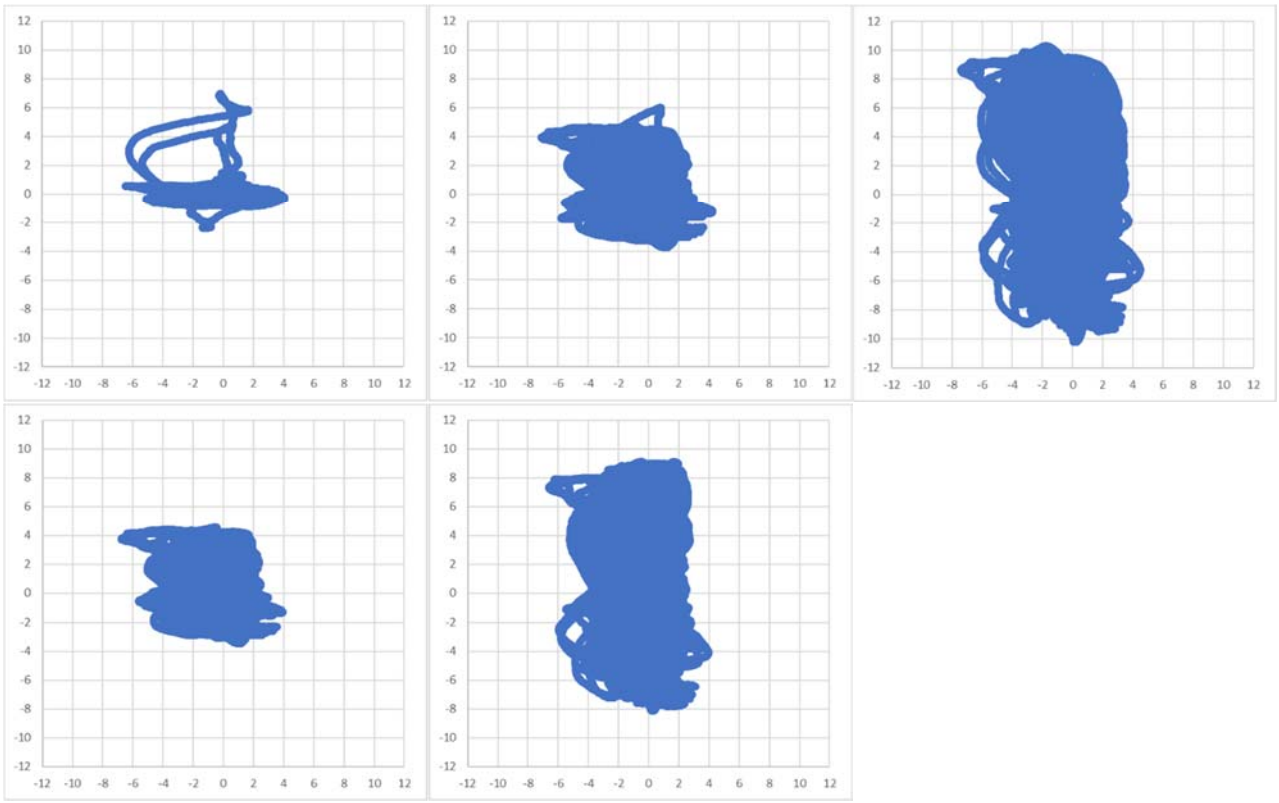

Figure 17 Surge (vertical) and sway (horizontal) motion relative to mean FSO turret position, for all Tp for the five environment cases in Table 29.

7.4 GASVESSEL DP footprint in HS 6m

For the GASVESSEL, the footprints from the operational environment cases are shown in Figure 18. The GASVESSEL is lighter, has smaller wind force, and have a smaller footprint than the FSO.

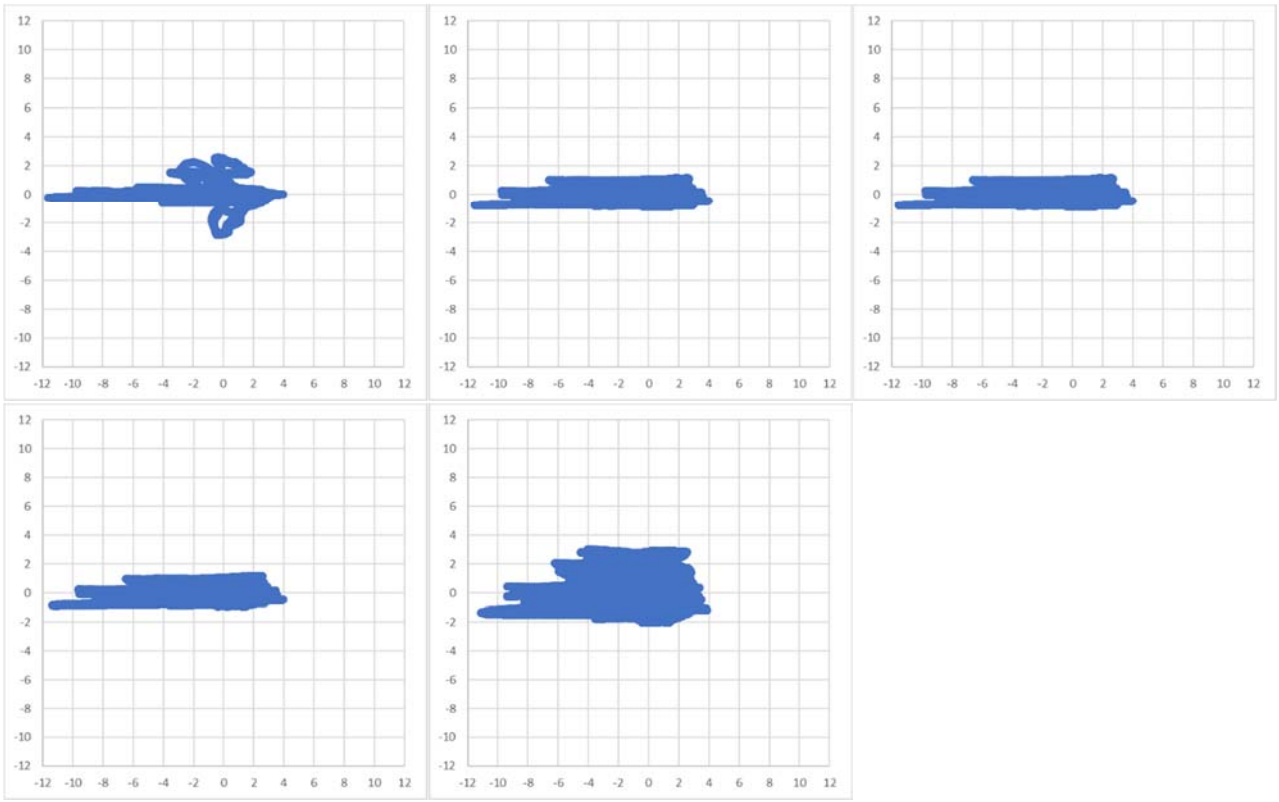

Figure 18 Surge (vertical) and sway (horizontal) motion relative to mean GASVESSEL position, for all Tp for the five environment cases in Table 29.

7.5 FSO and GASVESSEL combined

The FSO and the GASVESSEL was simulated together, and the distance between the coupling points calculated.

Each simulation was 3 hours, and the distance is plotted in Figure 19-Figure 23 for case 1-5 in Table 29 respectively. We make the following observations:

- Case 3, Figure 21, peaks outside the ESD limit at 116.0m for Tp 7s and 117.4m for Tp 8s.
- Case 4, Figure 22, is just outside with 115.4m for Tp 8s.
- The rest are within ESD1 of ±15m

To be inside the sector, the angle between the FSO and the hose must be less than 30 deg. Figure 24 shows the angle for all simulations with operational conditions. There are some peaks, but it is always within the ESD limit.

We conclude that for most environment cases, it is possible to operate in 6m Hs, but for cases with high sway loads it is on the limit that must be checked further.

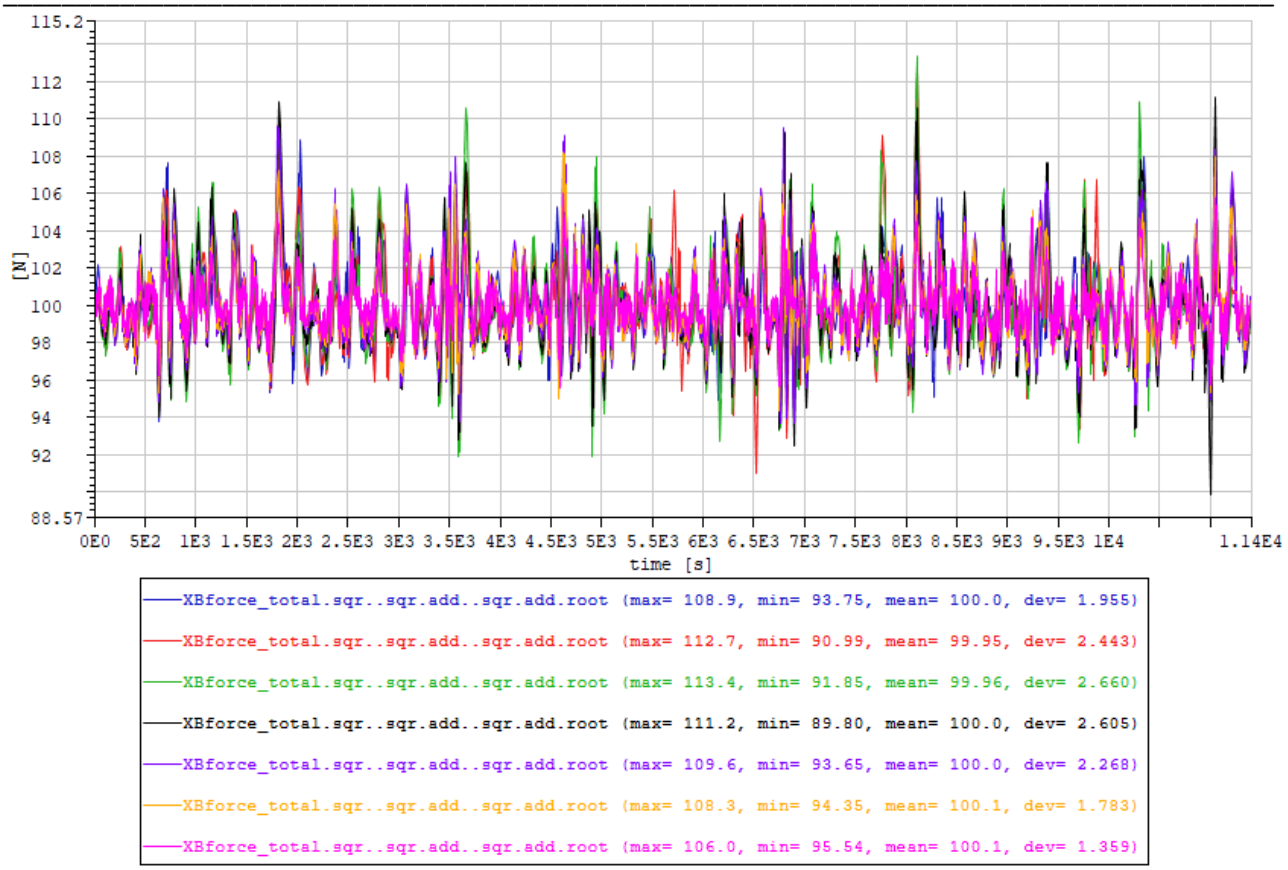

Figure 19 Length between the connection points on the two vessels for the collinear cases, case 1 in Table 29. 3 hours simulations for each Tp.

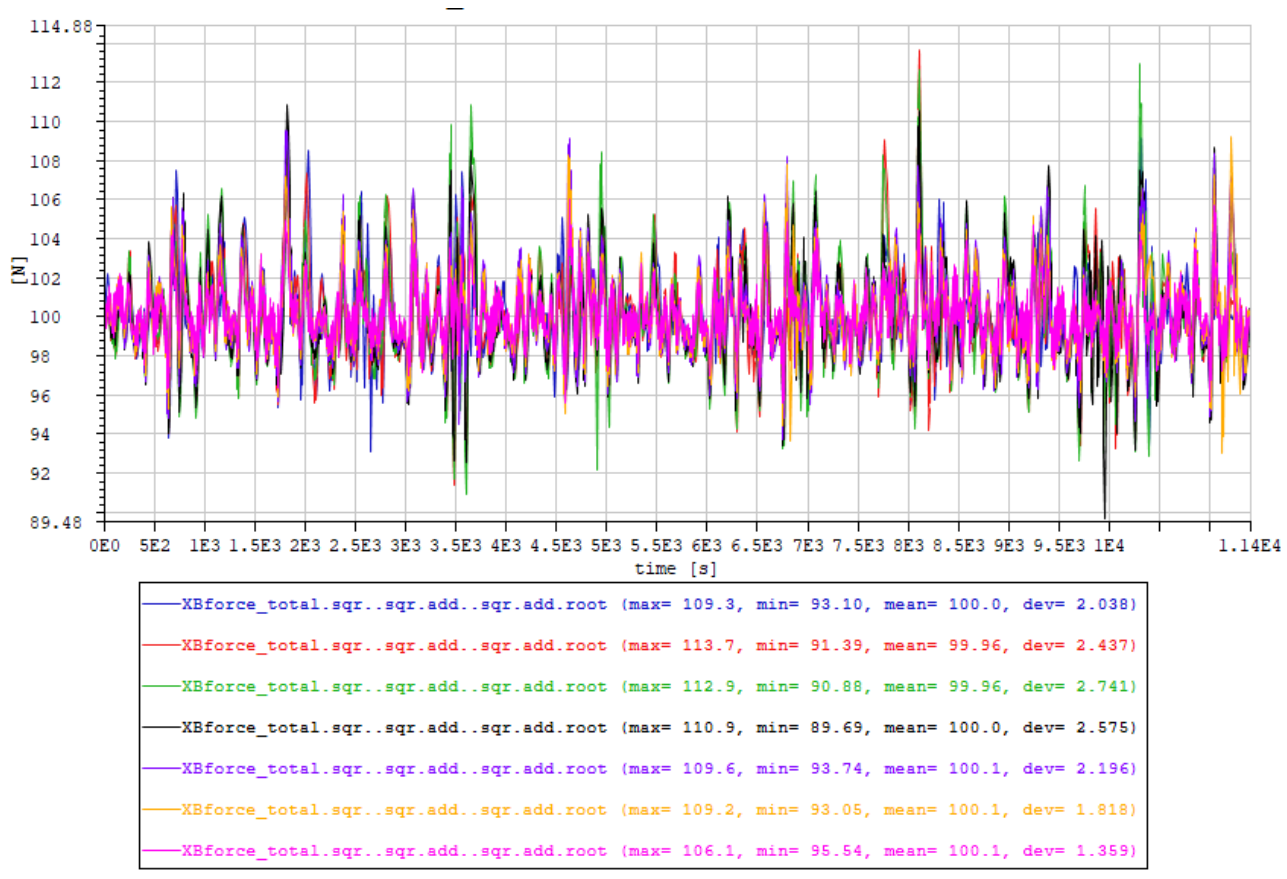

Figure 20 Length between the connection points on the two vessels for case 2 in Table 29.

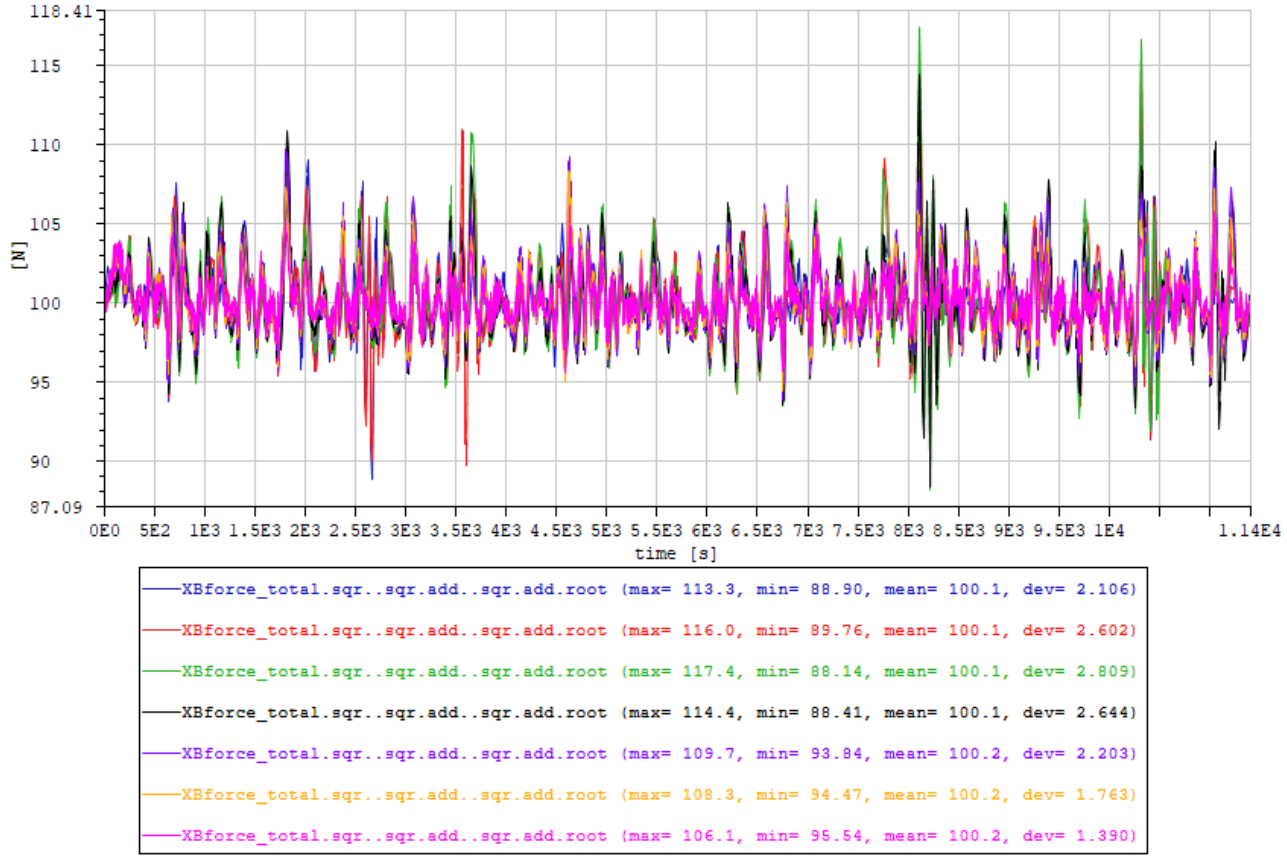

Figure 21 Length between the connection points on the two vessels for case 3 in Table 29.

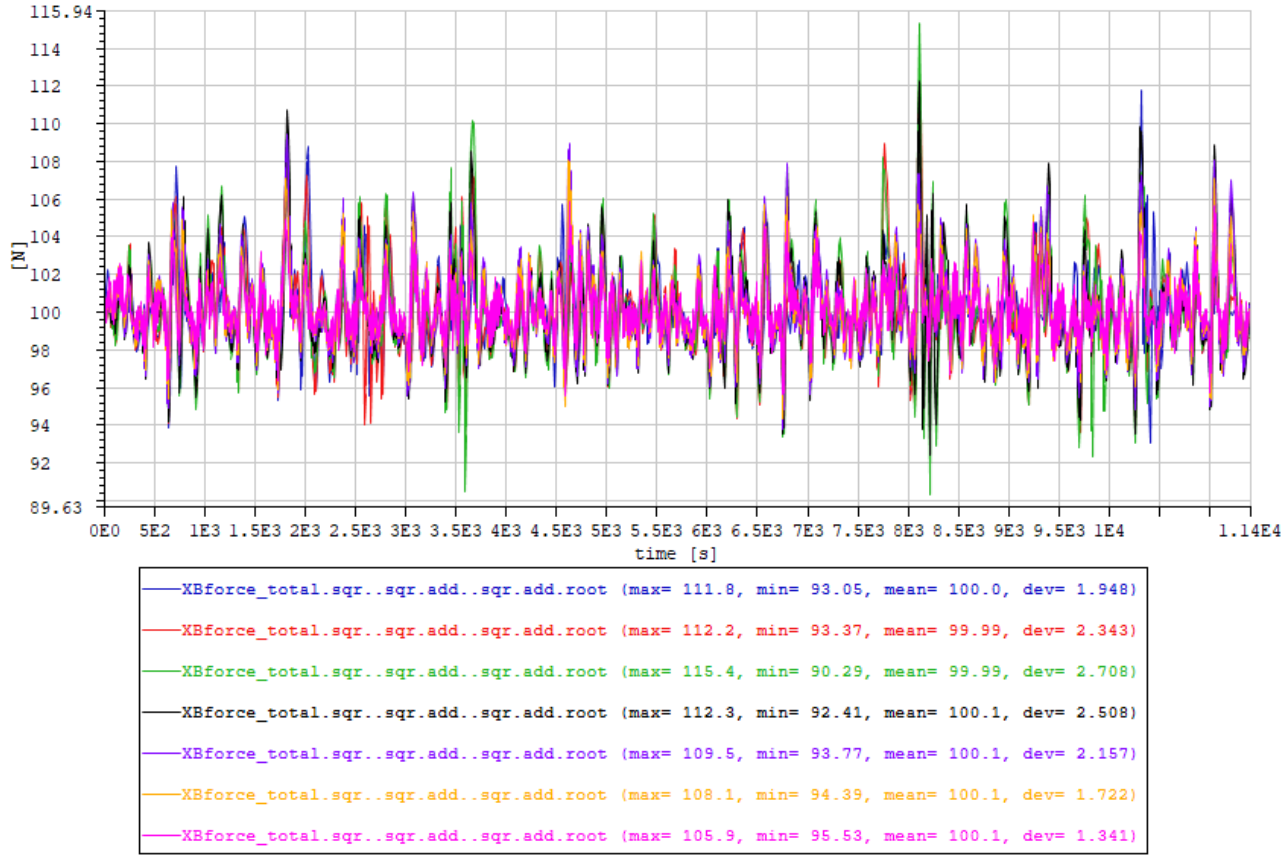

Figure 22 Length between the connection points on the two vessels for case 4 in Table 29.

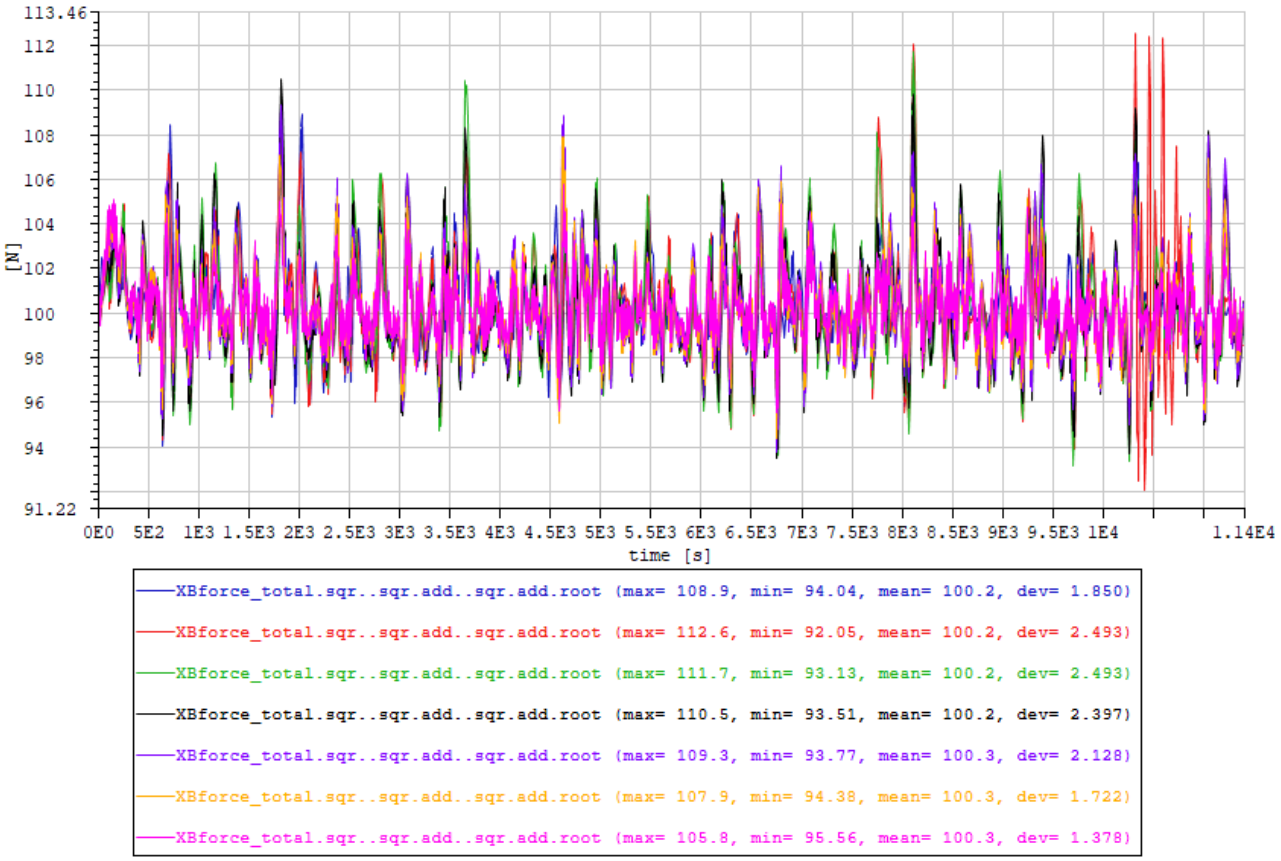

Figure 23 Length between the connection points on the two vessels for case 5 in Table 29.

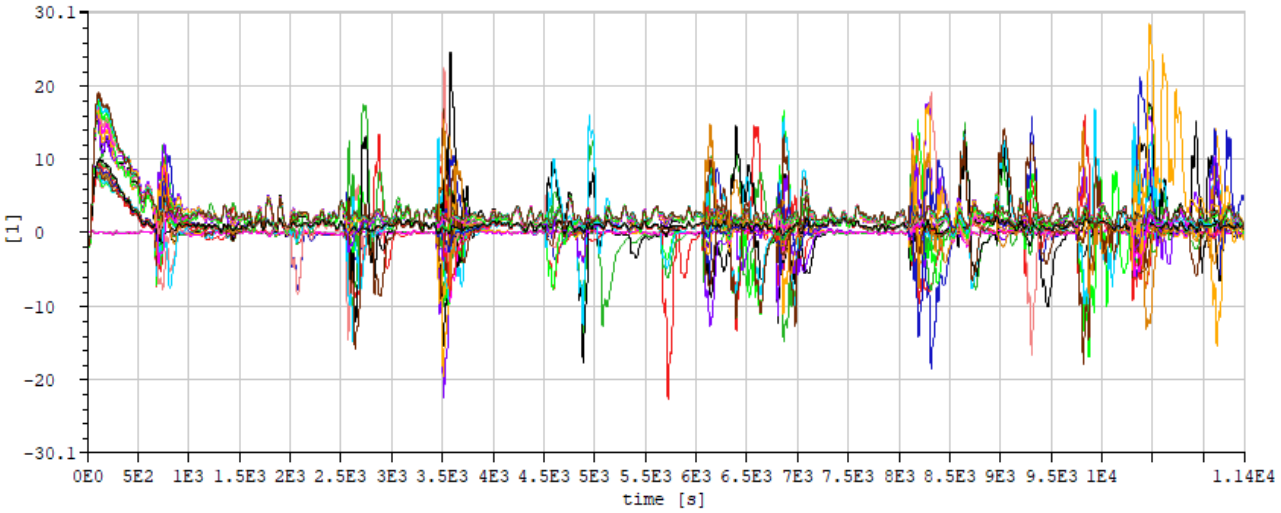

Figure 24 Hose angle behind FSO. The ESD sector is ±30 deg.

Reference

1. Yin, D., et al., *On the Design Considerations of New Offloading Hose Applied on a Turret Moored FPSO*, in *ASME 2017 36th International Conference on Ocean, Offshore and Arctic Engineering*. 2017: Trondheim, Norway.
2. Angelini, S., *GASVESSEL Deliverable No. D1.2 - Project Management Plan*. 2017.
3. Droushiotis, N., *GASVESSEL Deliverable NO. D2.1 - Scenario - Description and Characterization.* 2018.
4. Twomey, B., *Decommissioning process*, in *Presentation at CCOP/EPPM Workshop on End of Concession*. 2012.
5. Navalprogetti, *Drawing: 833-5.1B-0-002-A03 General Arrangement.dwg.* 2019.
6. Navalprogetti, *Drawing: WP5-D5.1-RV0-833-0-XXX-A01 B-Ship General Arrangement IN PROGRESS.dwg*. 2019.
7. Perosa, O., *Email from Oscar Perosa (Navalprogetti) to Decao Yin (SINTEF Ocean): RE: H2020-723030 GASVESSEL WP5 T5.2 Seakeeping tank tests*. 2019
8. Navalprogetti, *Drawing: Horizon 2020 723030 GASVESSEL Bow Thruster Grid*. 2019.
9. Navalprogetti, *Drawing: Horizon 2020 Propulsor Preliminary Arrangement*. 2018.
10. Perosa, O., *Email from Oscar Perosa (Navalprogetti) to Decao Yin (SINTEF Ocean) and Halvor Lie (SINTEF Ocean): RE: H2020 – Gasvessel 723030 – WP6 - RE: GASVESSEL: Technical meeting in Trieste*. 2019.
11. Lie, H., *Email from Halvor Lie (SINTEF Ocean) to Sukjoo Choi (Genesi Oil and Gas) and Djoni Sidarta (TechnipFMC): Inquiry of flexible riser data.* 2019.
12. D'All, B., *Email from Bill D'All (TechnipFMC) to Halvor Lie (SINTEF Ocean): RE: Inquiry of flexible riser data*. 2019.
13. MIB, *Emergency release systems*.
14. MIB, *Drawing: 330 barg DBV + QCDC INTEGRATED SYSTEM*.
15. TechnipFMC. *STRUCTURE 2.7 - TECHNICAL DATA SHEET REFERENCE FROM 355.20224 REV.0 INDATABASE SINCE 15/05/2019*. 2019 May 15.
16. Hoff, J., *Vessel hydrodynamic coefficients and motion RAOs*. 2019, SINTEF Ocean.
17. *Wind tunnel tests of gas carrier*. 2018, KRYLOV STATE RESEARCH CENTRE: St. Petersburg.
18. *Non-dimensional coefficients of hydrodynamic force*. 2019, CNG SHIP.

Appendix

A. Dynamic hose sensitivity study results presented in figures.

a. Round 1

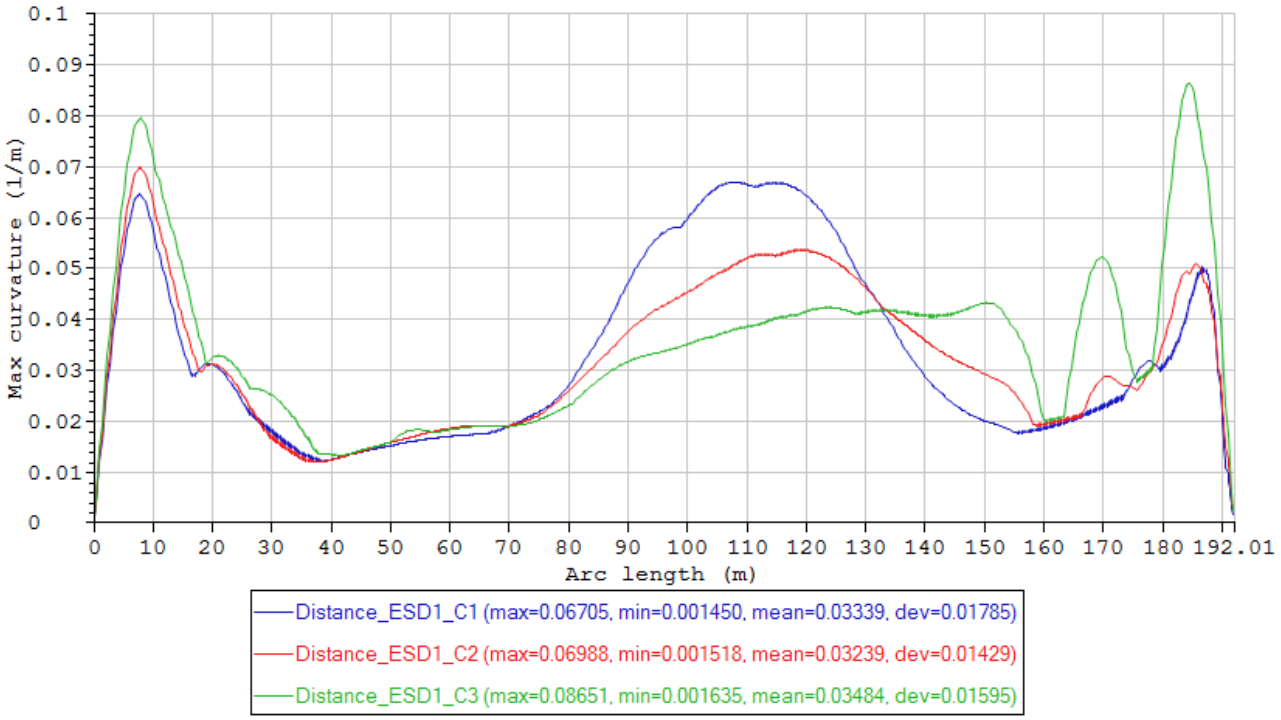

Figure 25 Maximum curvature envelope curves of the cases in Condition set - Distance_ESD1 (Table 15).

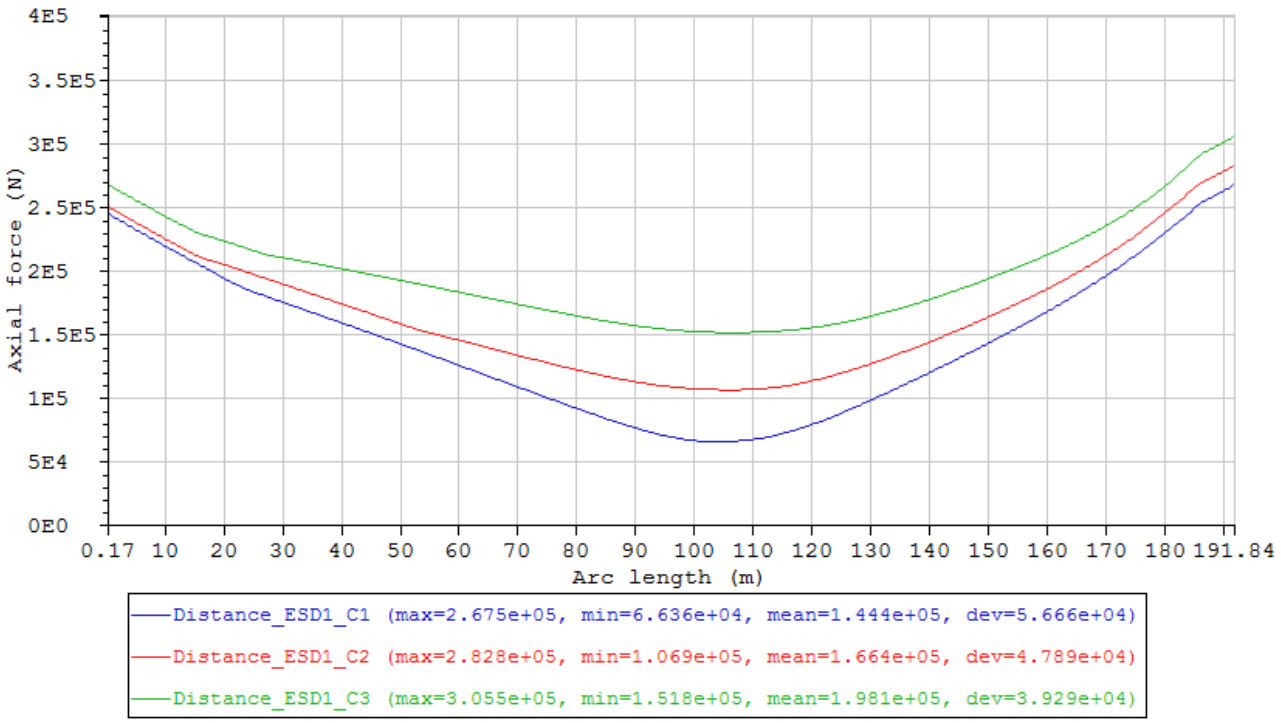

Figure 26 Maximum axial force envelope curves of the cases in Condition set - Distance_ESD1 (Table 15).

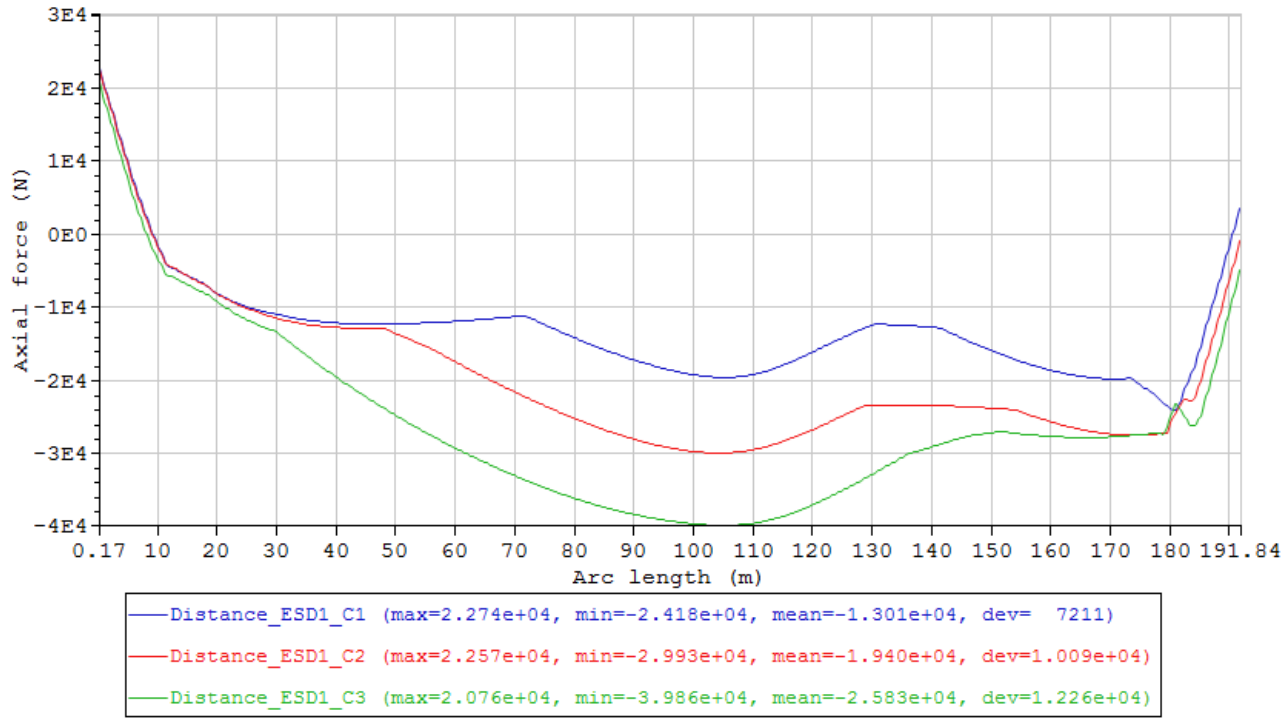

Figure 27 Minimum axial force envelope curves of the cases in Condition set - Distance_ESD1 (Table 15).

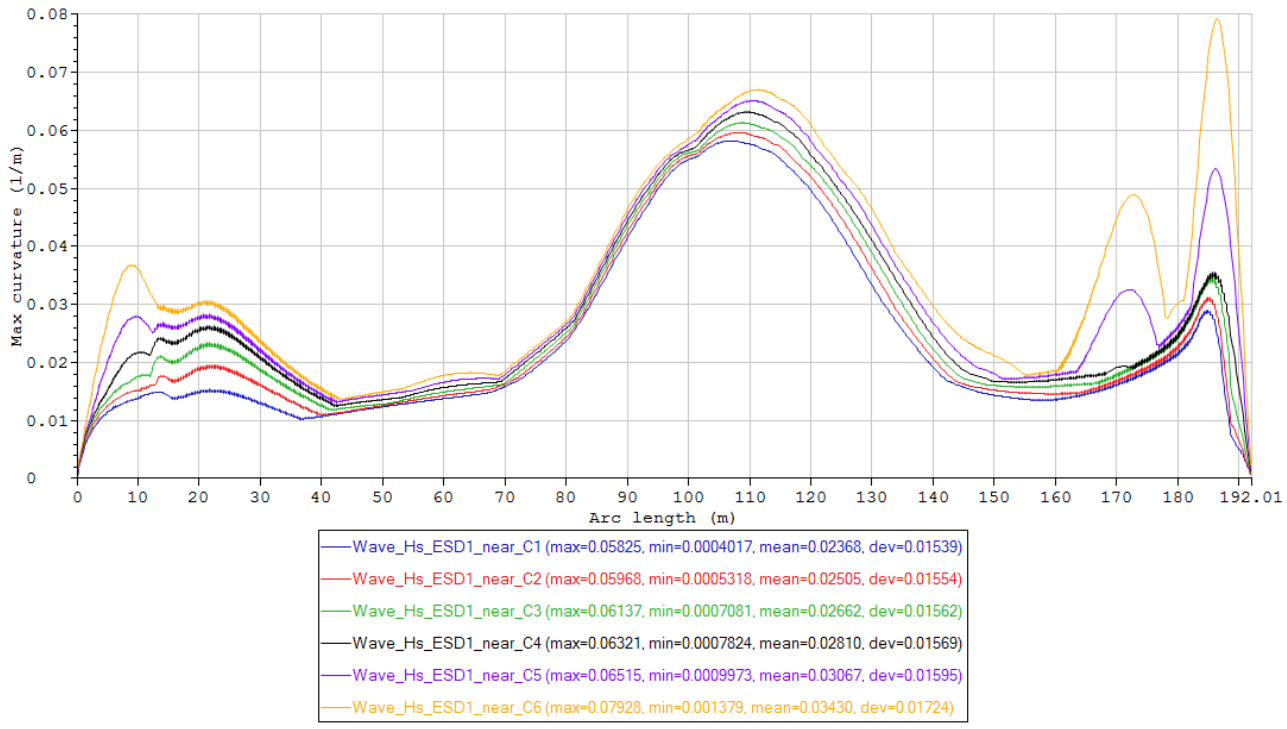

Figure 28 Maximum curvature envelope curves of the cases in Condition set – Wave_Hs_ESD1_near (Table 15).

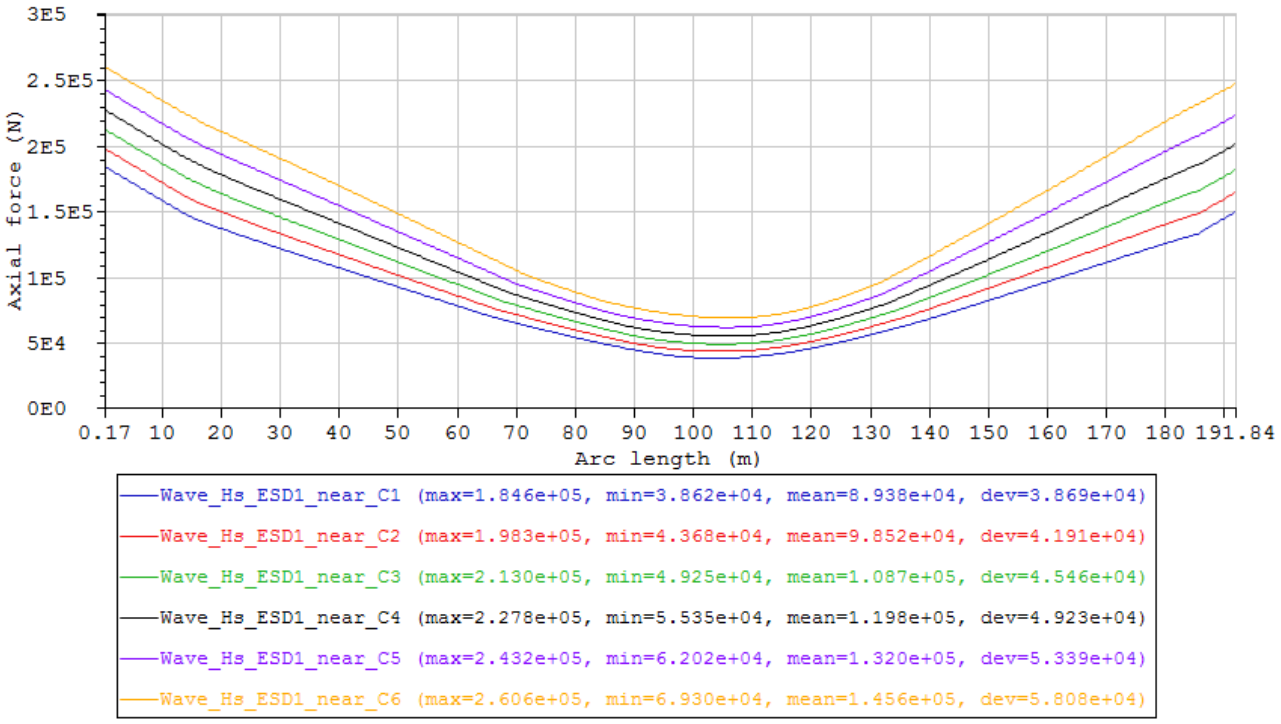

Figure 29 Maximum axial force envelope curves of the cases in Condition set – Wave_Hs_ESD1_near (Table 15).

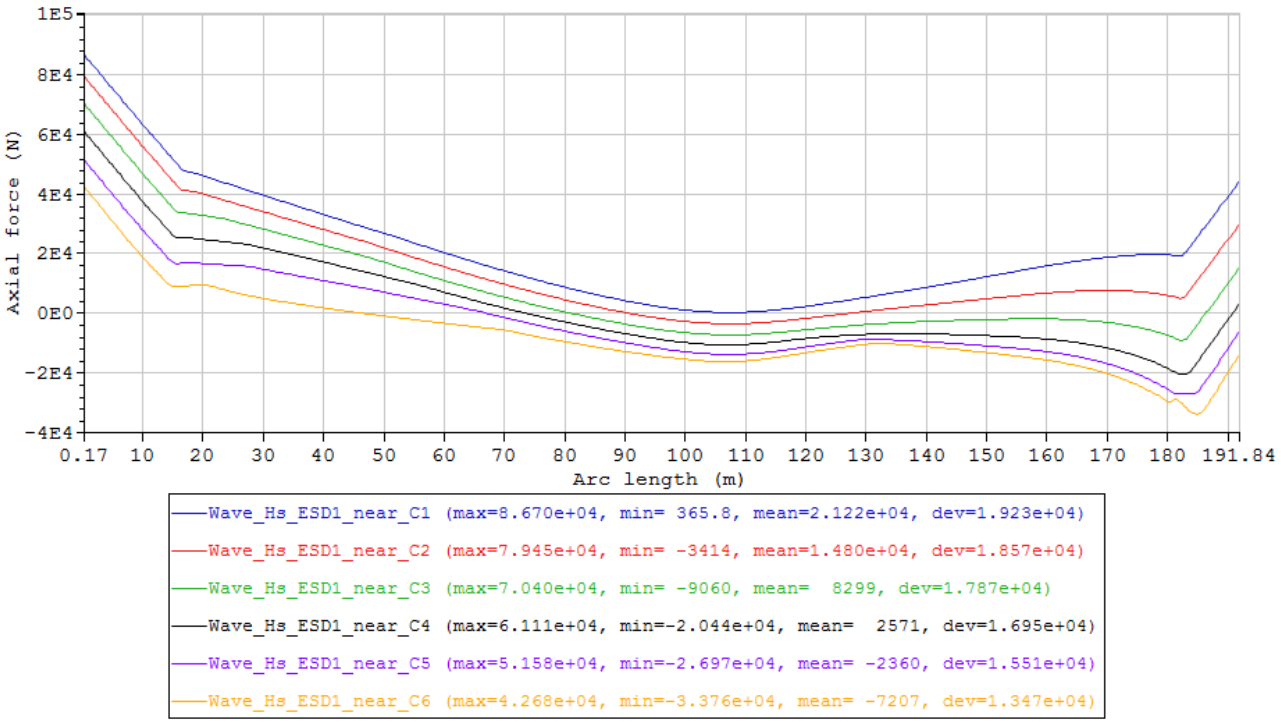

Figure 30 Minimum axial force envelope curves of the cases in Condition set – Wave_Hs_ESD1_near (Table 15).

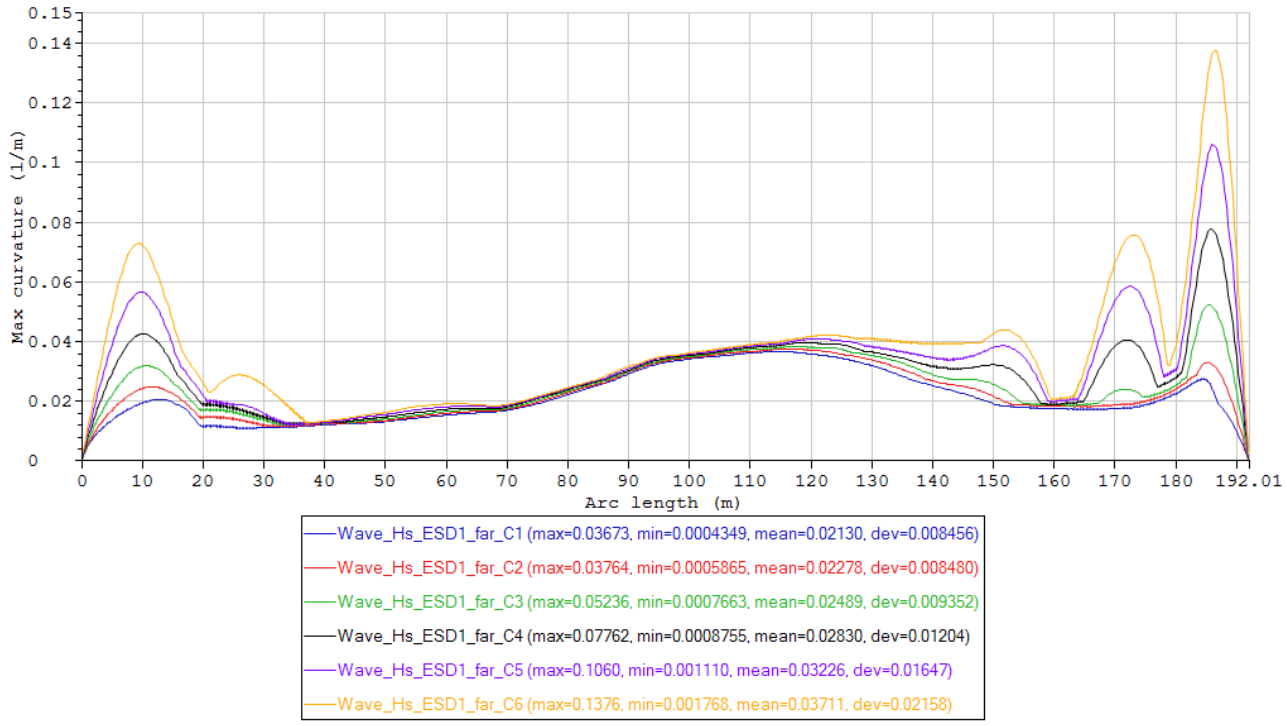

Figure 31 Maximum curvature envelope curves of the cases in Condition set – Wave_Hs_ESD1_far (Table 15).

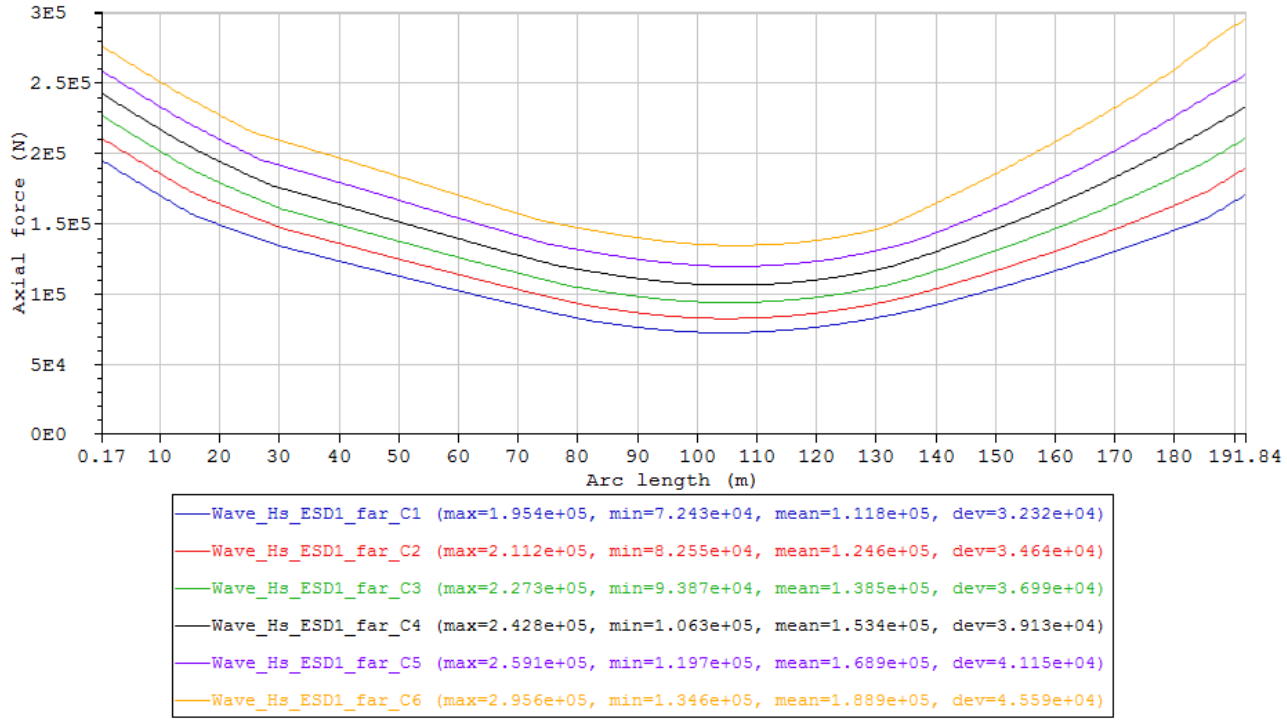

Figure 32 Maximum axial force envelope curves of the cases in Condition set – Wave_Hs_ESD1_far (Table 15).

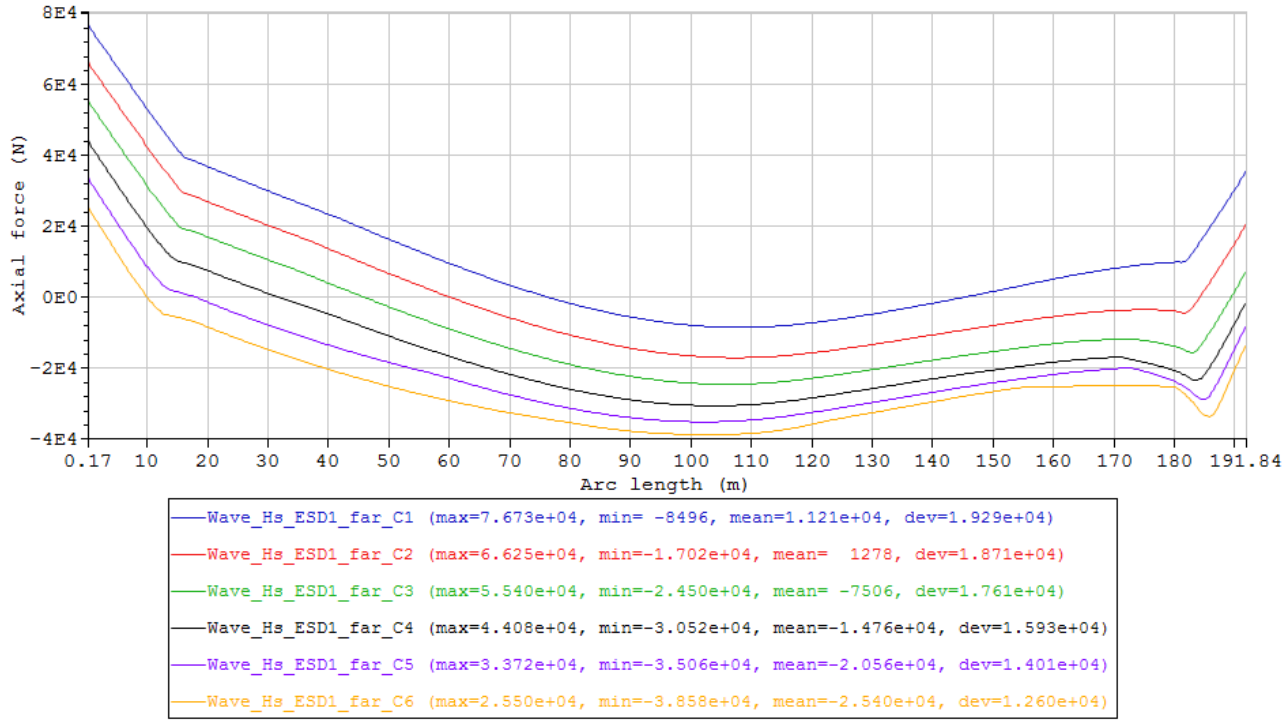

Figure 33 Minimum axial force envelope curves of the cases in Condition set – Wave_Hs_ESD1_far (Table 15).

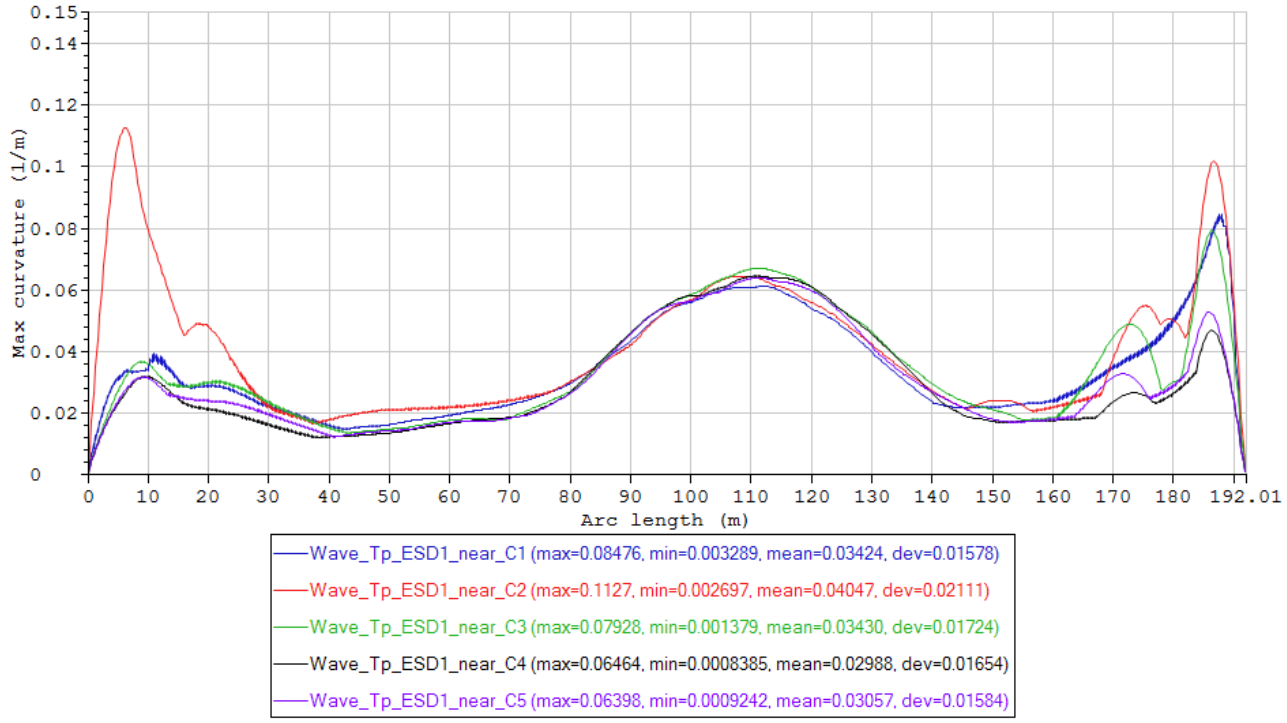

Figure 34 Maximum curvature envelope curves of the cases in Condition set – Wave_Tp_ESD1_near (Table 15).

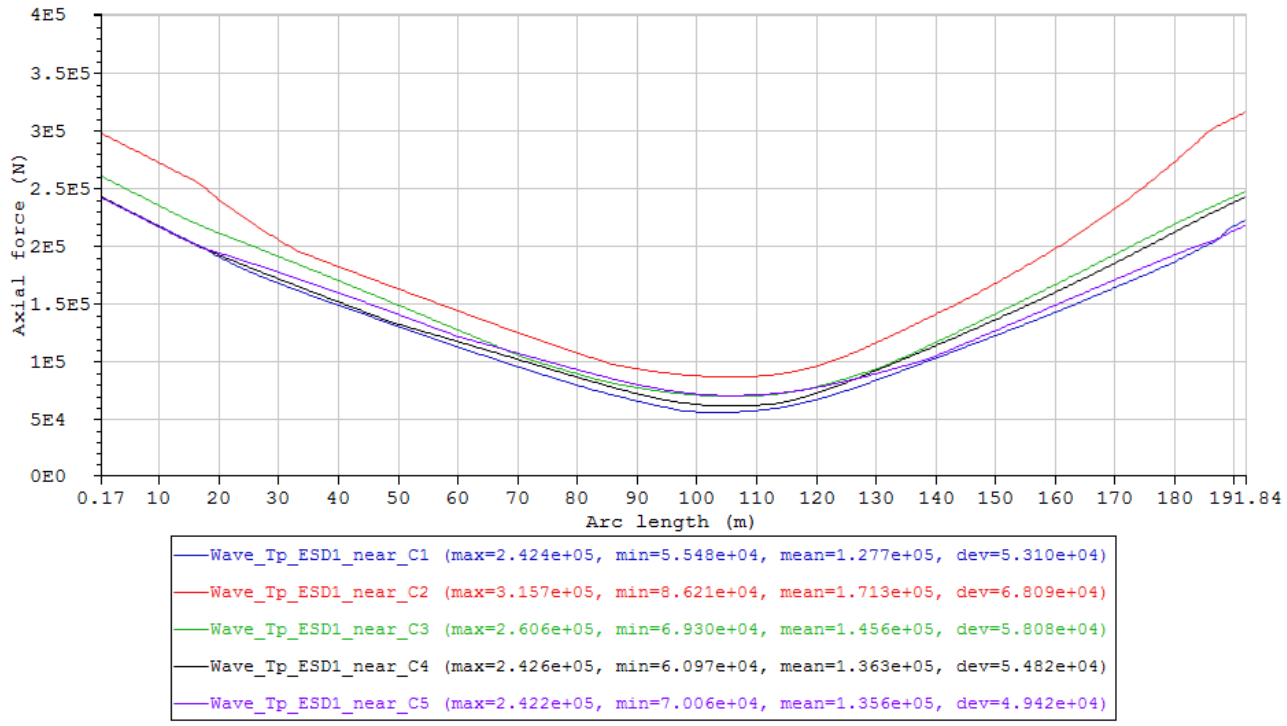

Figure 35 Maximum axial force envelope curves of the cases in Condition set – Wave_Tp_ESD1_near (Table 15).

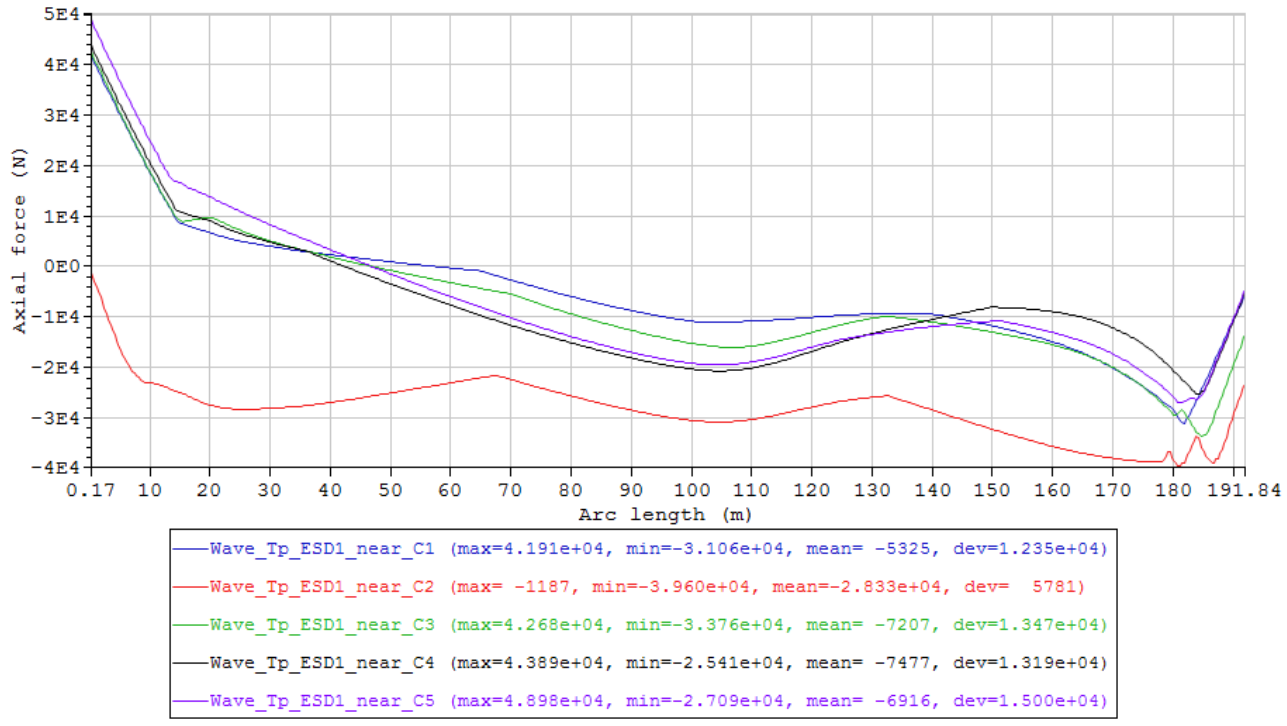

Figure 36 Minimum axial force envelope curves of the cases in Condition set – Wave_Tp_ESD1_near (Table 15).

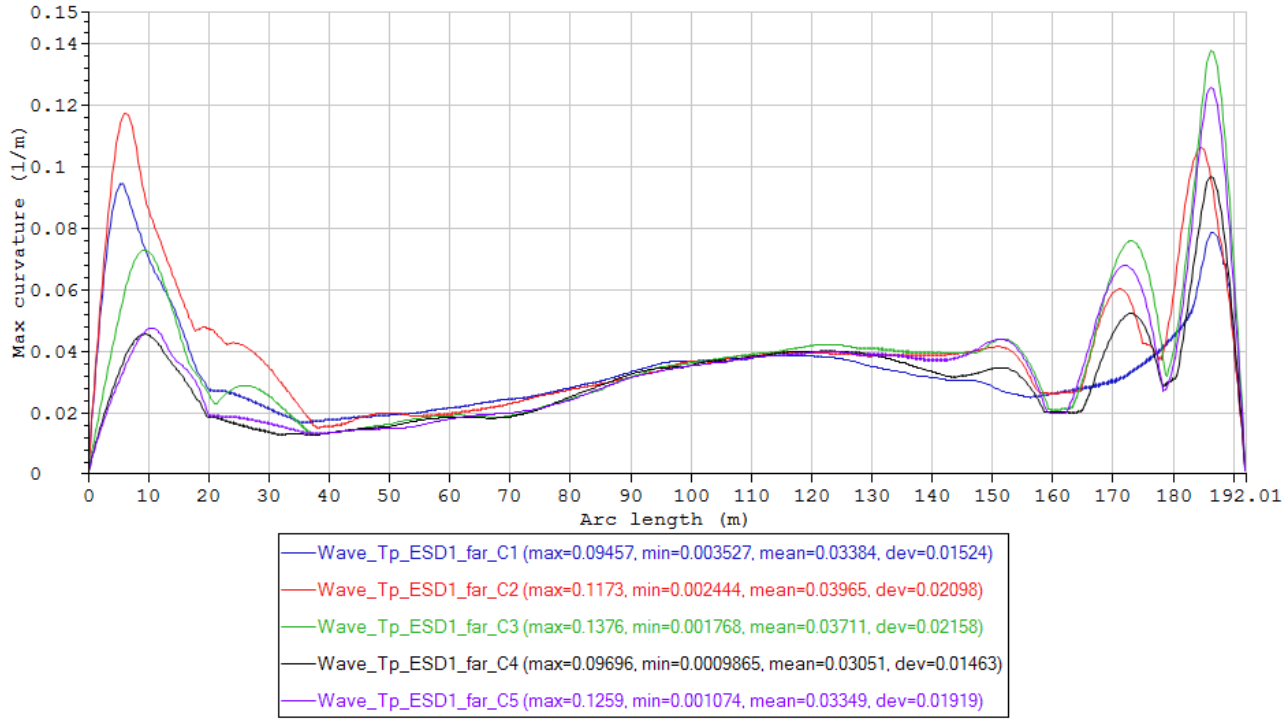

Figure 37 Maximum curvature envelope curves of the cases in Condition set – Wave_Tp_ESD1_far (Table 15).

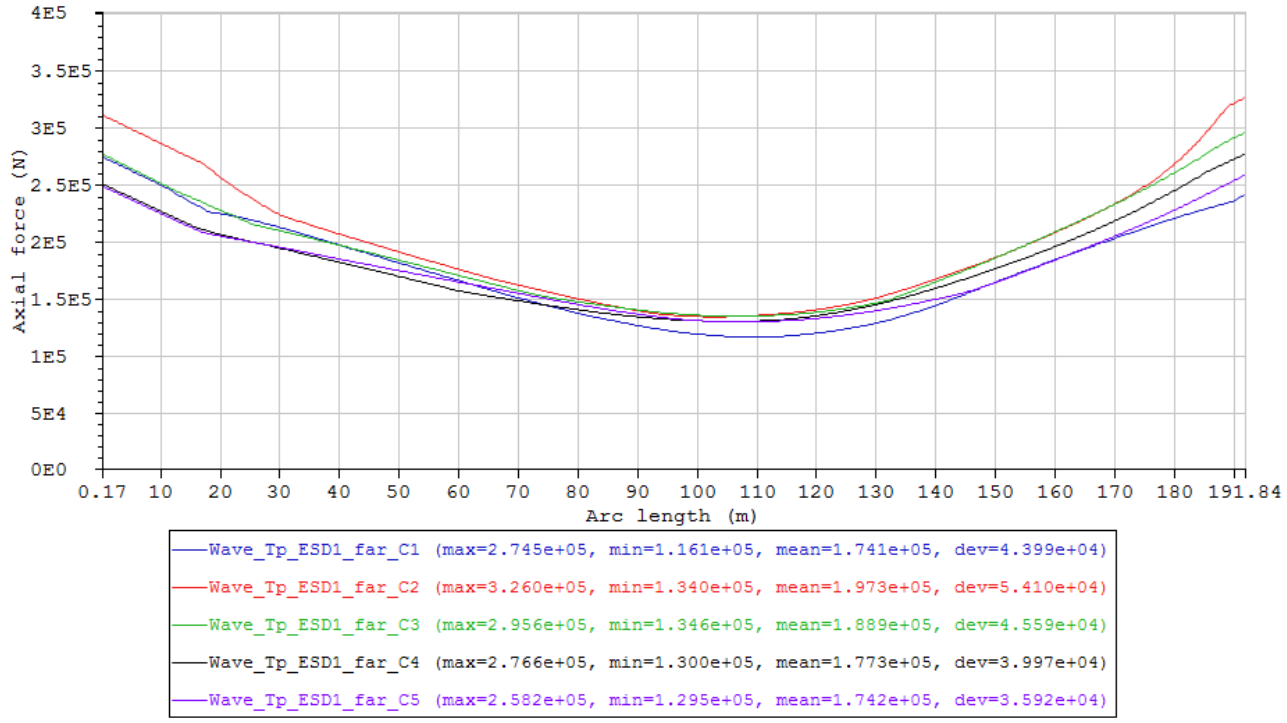

Figure 38 Maximum axial force envelope curves of the cases in Condition set – Wave_Tp_ESD1_far (Table 15).

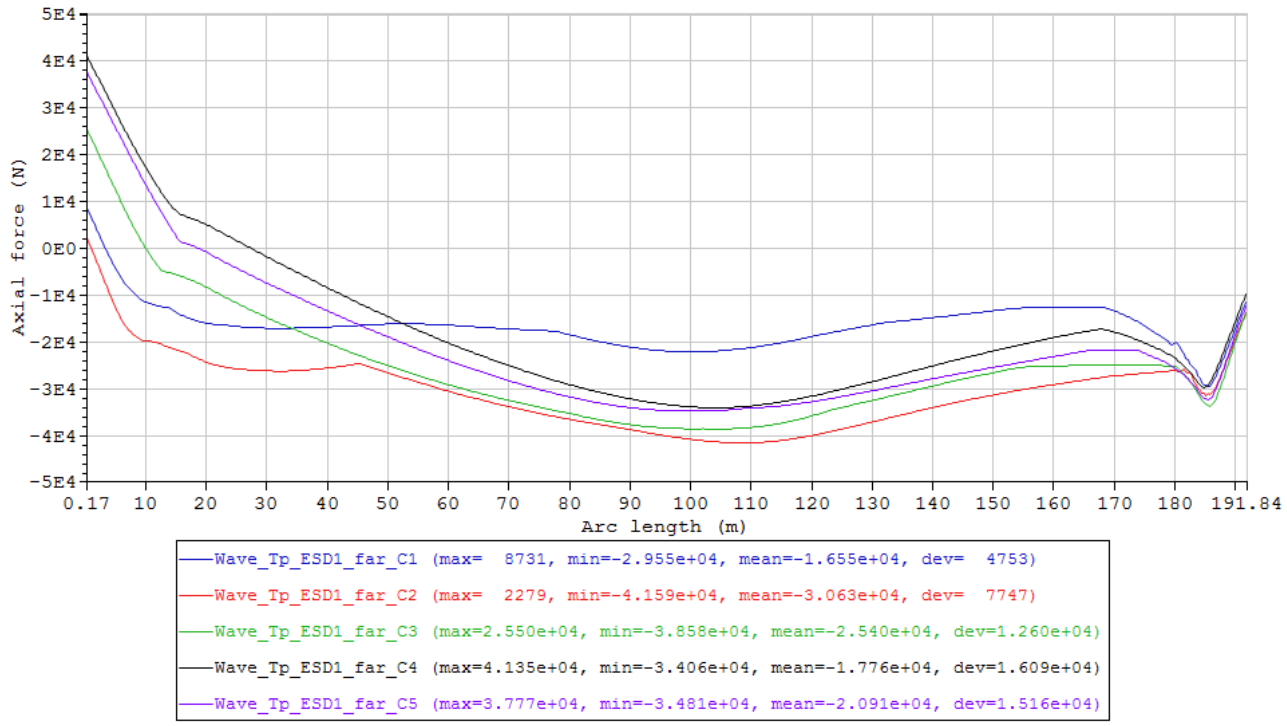

Figure 39 Minimum axial force envelope curves of the cases in Condition set – Wave_Tp_ESD1_far (Table 15).

b. Round 2

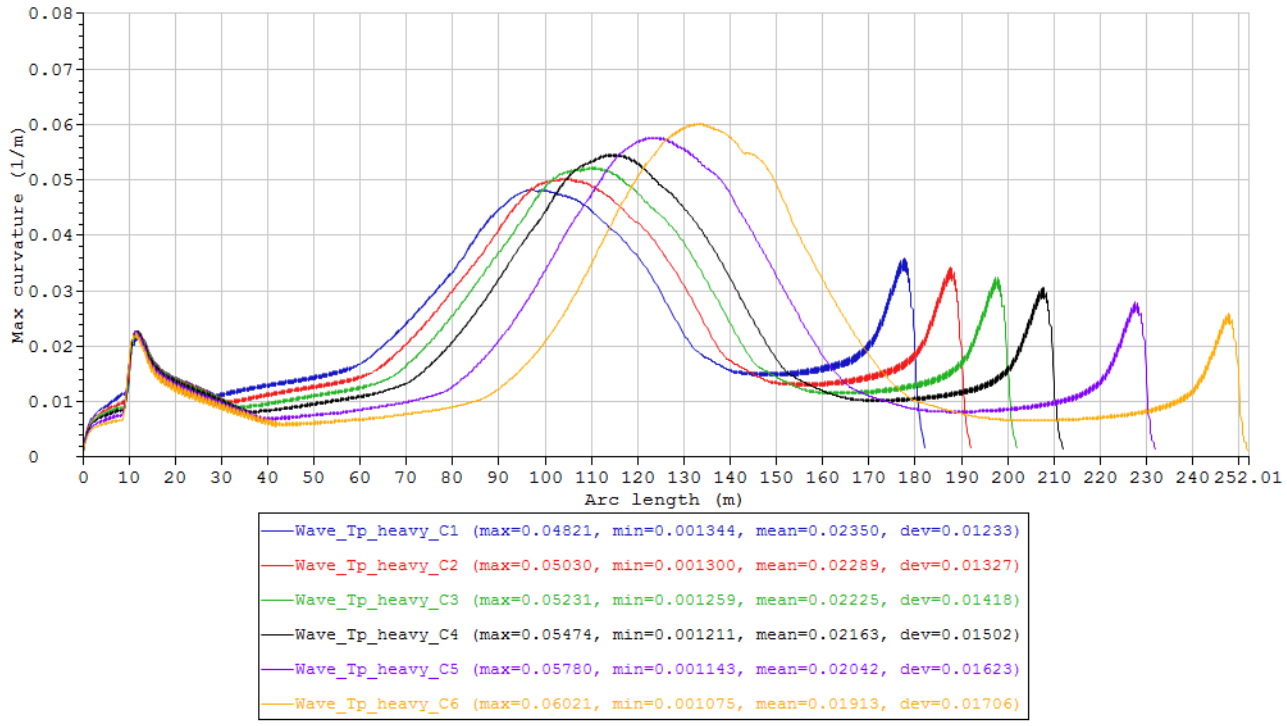

Figure 40 Maximum curvature envelope curves of the cases in Condition set – Wave_Tp_heavy (Table 17).

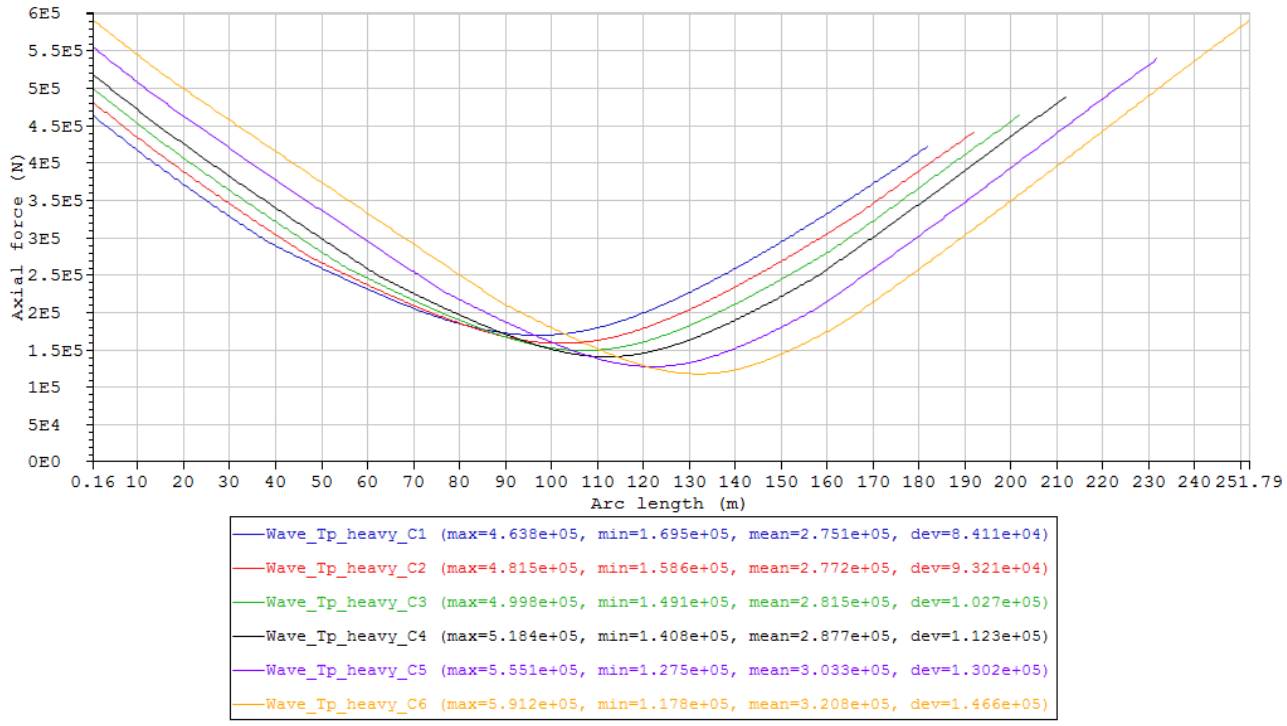

Figure 41 Maximum axial force envelope curves of the cases in Condition set – Wave_Tp_heavy (Table 17).

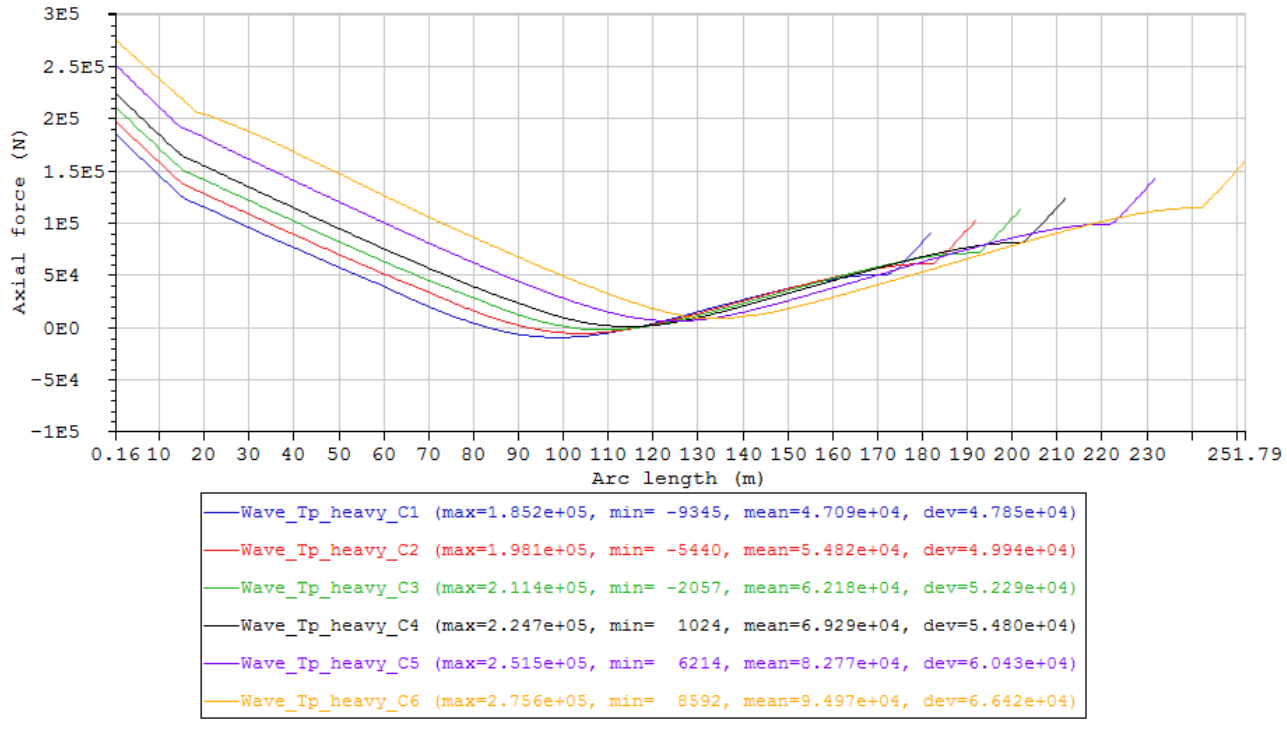

Figure 42 Minimum axial force envelope curves of the cases in Condition set – Wave_Tp_heavy (Table 17).

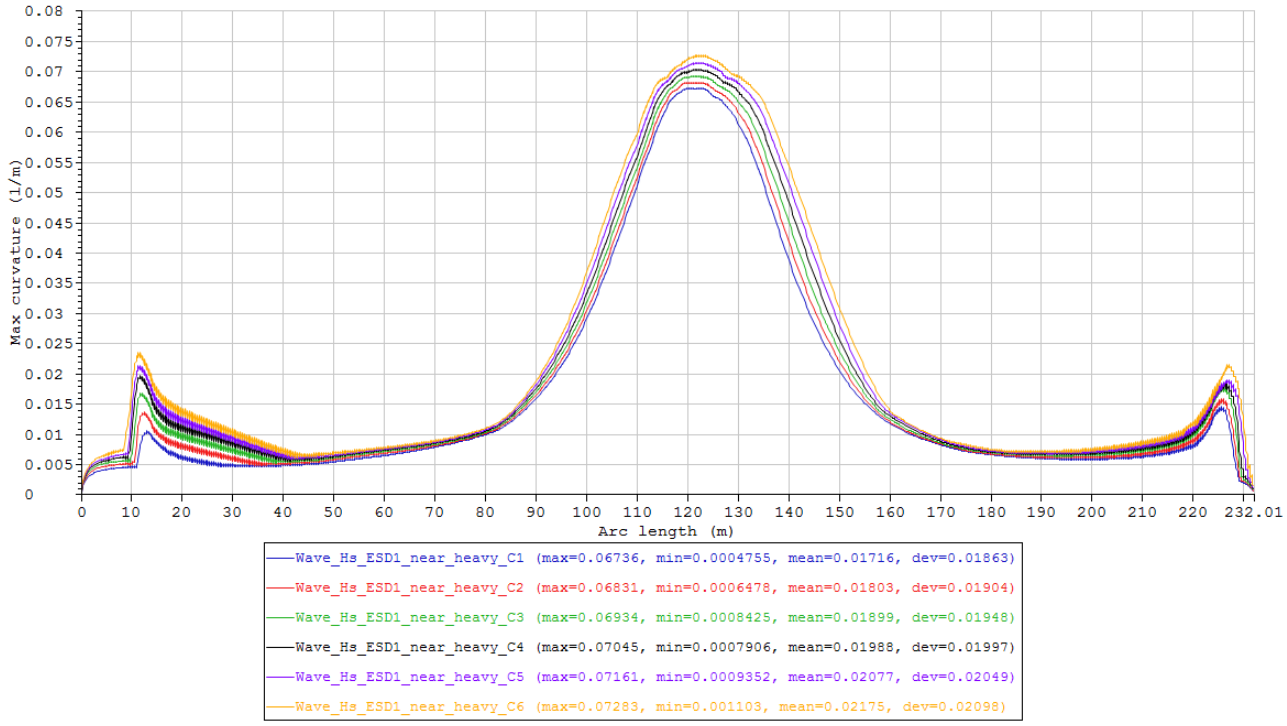

Figure 43 Maximum curvature envelope curves of the cases in Condition set – Wave_Hs_ESD1_near_heavy (Table 17).

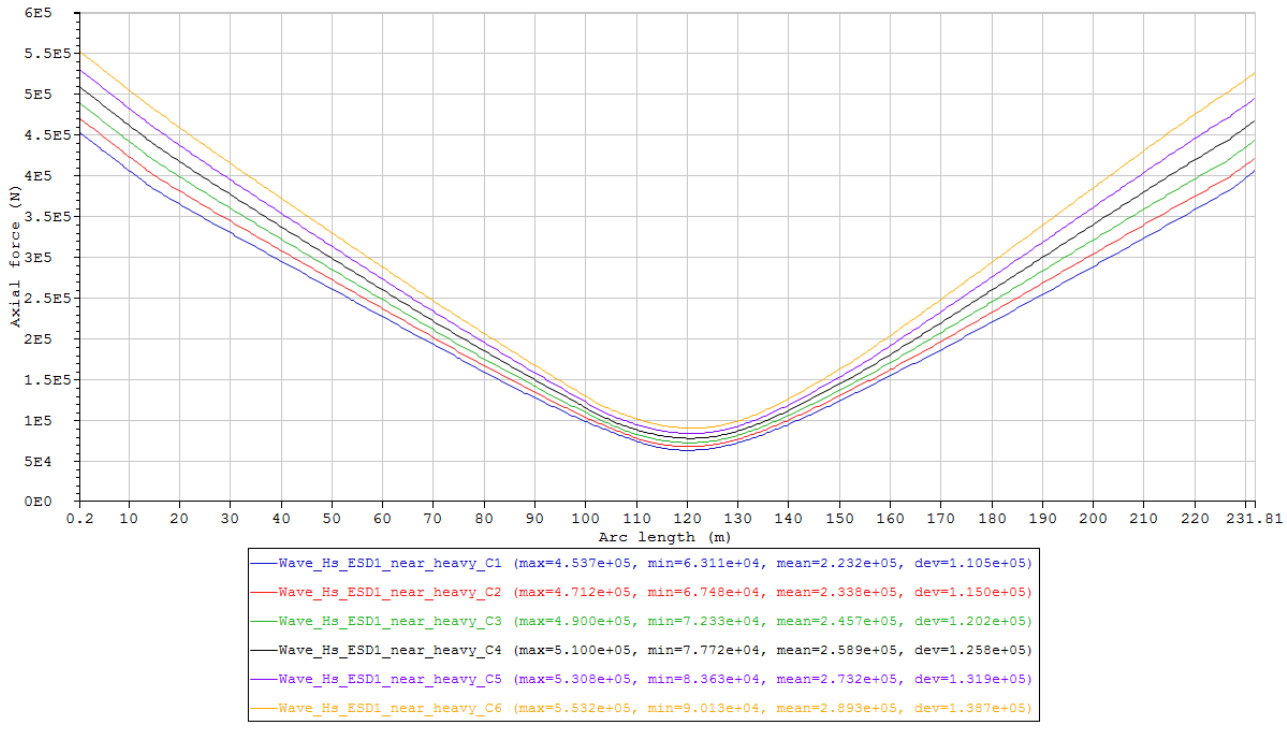

Figure 44 Maximum axial force envelope curves of the cases in Condition set – Wave_Hs_ESD1_near_heavy (Table 17).

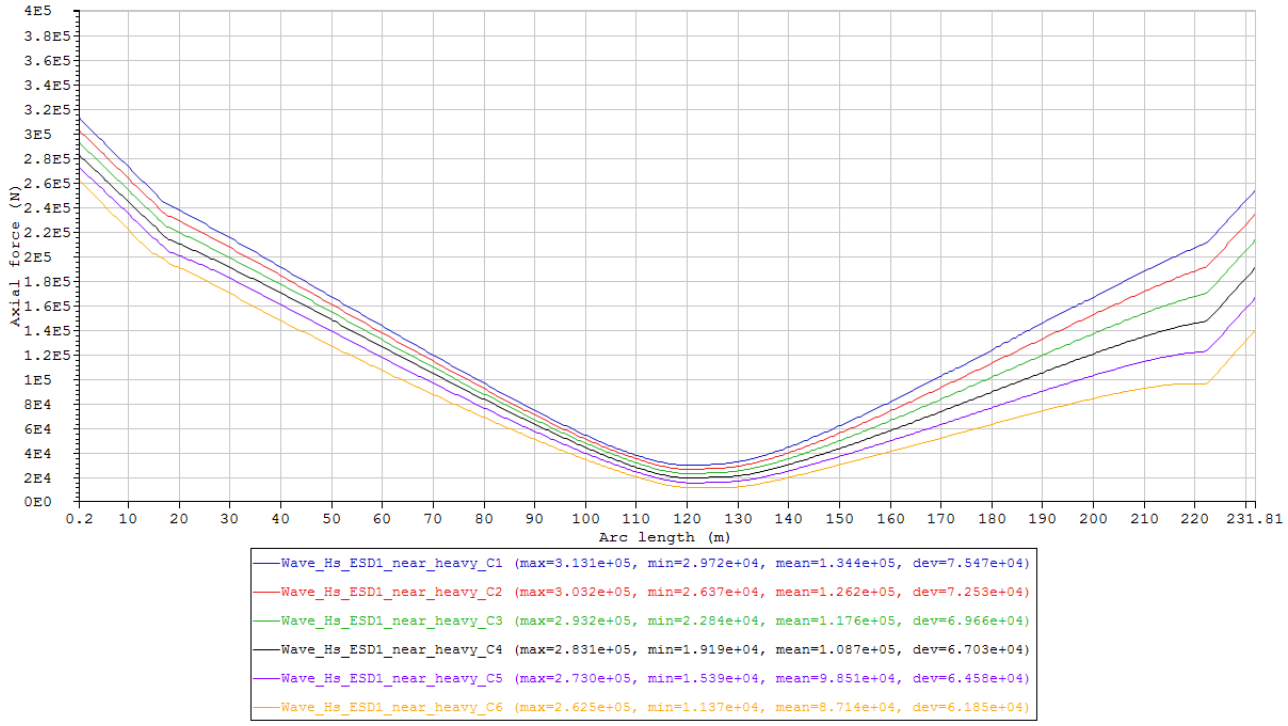

Figure 45 Minimum axial force envelope curves of the cases in Condition set – Wave_Hs_ESD1_near_heavy (Table 17).

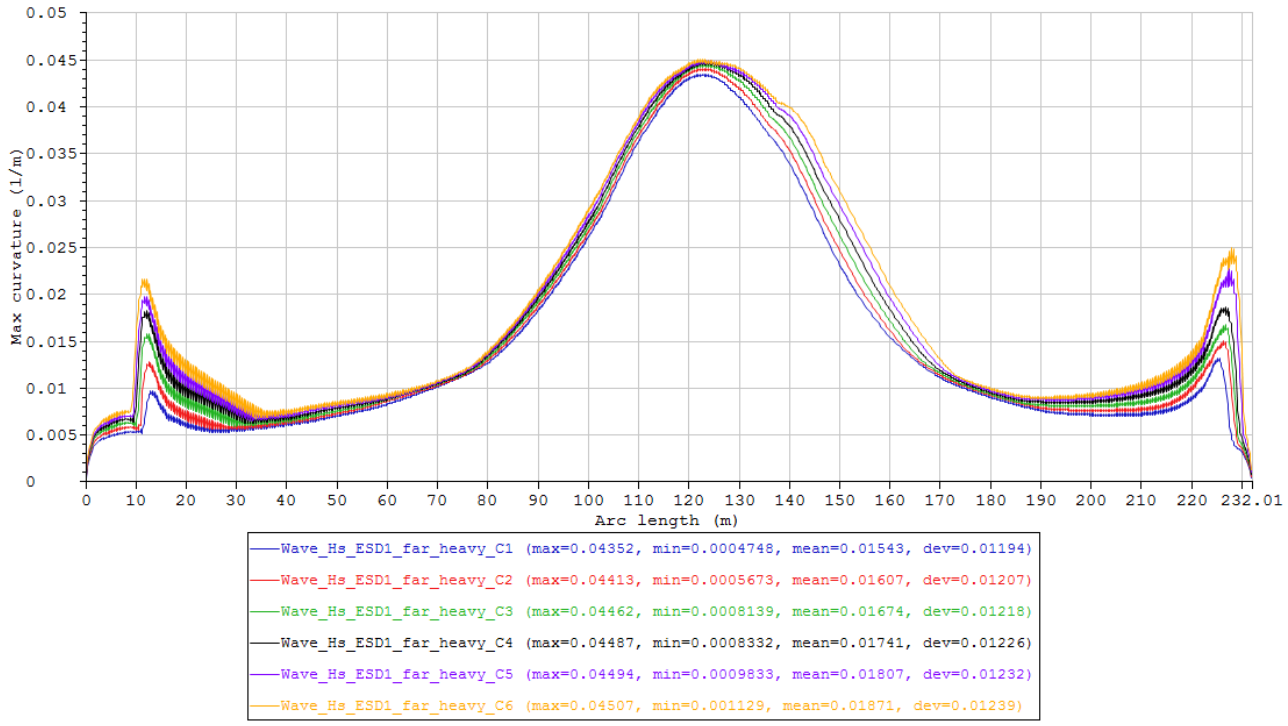

Figure 46 Maximum curvature envelope curves of the cases in Condition set – Wave_Hs_ESD1_far_heavy (Table 17).

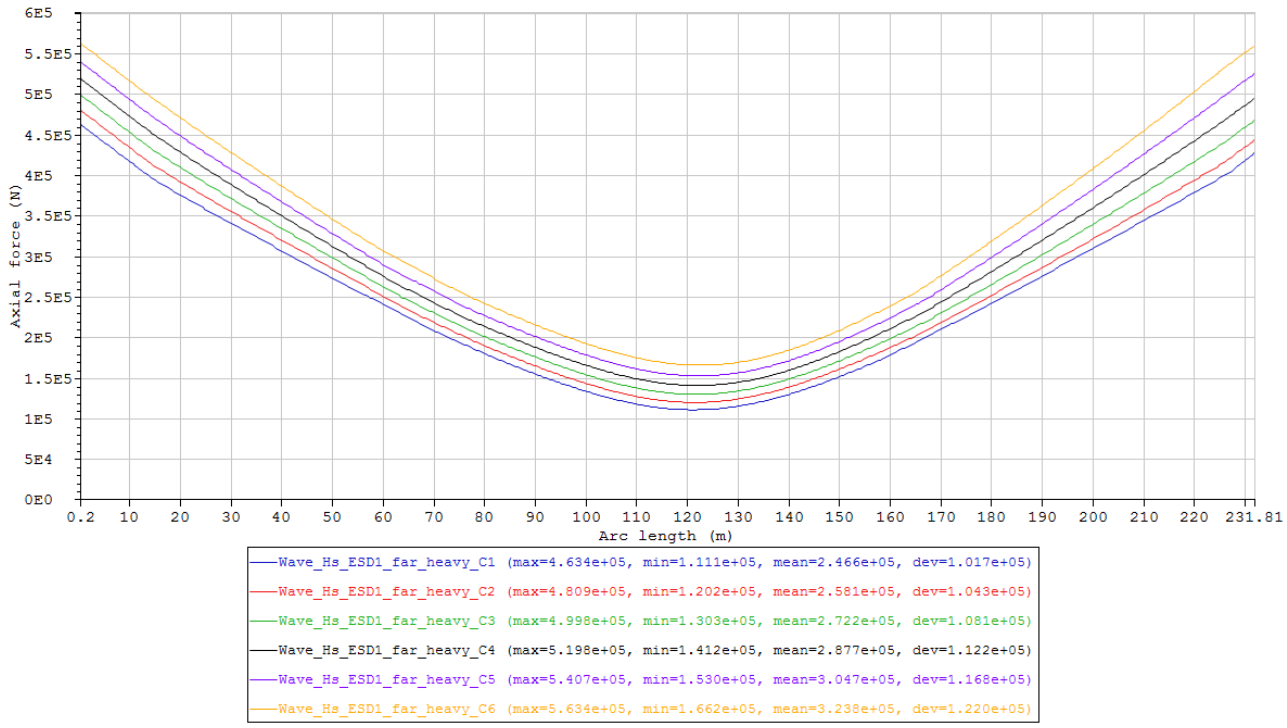

Figure 47 Maximum axial force envelope curves of the cases in Condition set – Wave_Hs_ESD1_far_heavy (Table 17).

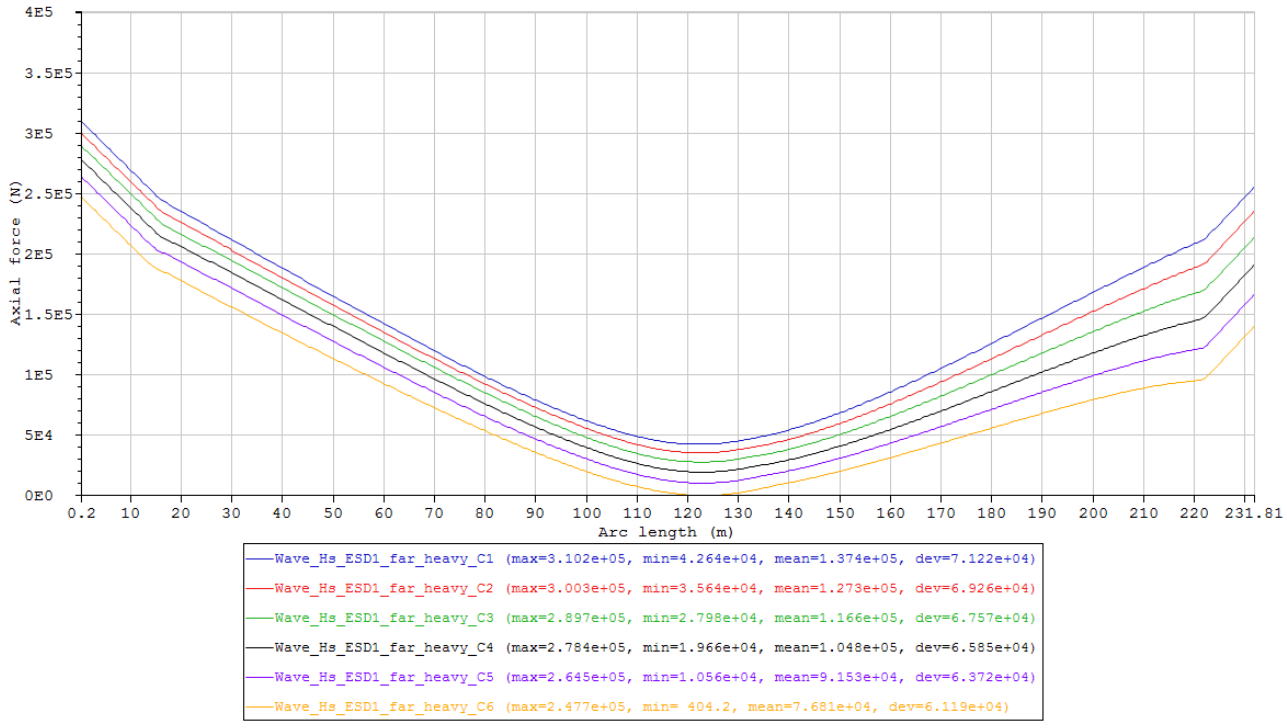

Figure 48 Minimum axial force envelope curves of the cases in Condition set – Wave_Hs_ESD1_far_heavy (Table 17).

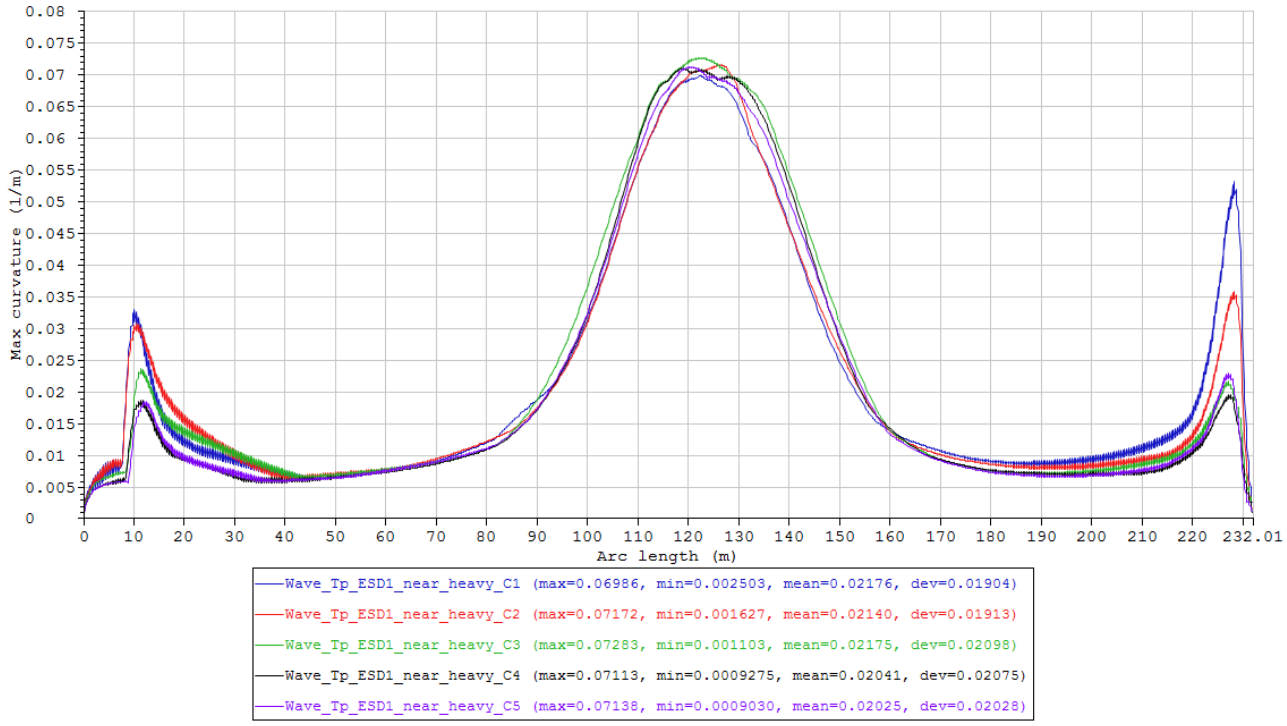

Figure 49 Maximum curvature envelope curves of the cases in Condition set – Wave_Tp_ESD1_near_heavy (Table 17).

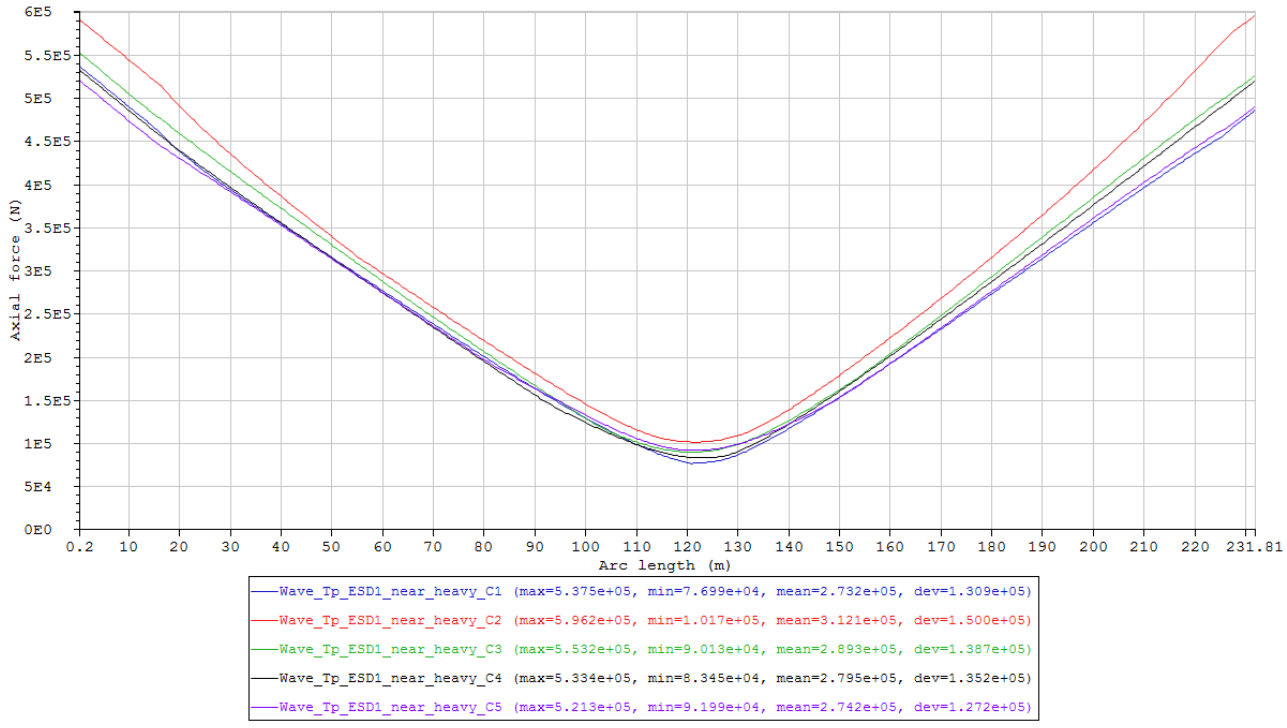

Figure 50 Maximum axial force envelope curves of the cases in Condition set – Wave_Tp_ESD1_near_heavy (Table 17).

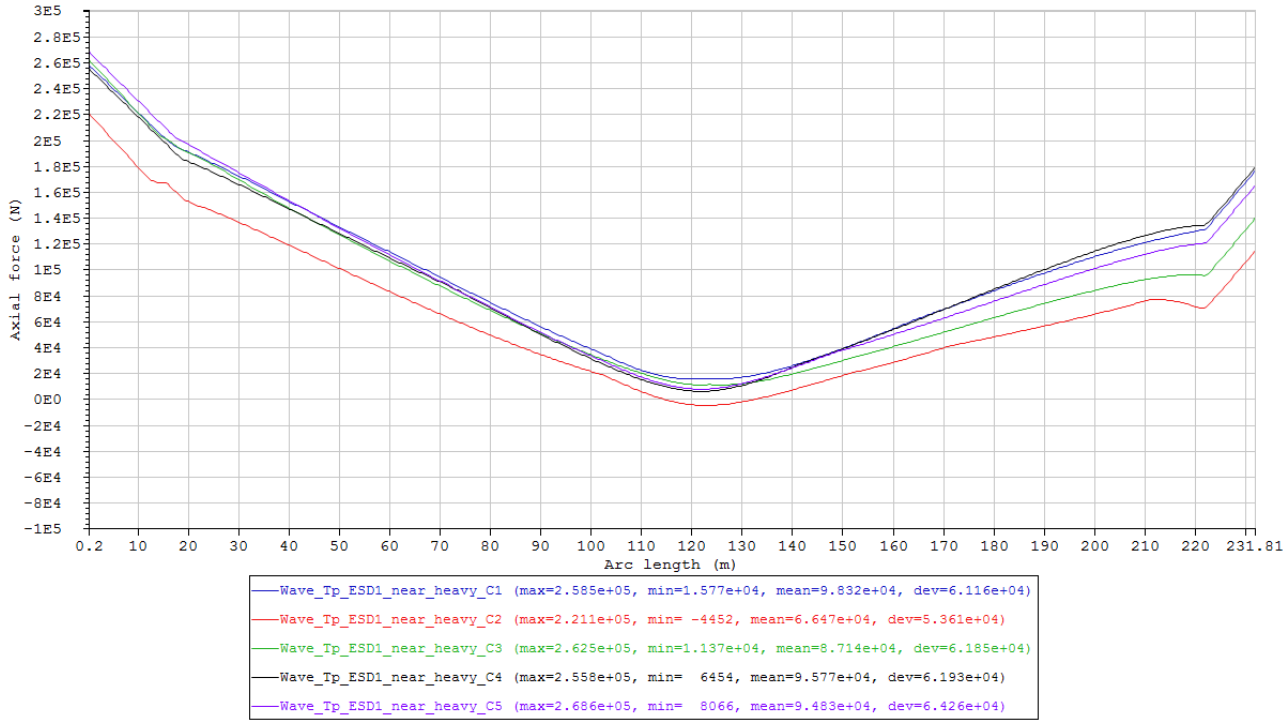

Figure 51 Minimum axial force envelope curves of the cases in Condition set – Wave_Tp_ESD1_near_heavy (Table 17).

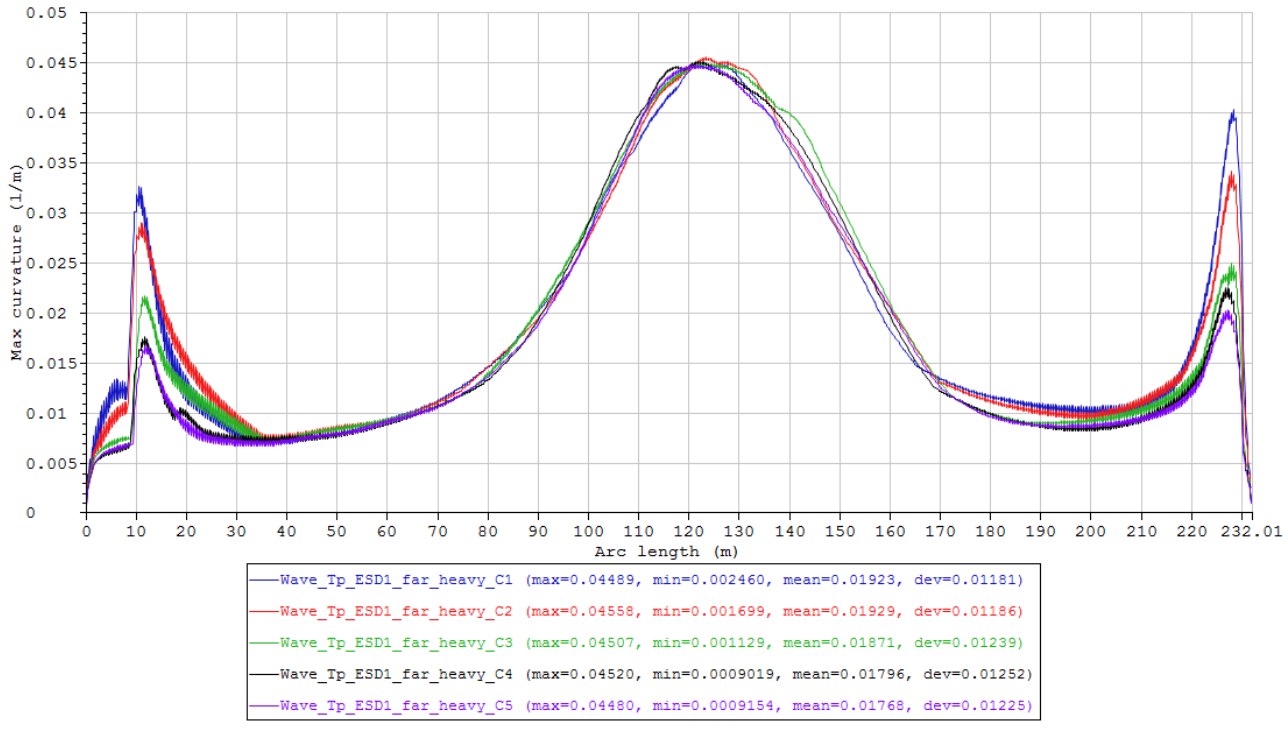

Figure 52 Maximum curvature envelope curves of the cases in Condition set – Wave_Tp_ESD1_far_heavy (Table 17).

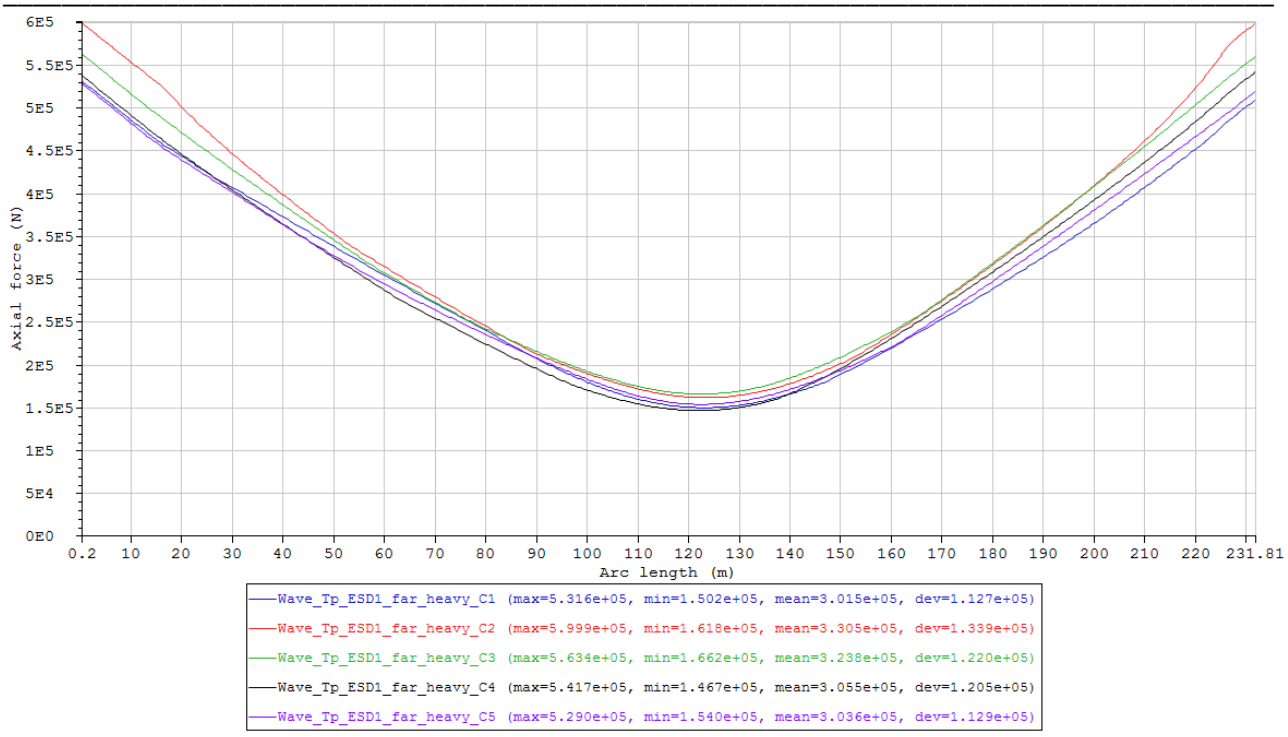

Figure 53 Maximum axial force envelope curves of the cases in Condition set – Wave_Tp_ESD1_far_heavy (Table 17).

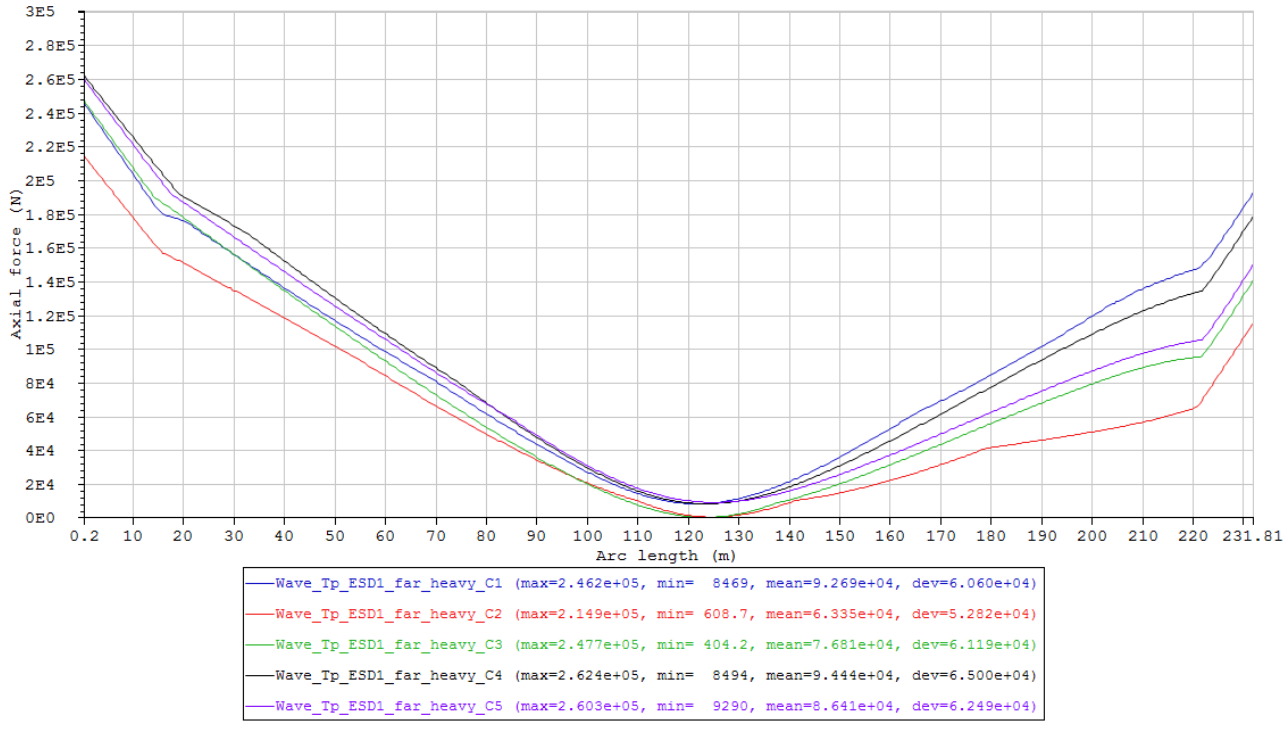

Figure 54 Minimum axial force envelope curves of the cases in Condition set – Wave_Tp_ESD1_far_heavy (Table 17).

c. Round 3

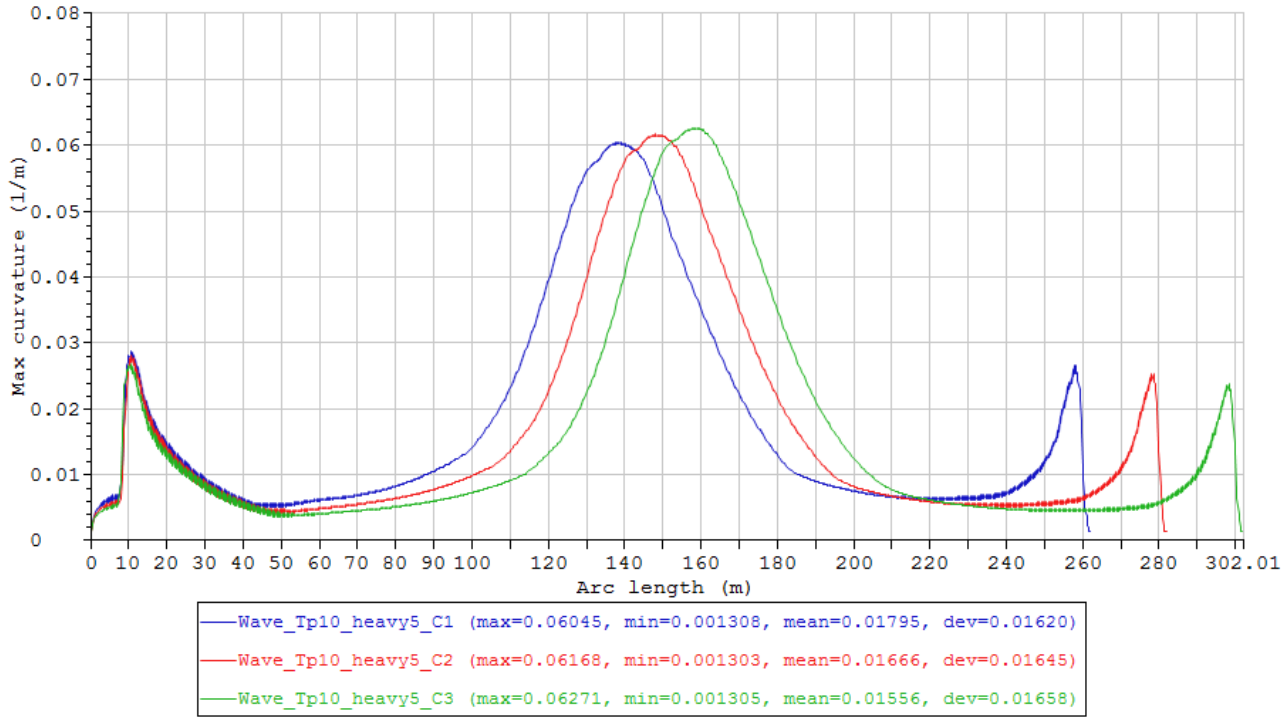

Figure 55 Maximum curvature envelope curves of the cases in Condition set – Wave_Tp10_heavy5, first 3 cases with length variation (Table 19).

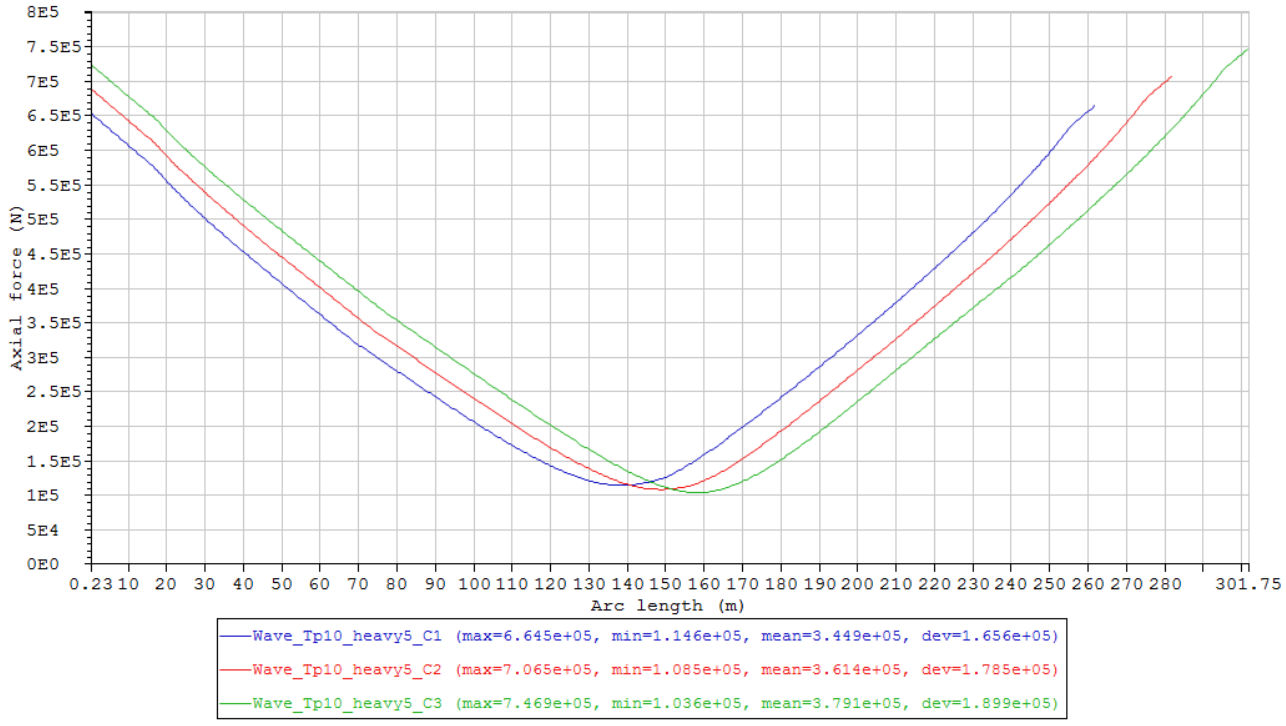

Figure 56 Maximum axial force envelope curves of the cases in Condition set - Wave_Tp10_heavy5, first 3 cases with length variation (Table 19).

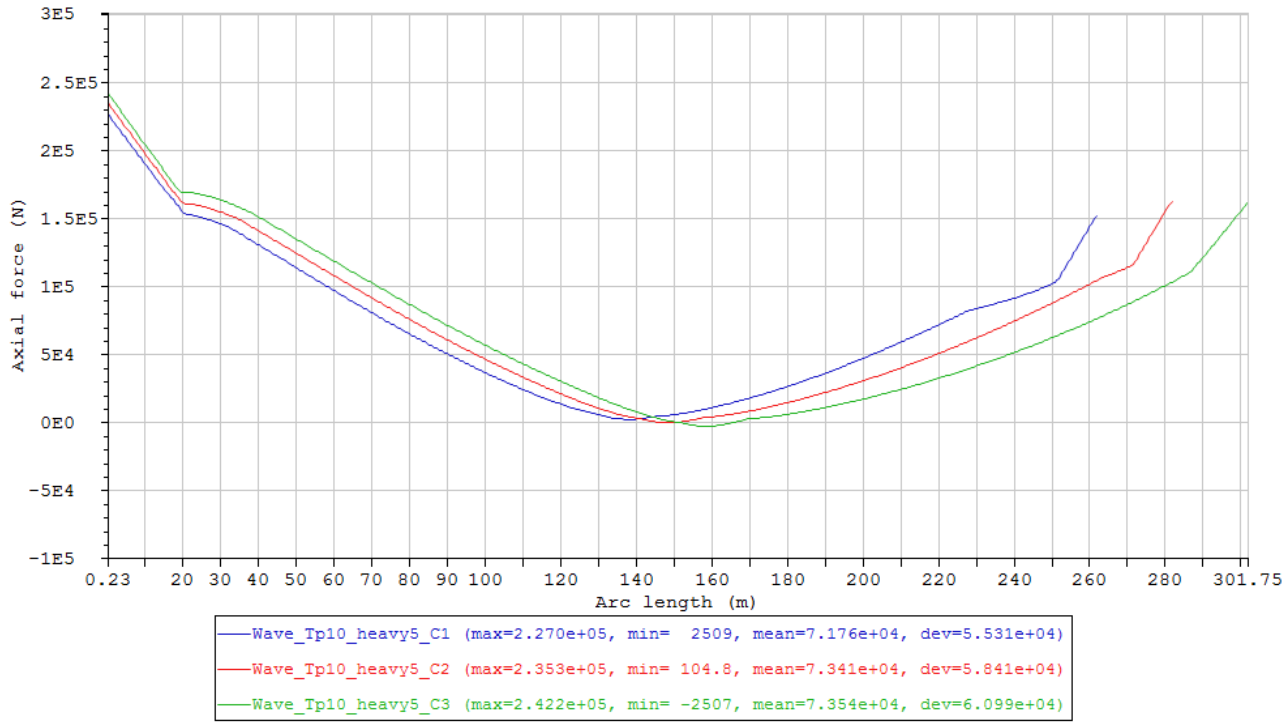

Figure 57 Minimum axial force envelope curves of the cases in Condition set - Wave_Tp10_heavy5, first 3 cases with length variation (Table 19).

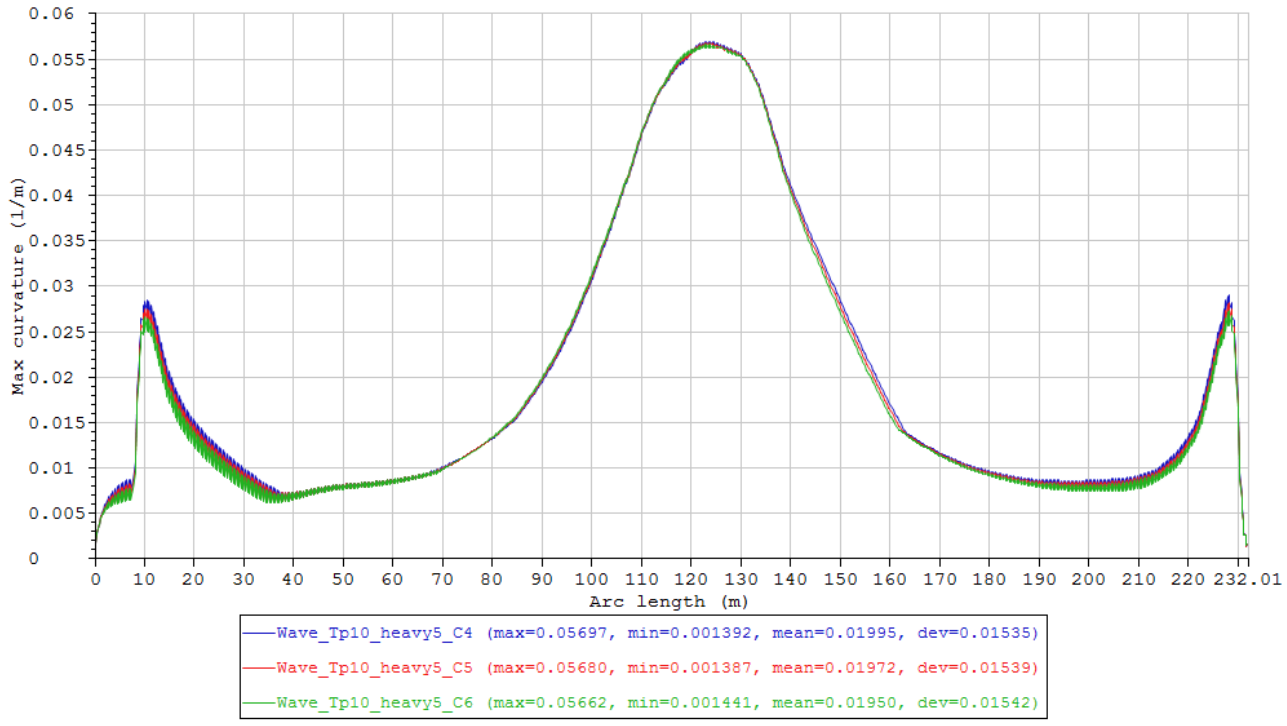

Figure 58 Maximum curvature envelope curves of the cases in Condition set – Wave_Tp10_heavy5, last 3 cases with mass/length variation (Table 19).

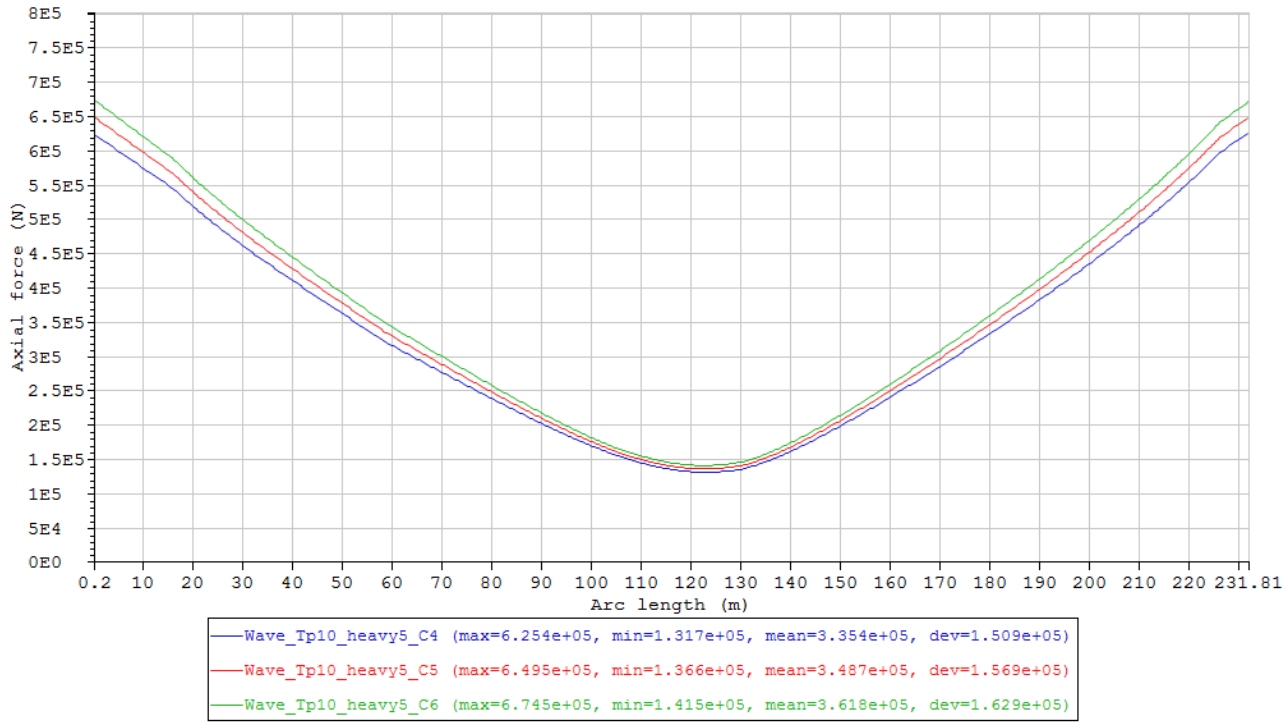

Figure 59 Maximum axial force envelope curves of the cases in Condition set - Wave_Tp10_heavy5, last 3 cases with mass/length variation (Table 19).

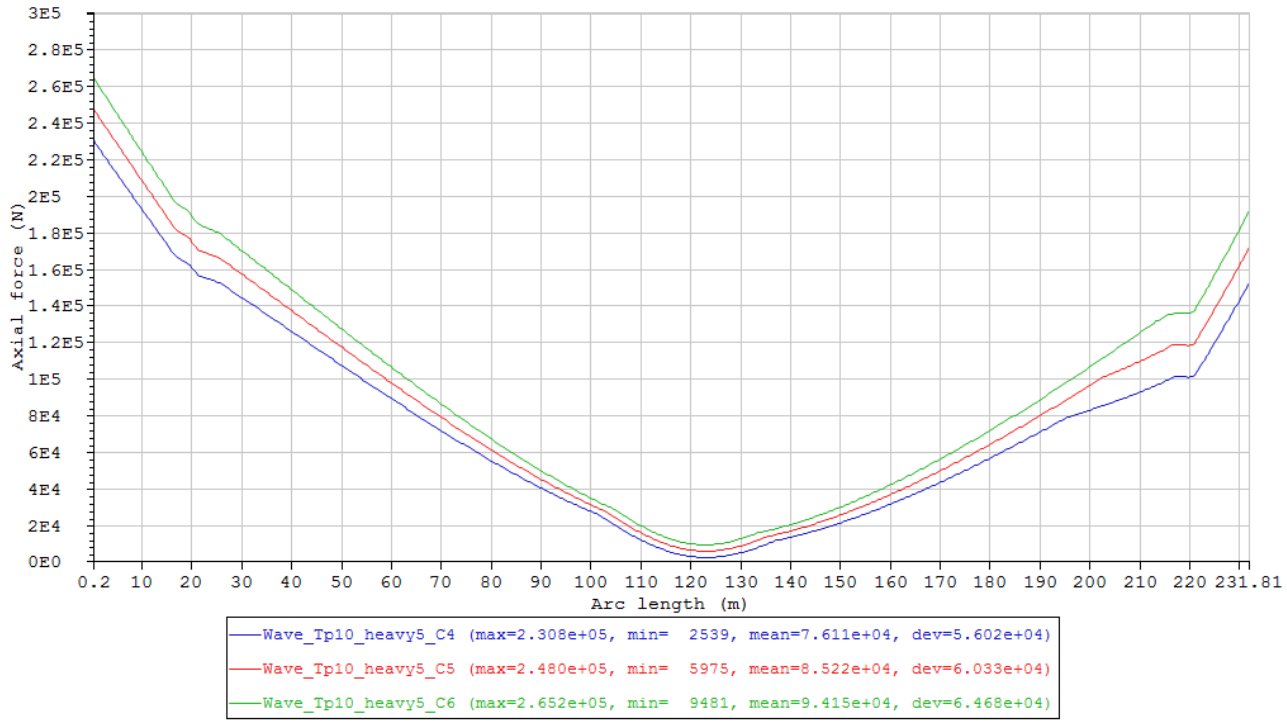

Figure 60 Minimum axial force envelope curves of the cases in Condition set - Wave_Tp10_heavy5, last 3 cases with mass/length variation (Table 19).

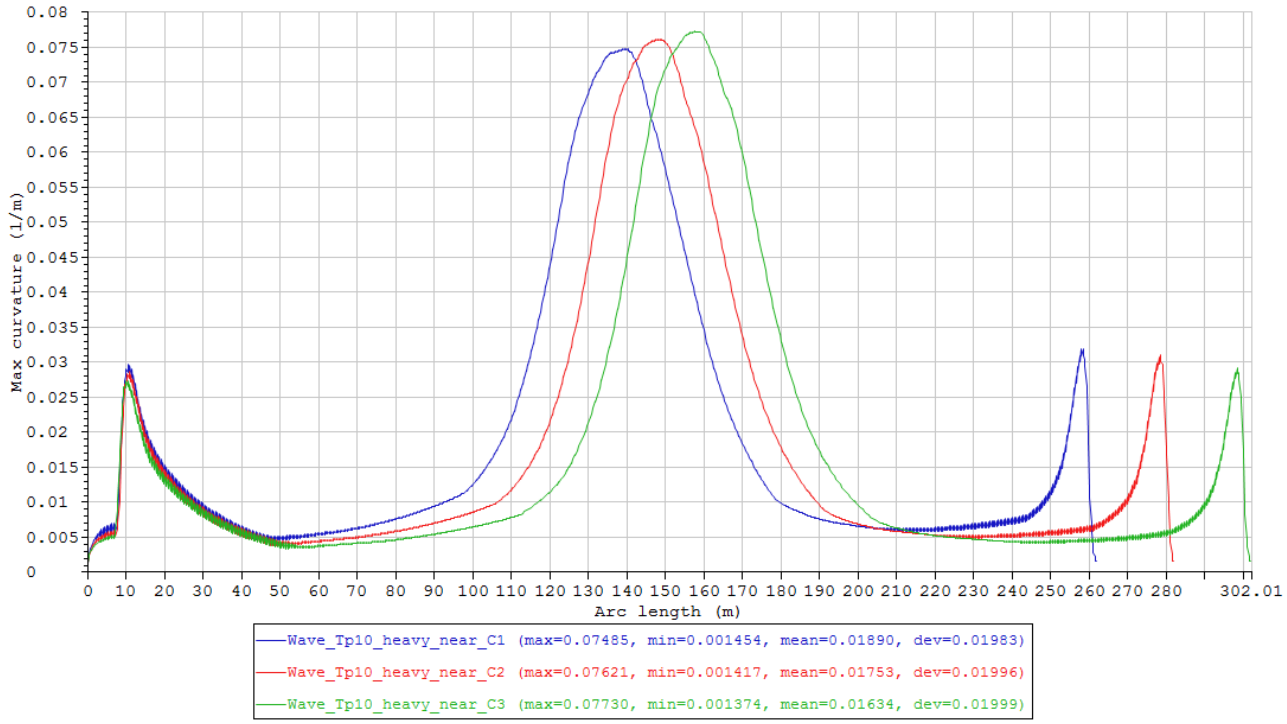

Figure 61 Maximum curvature envelope curves of the cases in Condition set – Wave_Tp10_heavy5_near, first 3 cases with length variation (Table 19).

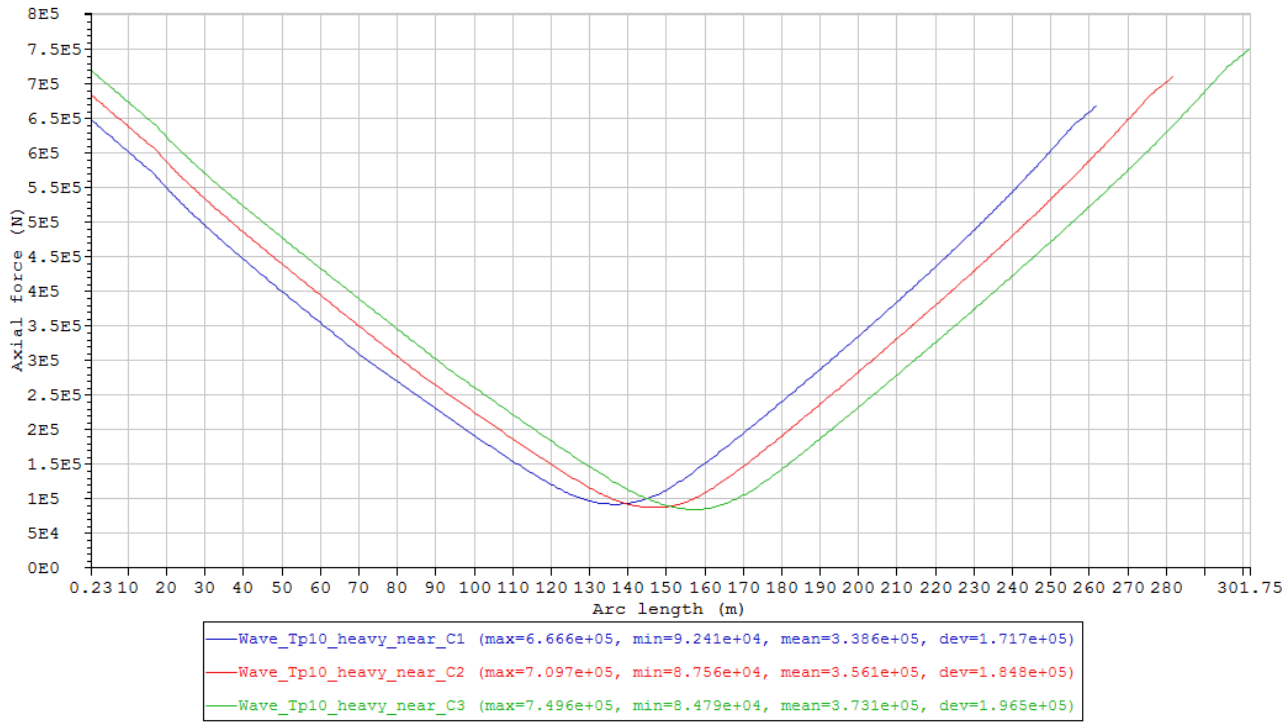

Figure 62 Maximum axial force envelope curves of the cases in Condition set - Wave_Tp10_heavy5_near, first 3 cases with length variation (Table 19).

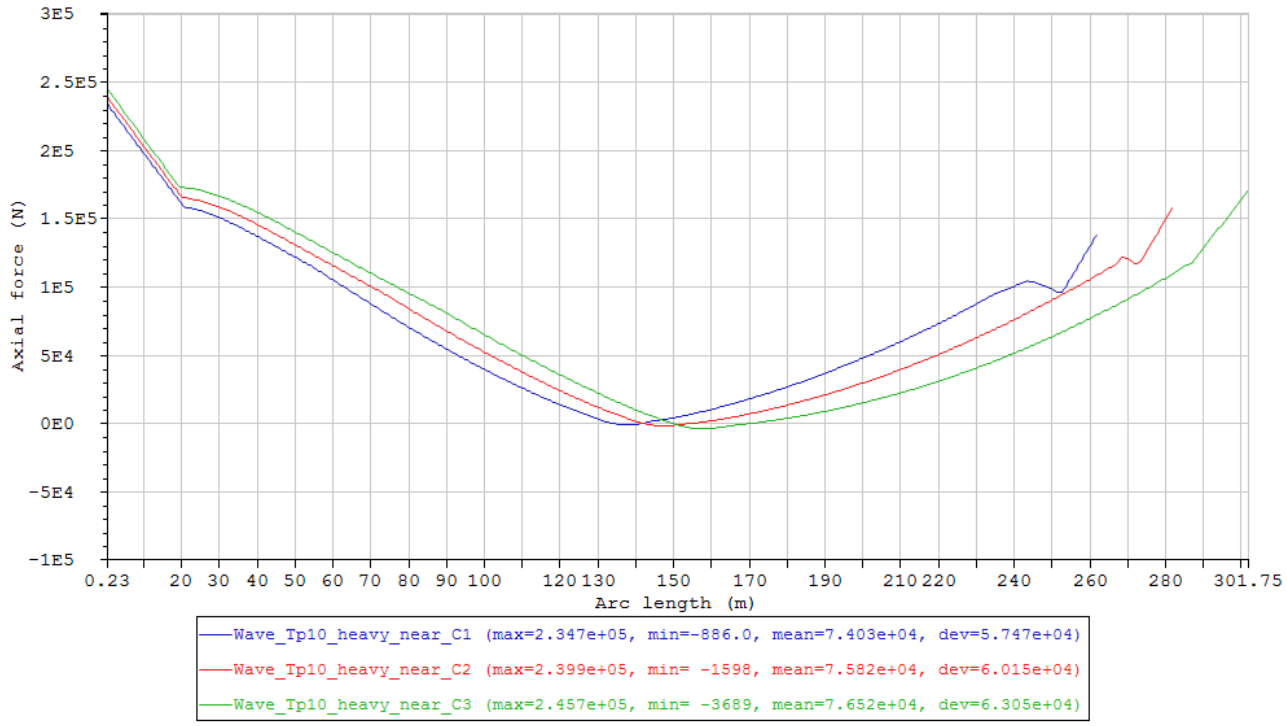

Figure 63 Minimum axial force envelope curves of the cases in Condition set - Wave_Tp10_heavy5_near, first 3 cases with length variation (Table 19).

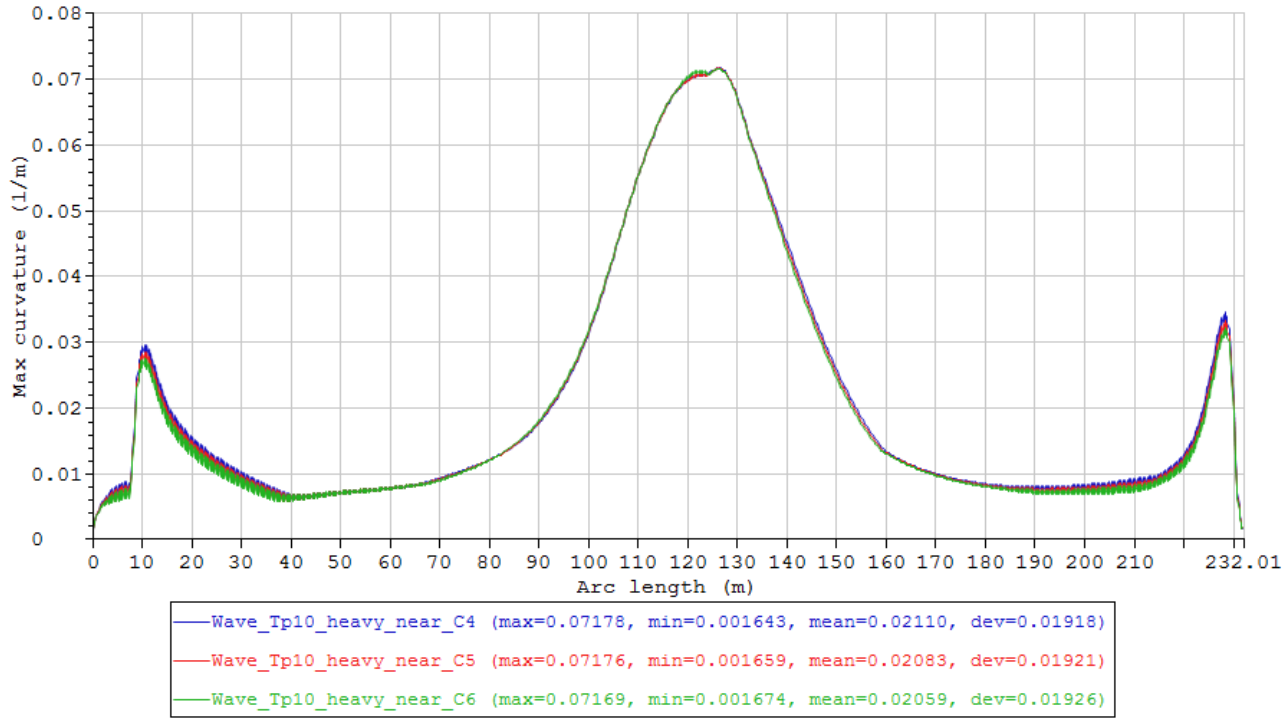

Figure 64 Maximum curvature envelope curves of the cases in Condition set – Wave_Tp10_heavy5_near, last 3 cases with mass/length variation (Table 19).

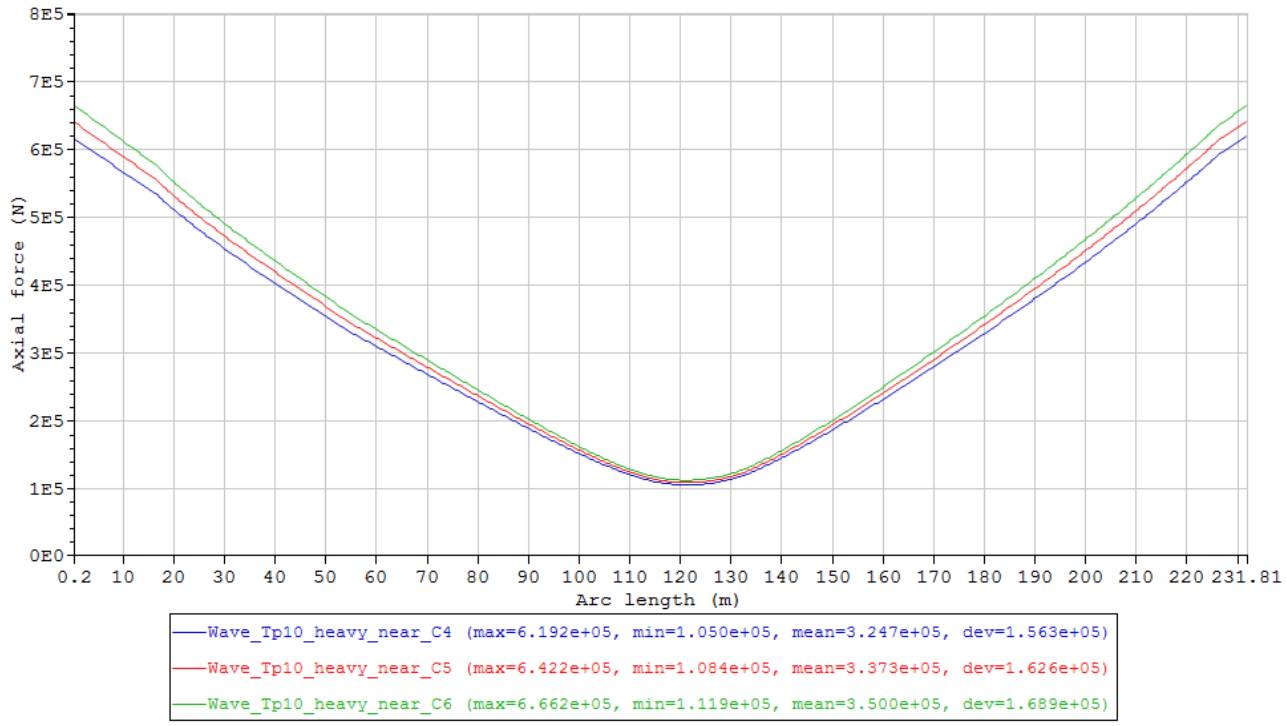

Figure 65 Maximum axial force envelope curves of the cases in Condition set – Wave_Tp10_heavy5_near, last 3 cases with mass/length variation (Table 19).

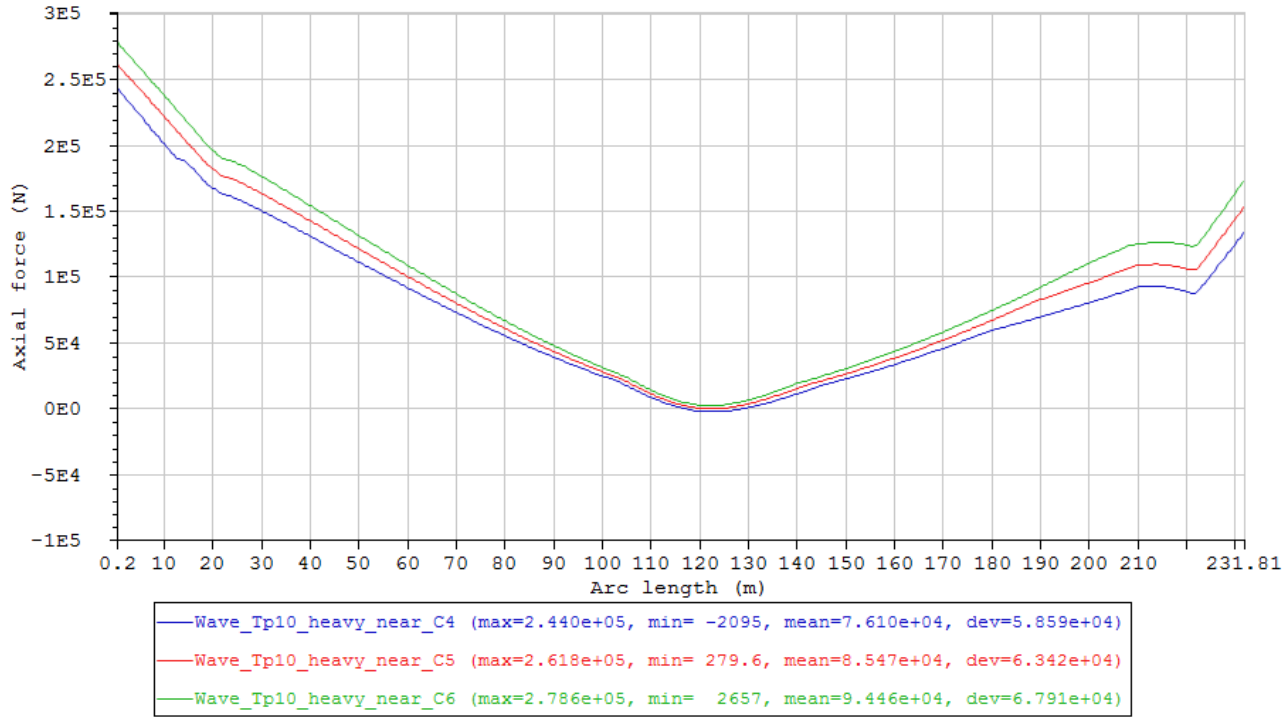

Figure 66 Minimum axial force envelope curves of the cases in Condition set – Wave_Tp10_heavy5_near, last 3 cases with mass/length variation (Table 19).

d. Round 4

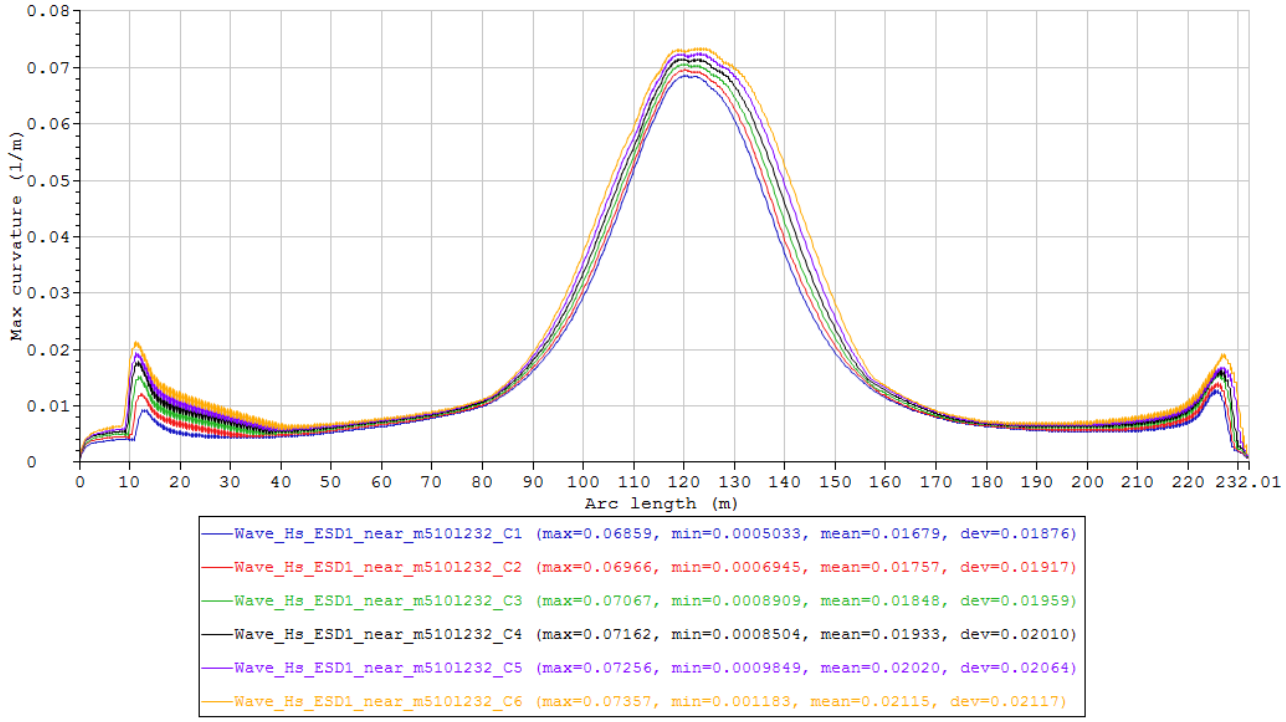

Figure 67 Maximum curvature envelope curves of the cases in Condition set – Wave_Hs_ESD1_near_m510l232 (Table 21).

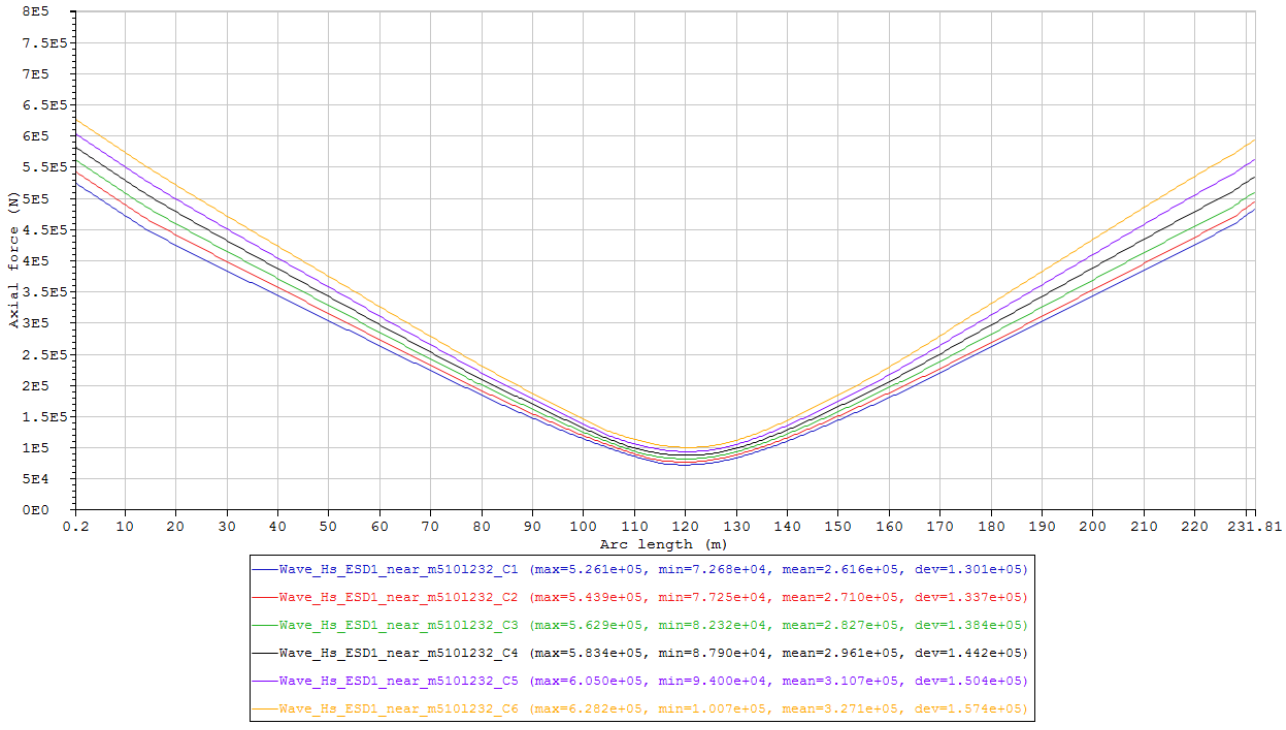

Figure 68 Maximum axial force envelope curves of the cases in Condition set – Wave_Hs_ESD1_near_m510l232 (Table 21).

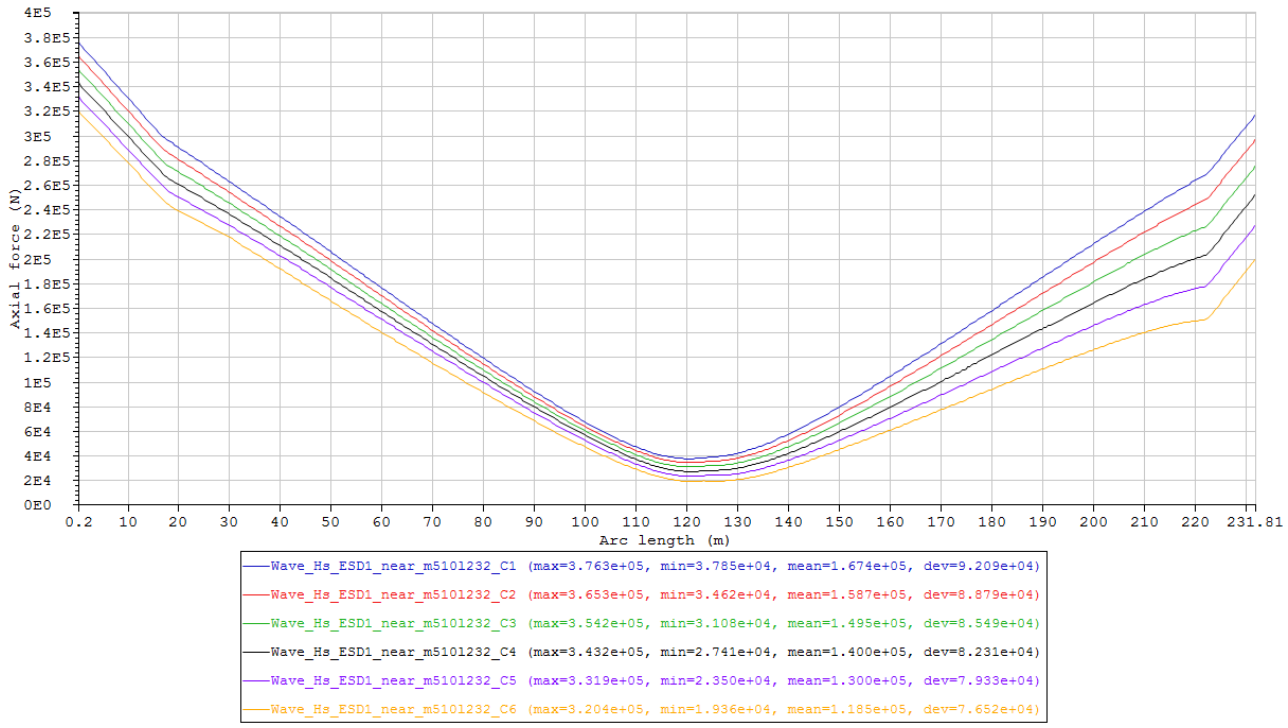

Figure 69 Minimum axial force envelope curves of the cases in Condition set – Wave_Hs_ESD1_near_m510l232 (Table 21).

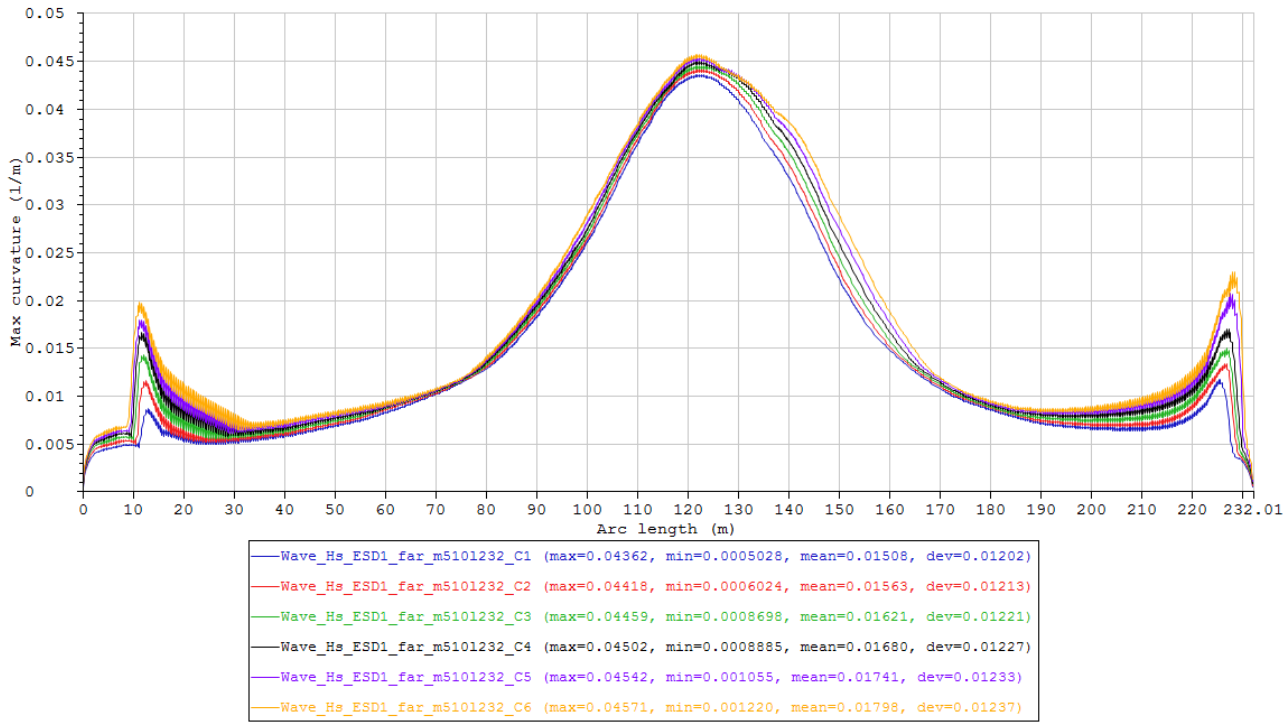

Figure 70 Maximum curvature envelope curves of the cases in Condition set – Wave_Hs_ESD1_far_m510l232 (Table 21).

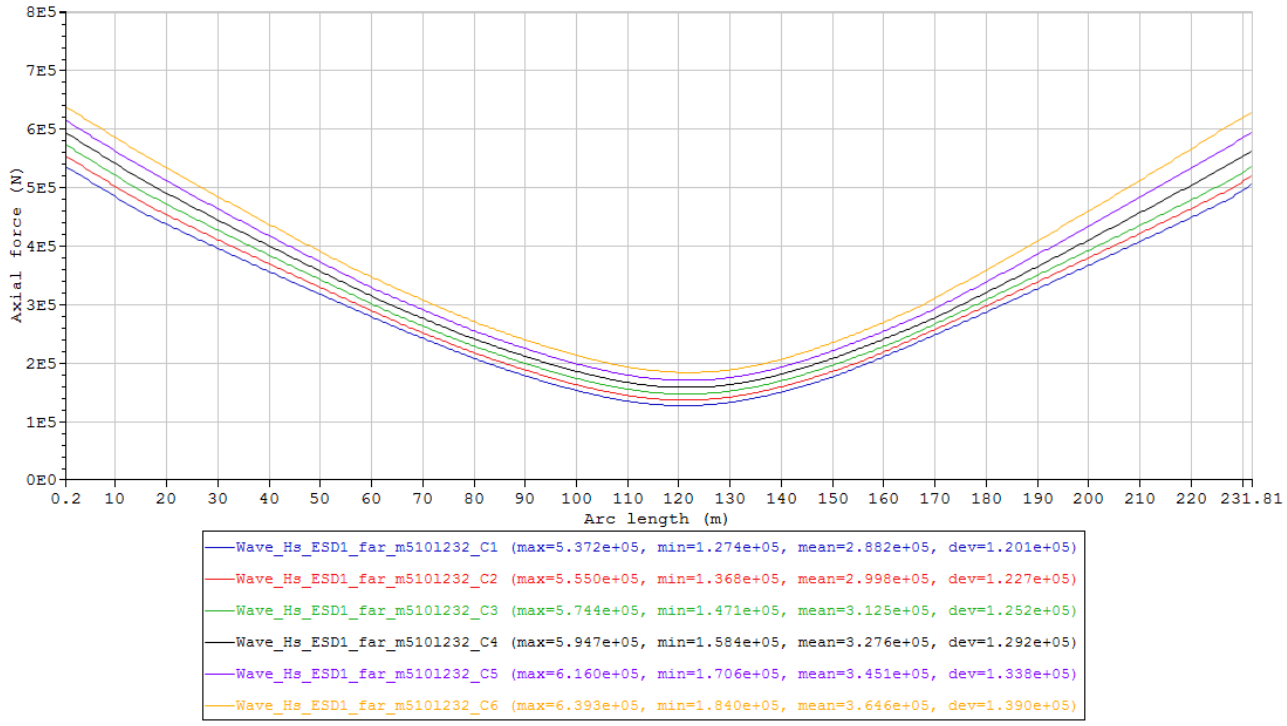

Figure 71 Maximum axial force envelope curves of the cases in Condition set – Wave_Hs_ESD1_far_m510l232 (Table 21).

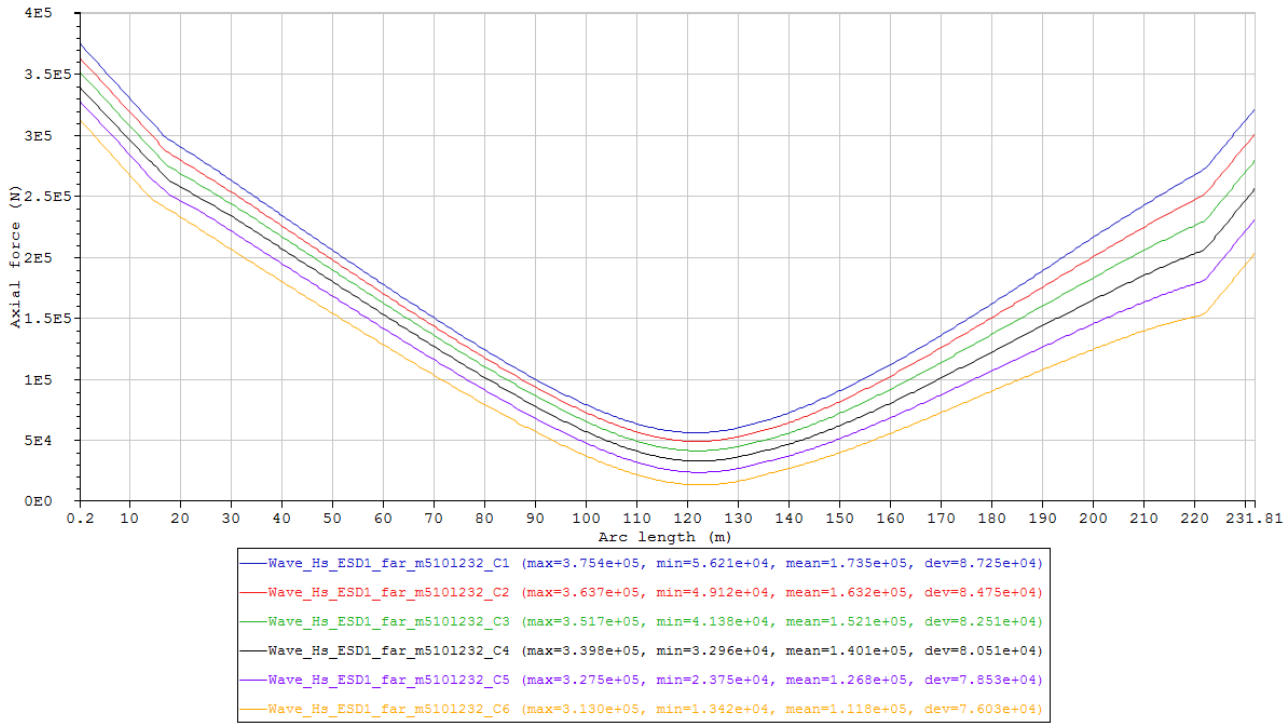

Figure 72 Minimum axial force envelope curves of the cases in Condition set – Wave_Hs_ESD1_far_m510l232 (Table 21).

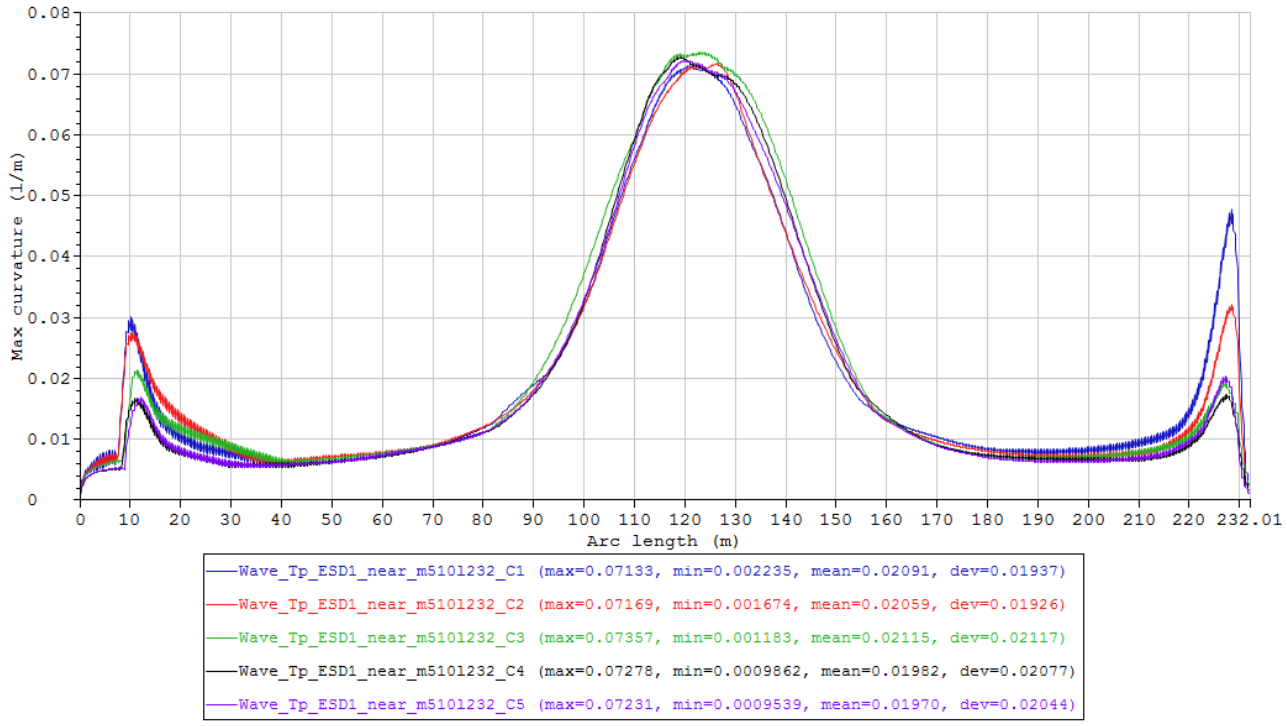

Figure 73 Maximum curvature envelope curves of the cases in Condition set – Wave_Tp_ESD1_near_m510l232 (Table 21).

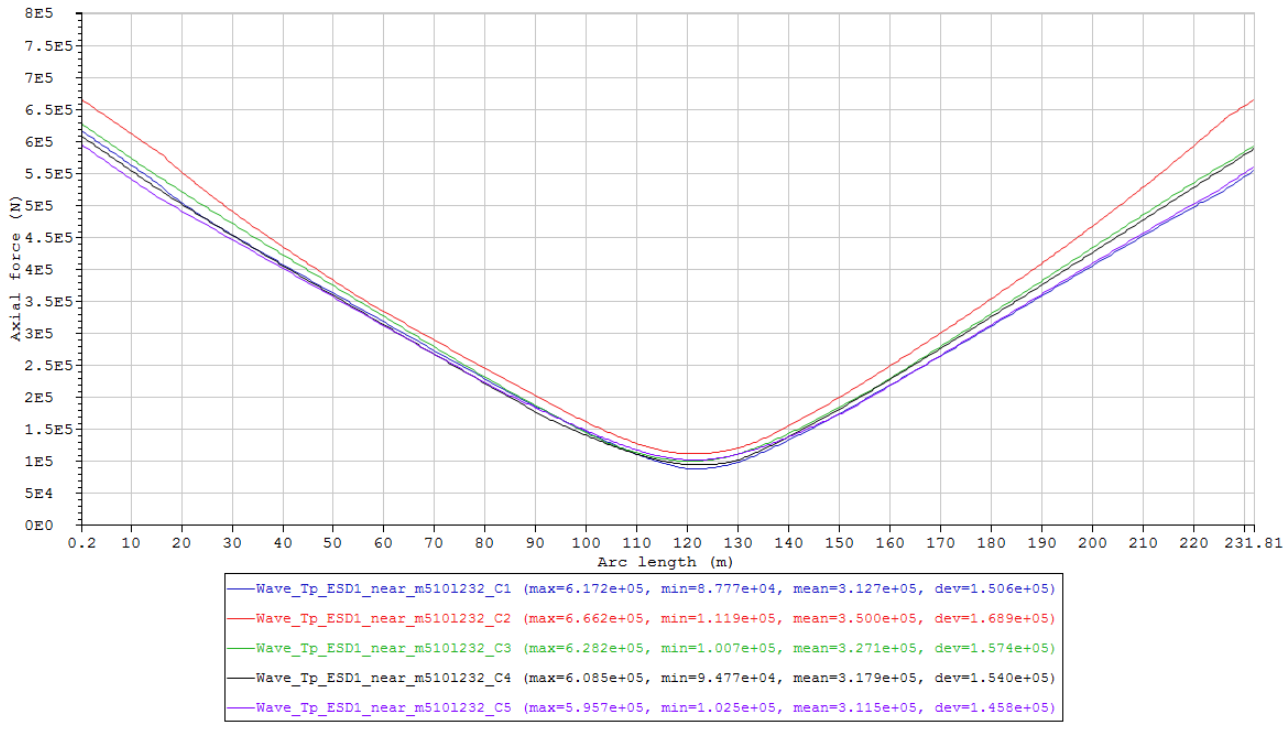

Figure 74 Maximum axial force envelope curves of the cases in Condition set – Wave_Tp_ESD1_near_m510l232 (Table 21).

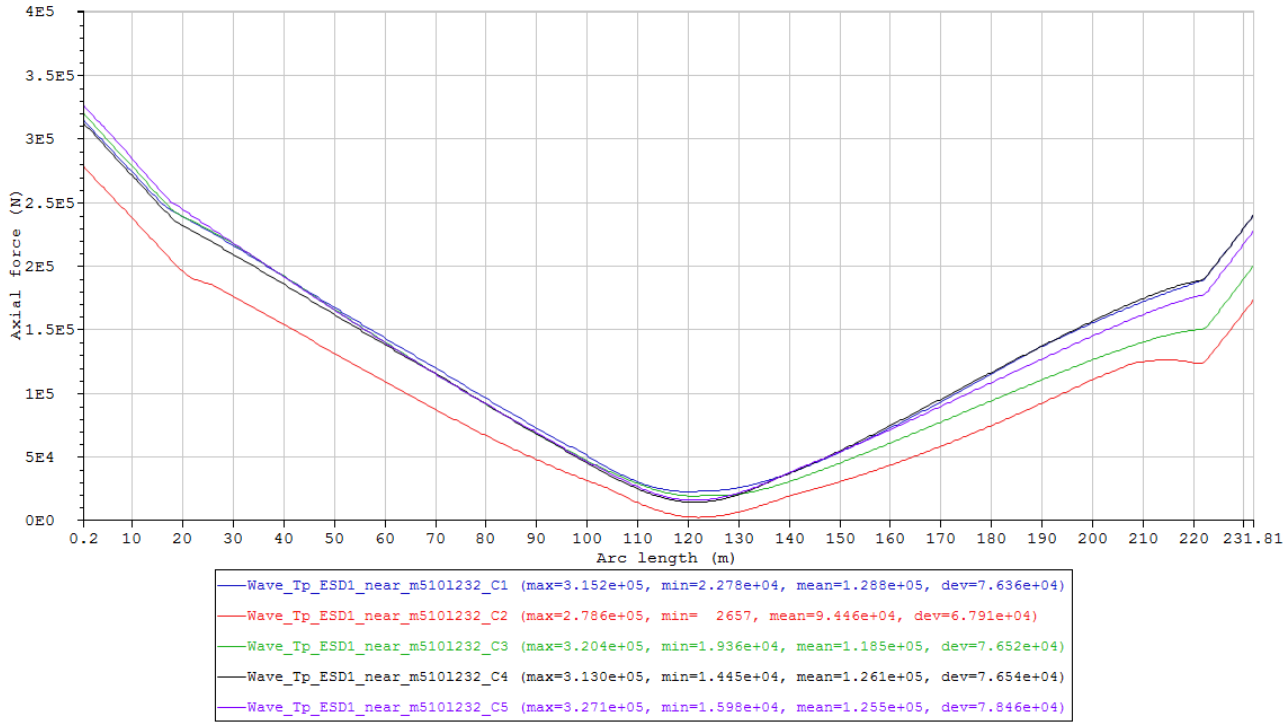

Figure 75 Minimum axial force envelope curves of the cases in Condition set – Wave_Tp_ESD1_near_m510l232 (Table 21).

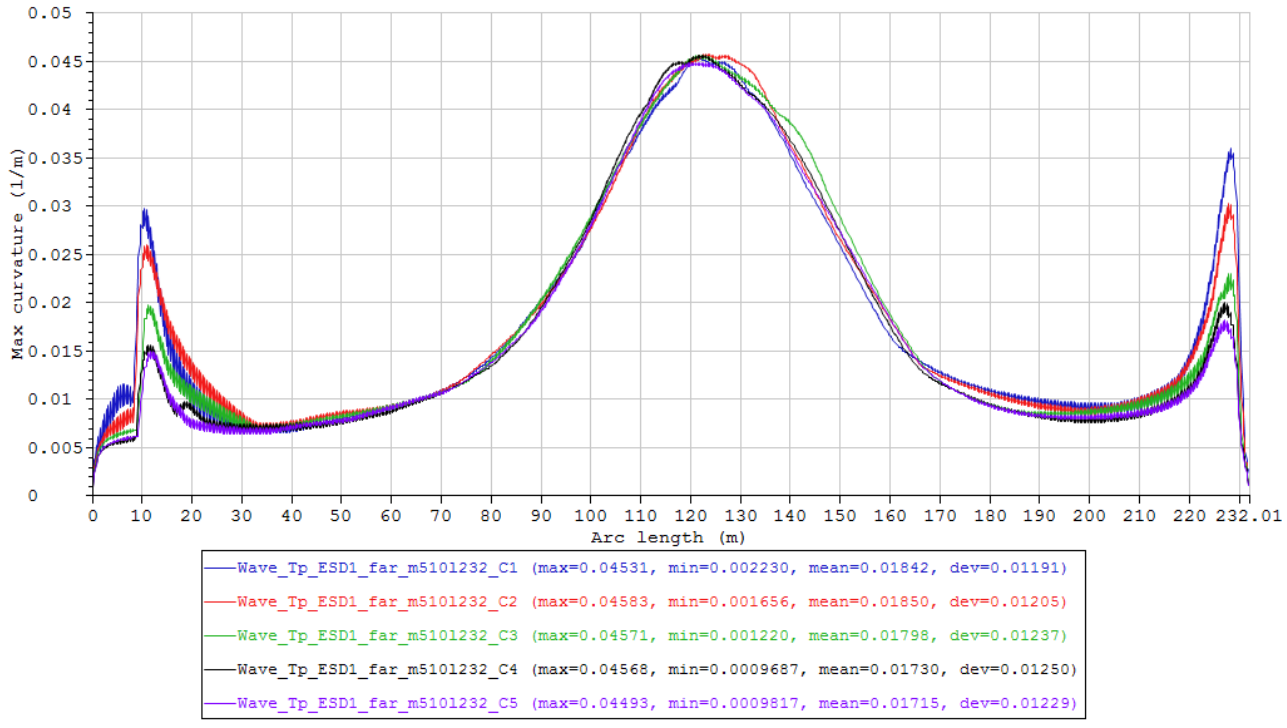

Figure 76 Maximum curvature envelope curves of the cases in Condition set – Wave_Tp_ESD1_far_m510l232 (Table 21).

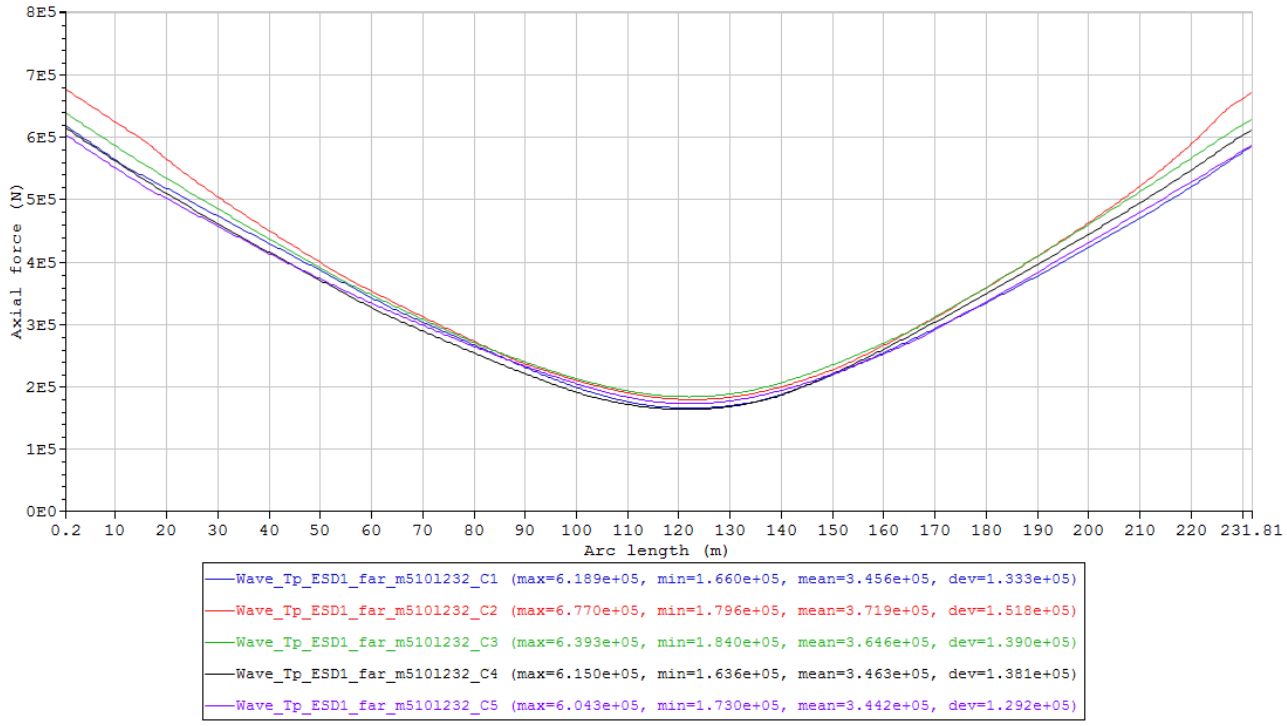

Figure 77 Maximum axial force envelope curves of the cases in Condition set – Wave_Tp_ESD1_far_m510l232 (Table 21).

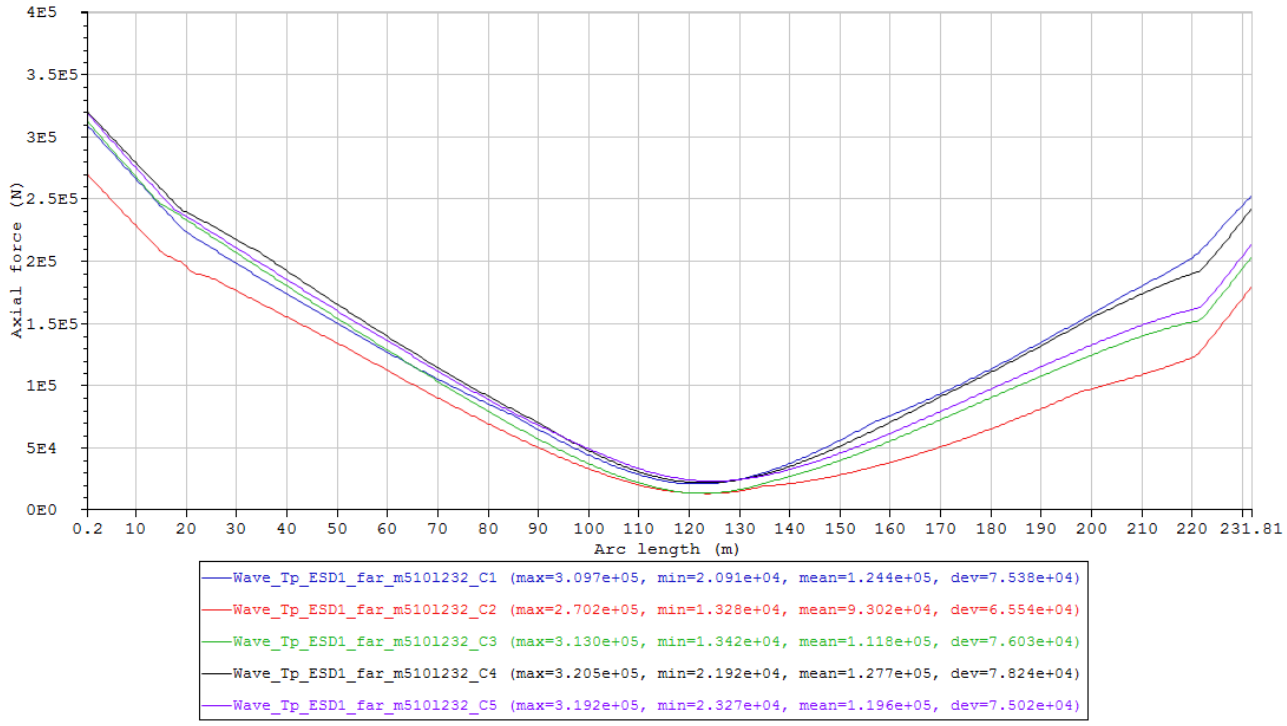

Figure 78 Minimum axial force envelope curves of the cases in Condition set – Wave_Tp_ESD1_far_m510l232 (Table 21).

e. Round 5

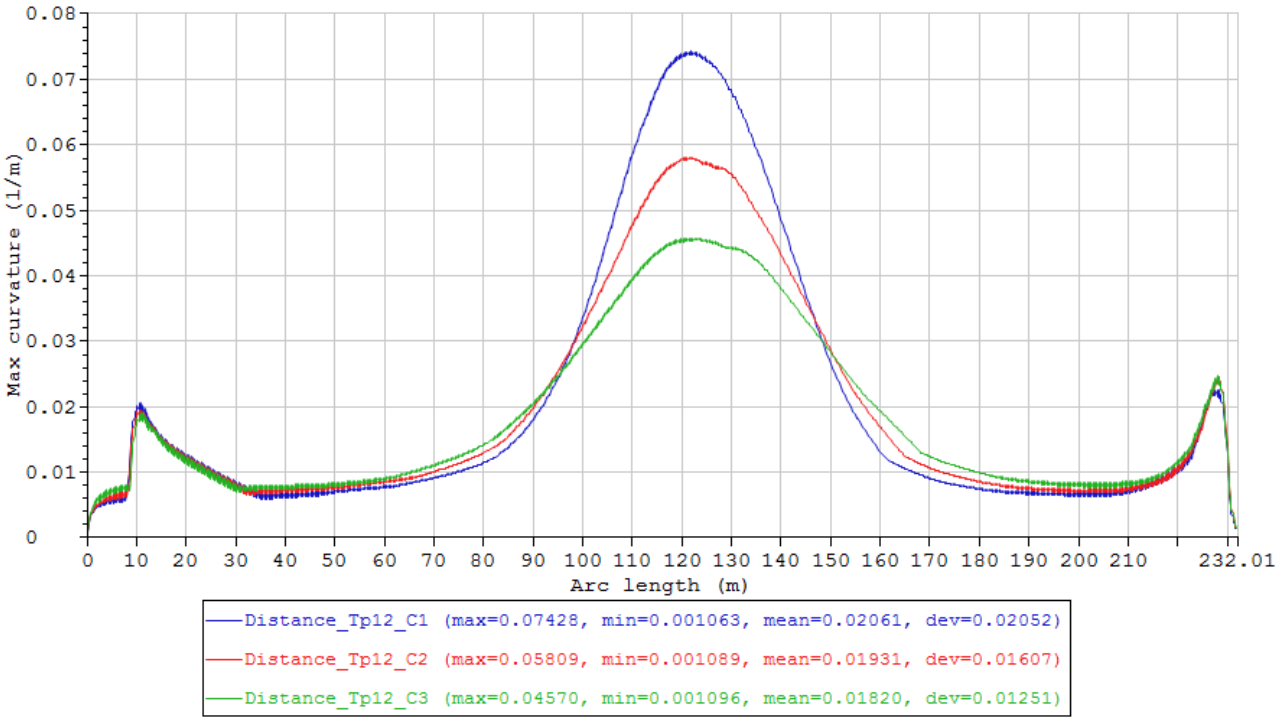

Figure 79 Maximum curvature envelope curves of the cases in Condition set – Distance_Tp12 (Table 23).

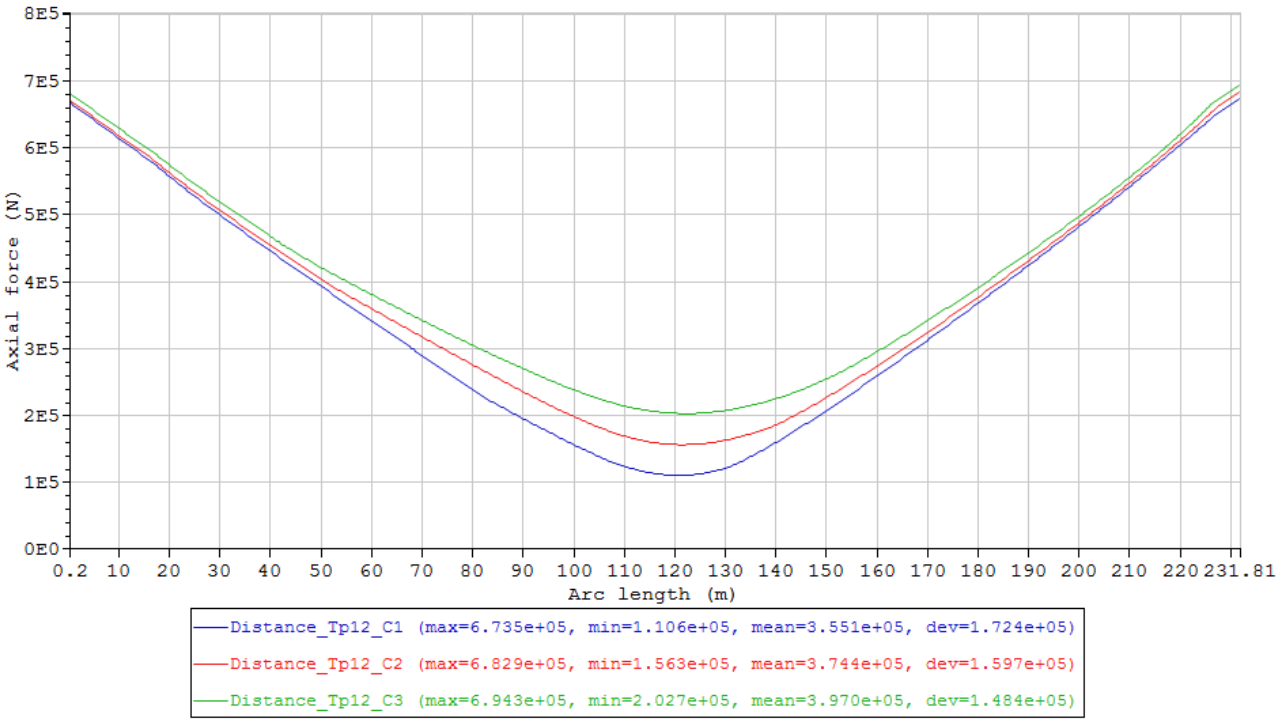

Figure 80 Maximum axial force envelope curves of the cases in Condition set – Distance_Tp12 (Table 23).

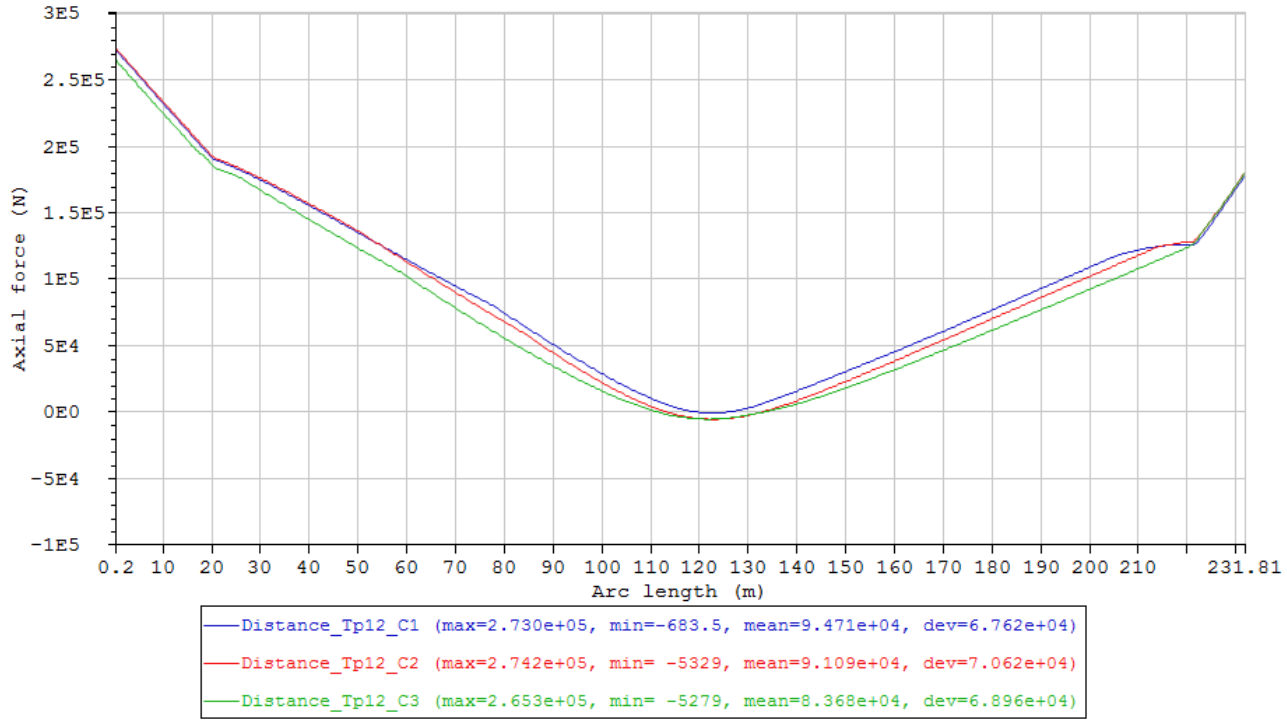

Figure 81 Minimum axial force envelope curves of the cases in Condition set – Distance_Tp12 (Table 23).

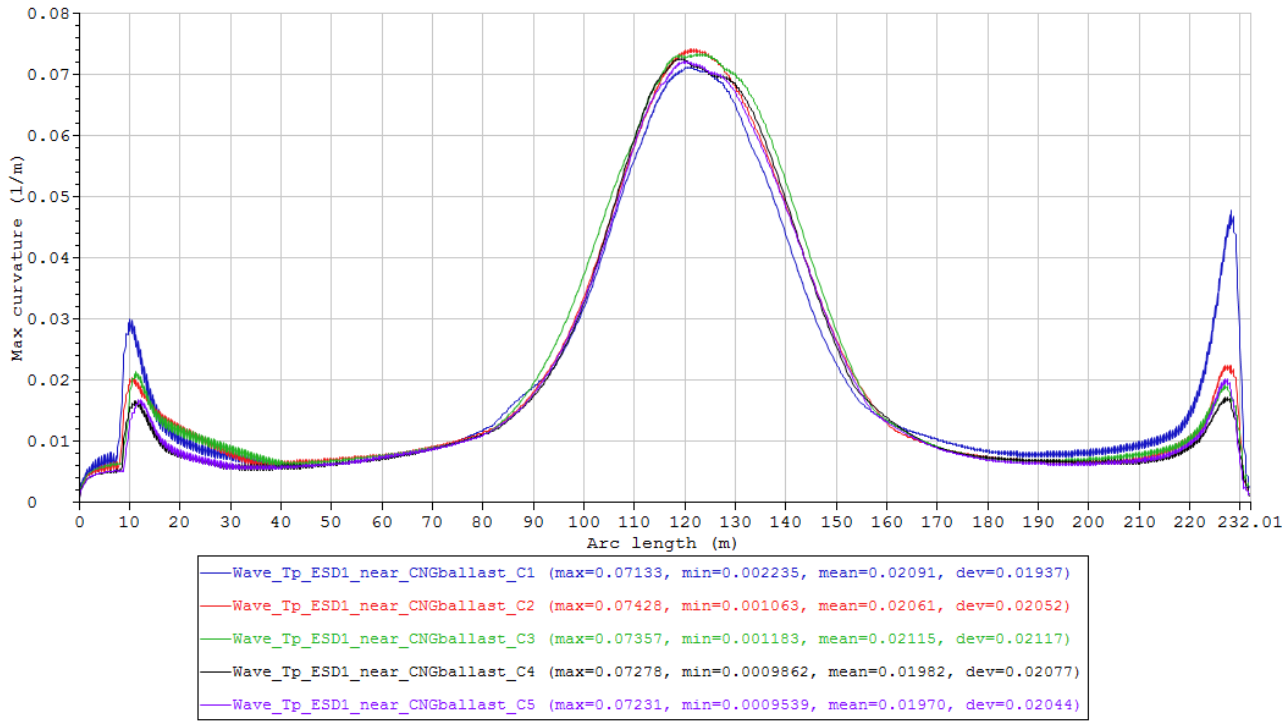

Figure 82 Maximum curvature envelope curves of the cases in Condition set – Wave_Tp_ESD1_near_CNGballast (Table 23).

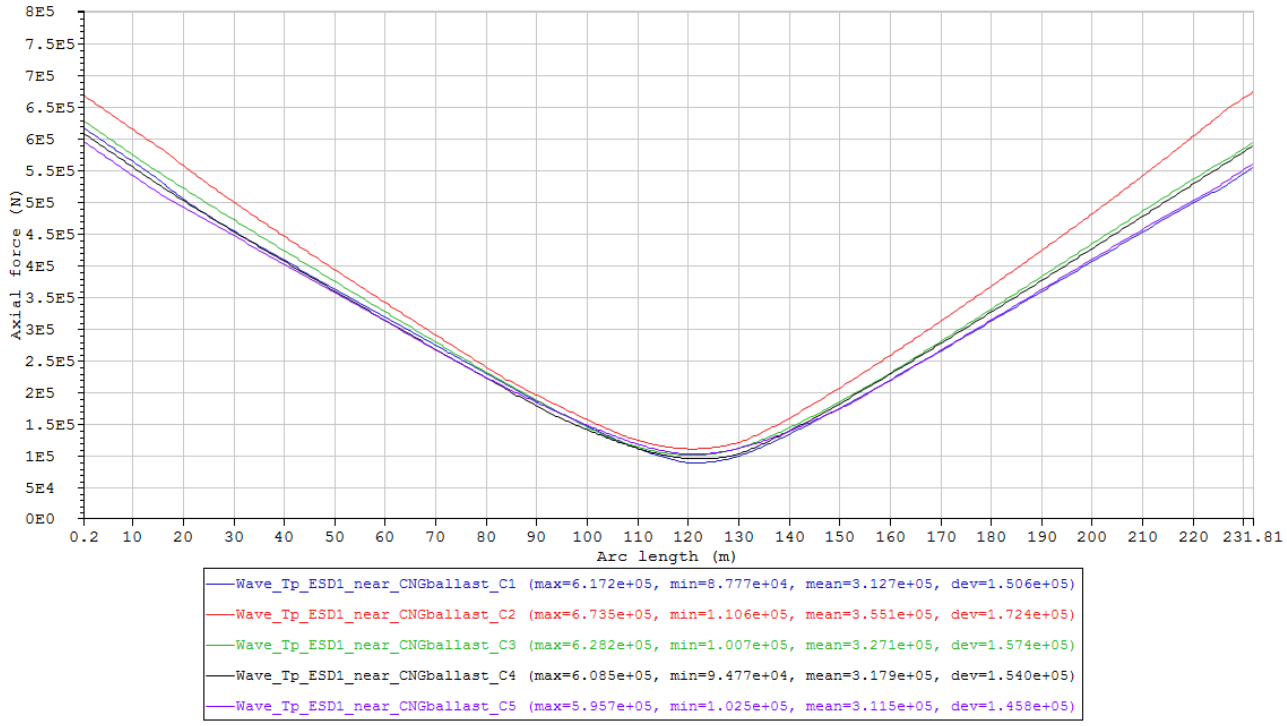

Figure 83 Maximum axial force envelope curves of the cases in Condition set – Wave_Tp_ESD1_near_CNGballast (Table 23).

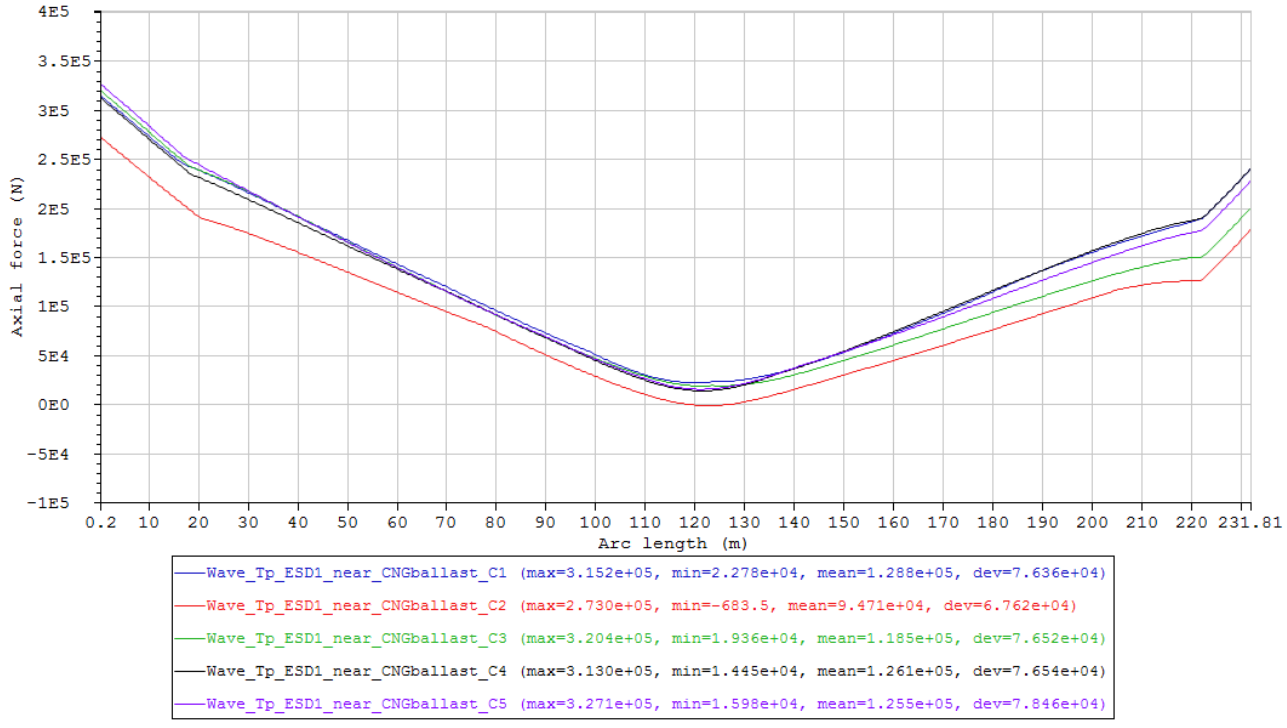

Figure 84 Minimum axial force envelope curves of the cases in Condition set – Wave_Tp_ESD1_near_CNGballast (Table 23).

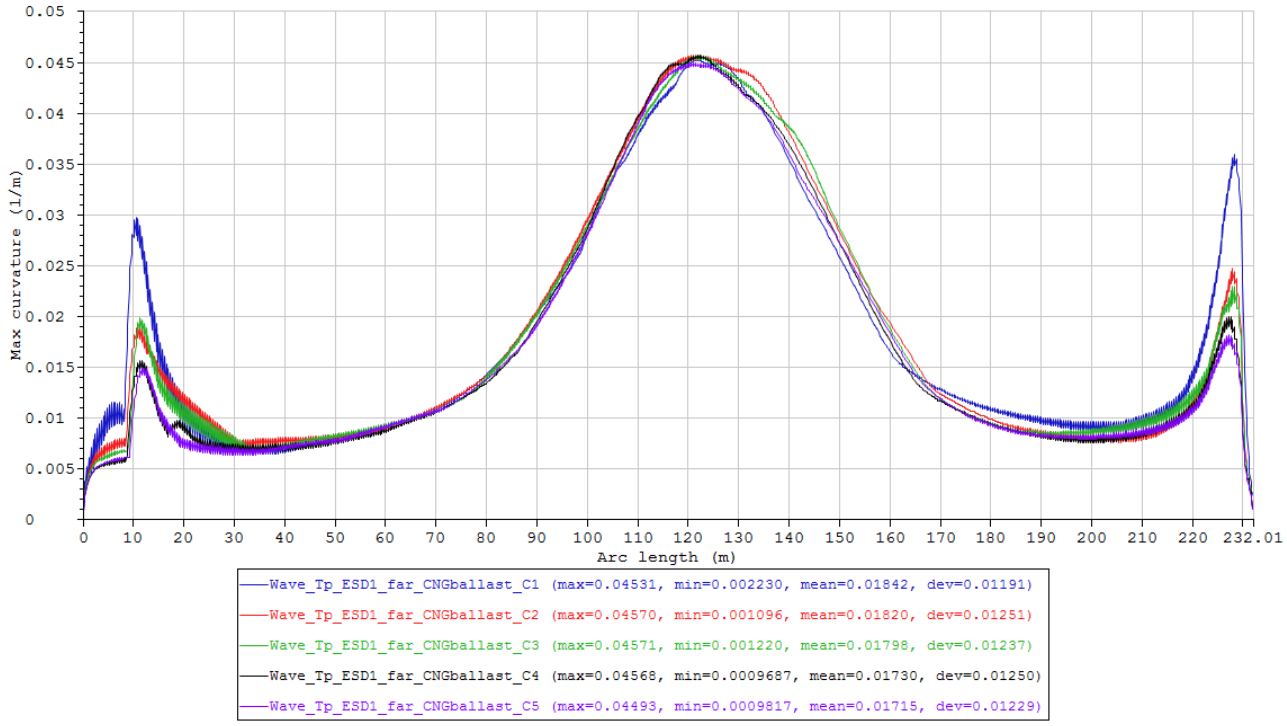

Figure 85 Maximum curvature envelope curves of the cases in Condition set – Wave_Tp_ESD1_far_CNGballast (Table 23).

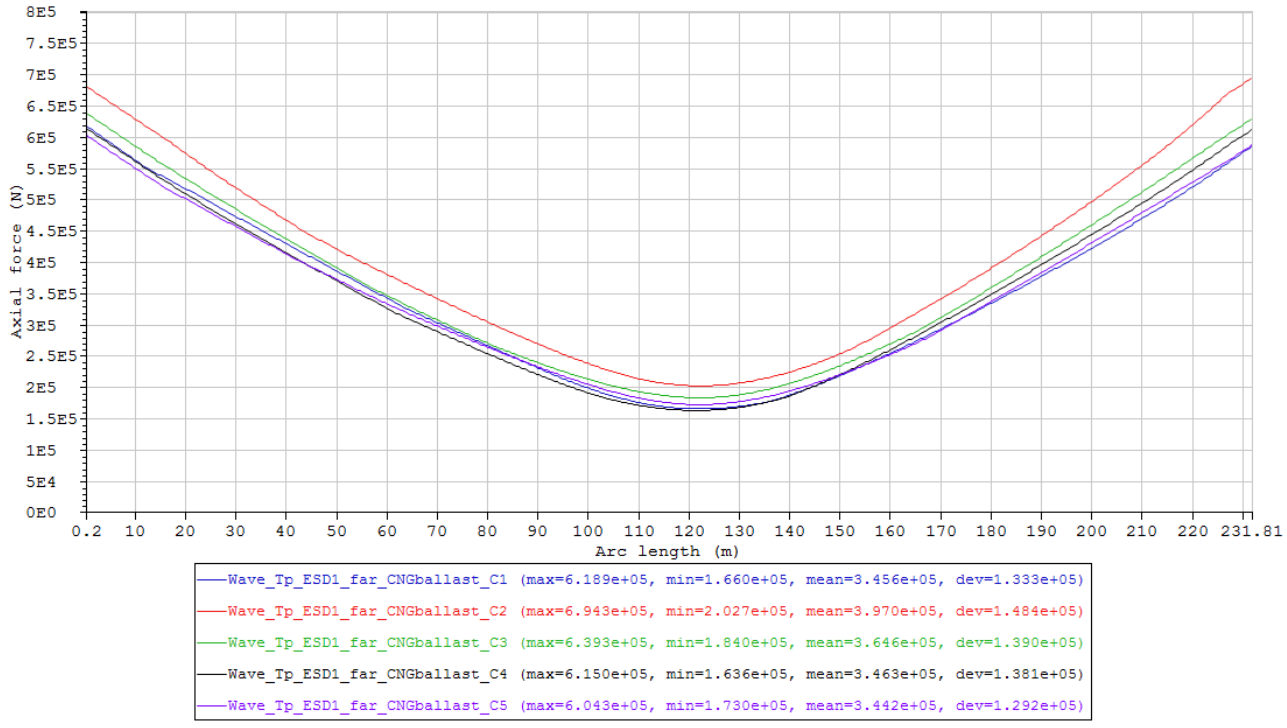

Figure 86 Maximum axial force envelope curves of the cases in Condition set – Wave_Tp_ESD1_far_CNGballast (Table 23).

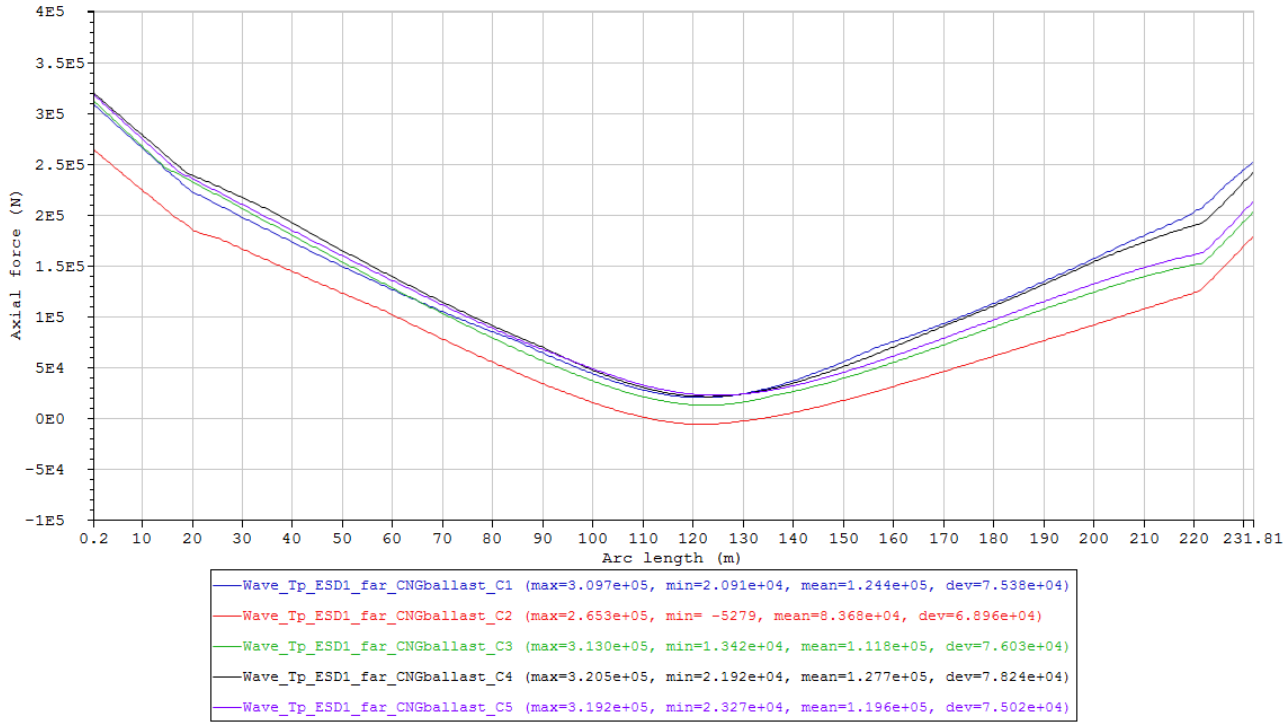

Figure 87 Minimum axial force envelope curves of the cases in Condition set – Wave_Tp_ESD1_far_CNGballast (Table 23).

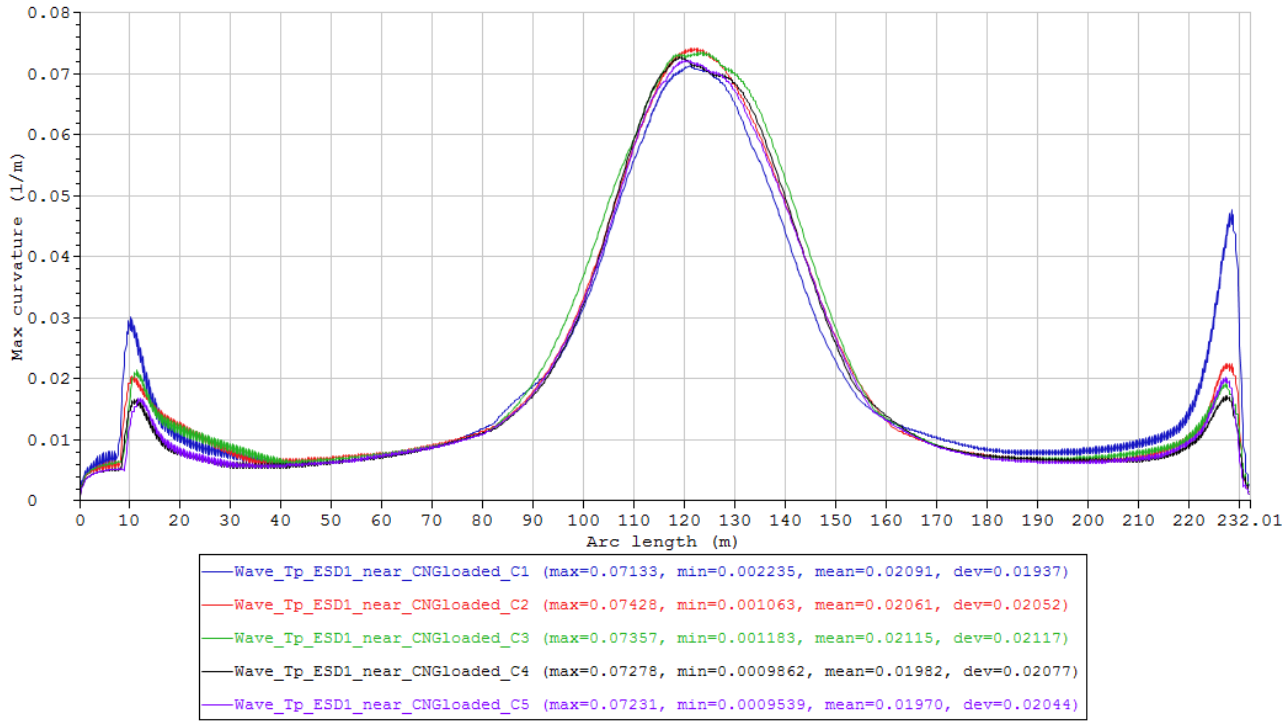

Figure 88 Maximum curvature envelope curves of the cases in Condition set – Wave_Tp_ESD1_near_CNGloaded (Table 23).

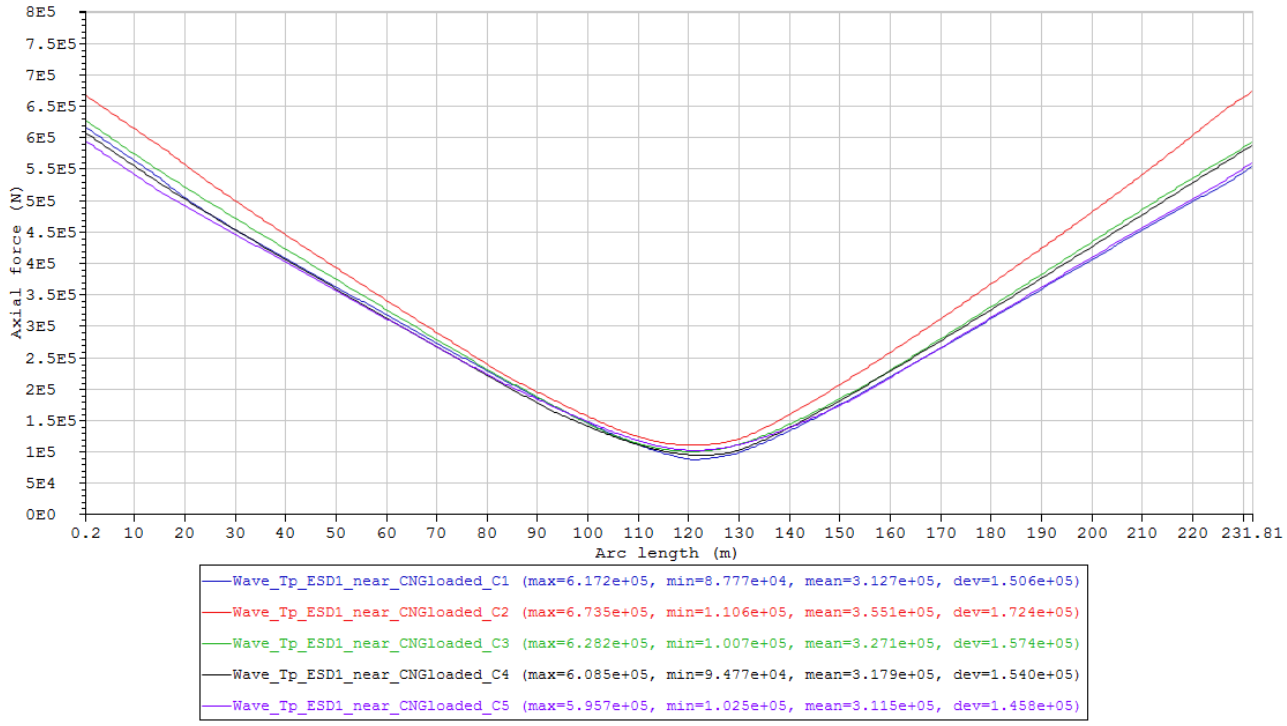

Figure 89 Maximum axial force envelope curves of the cases in Condition set – Wave_Tp_ESD1_near_CNGloaded (Table 23).

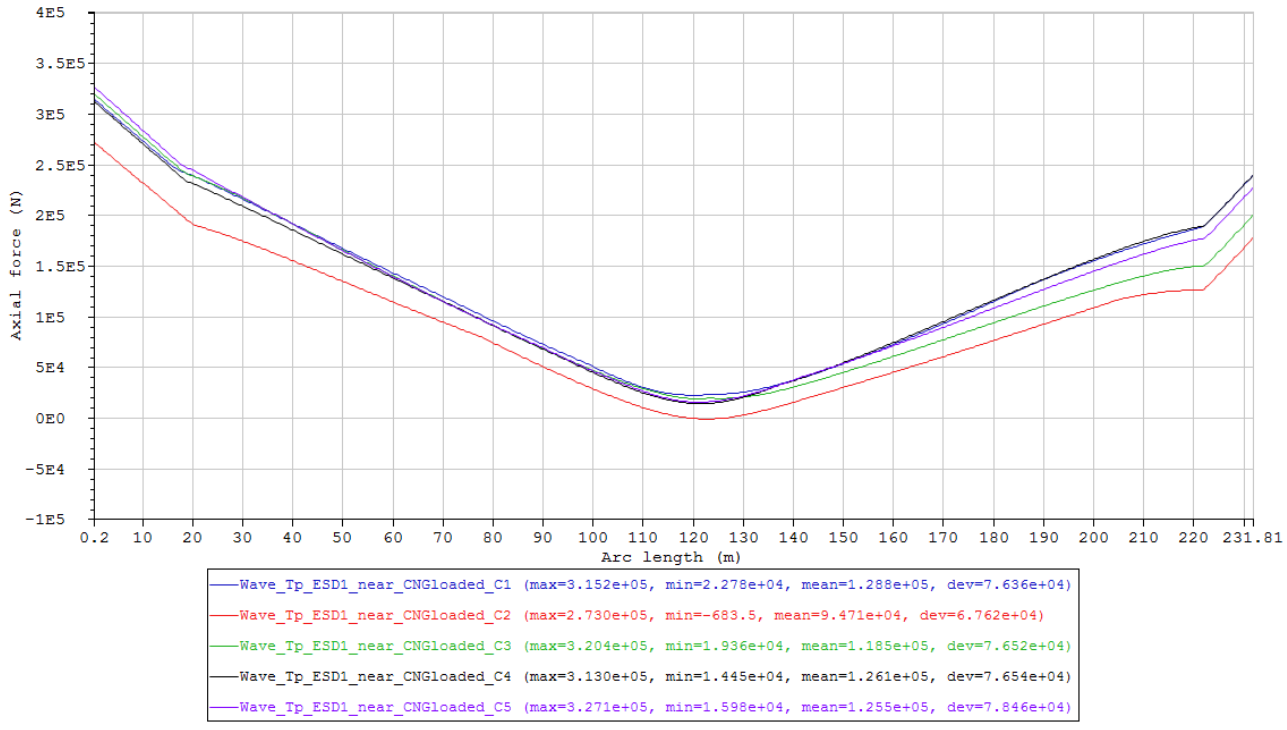

Figure 90 Minimum axial force envelope curves of the cases in Condition set – Wave_Tp_ESD1_near_CNGloaded (Table 23).

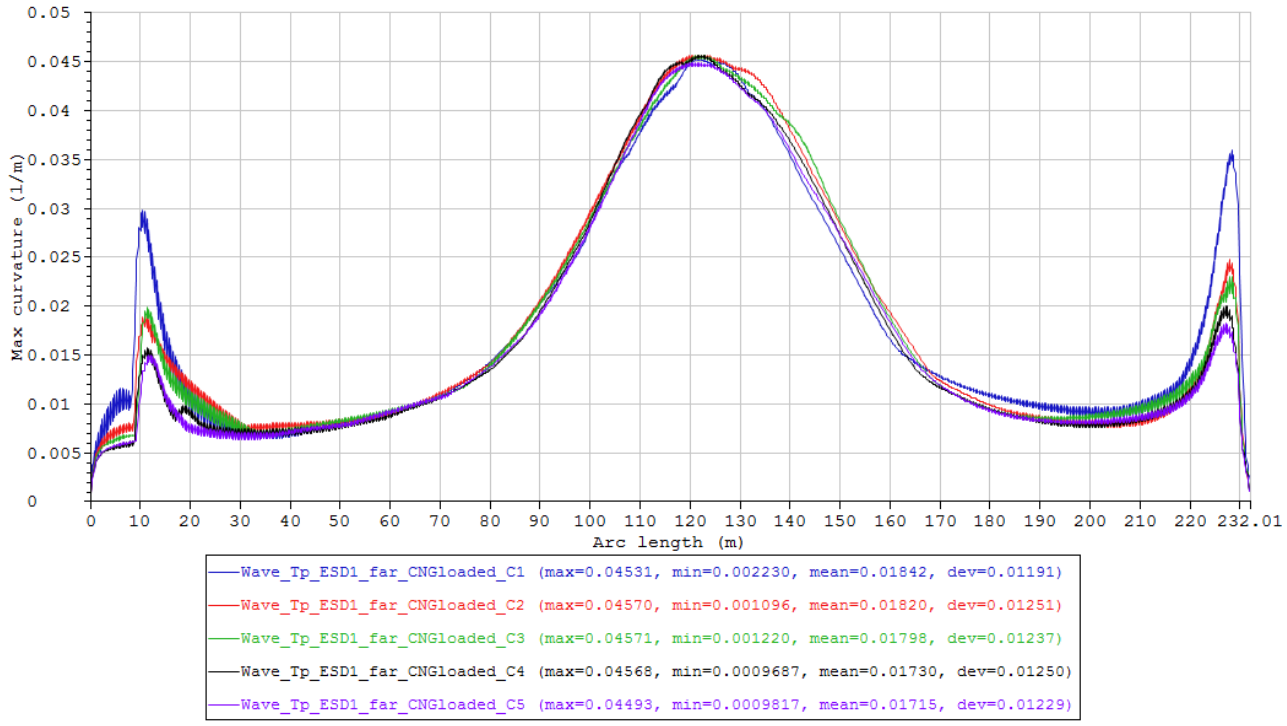

Figure 91 Maximum curvature envelope curves of the cases in Condition set – Wave_Tp_ESD1_far_CNGloaded (Table 23).

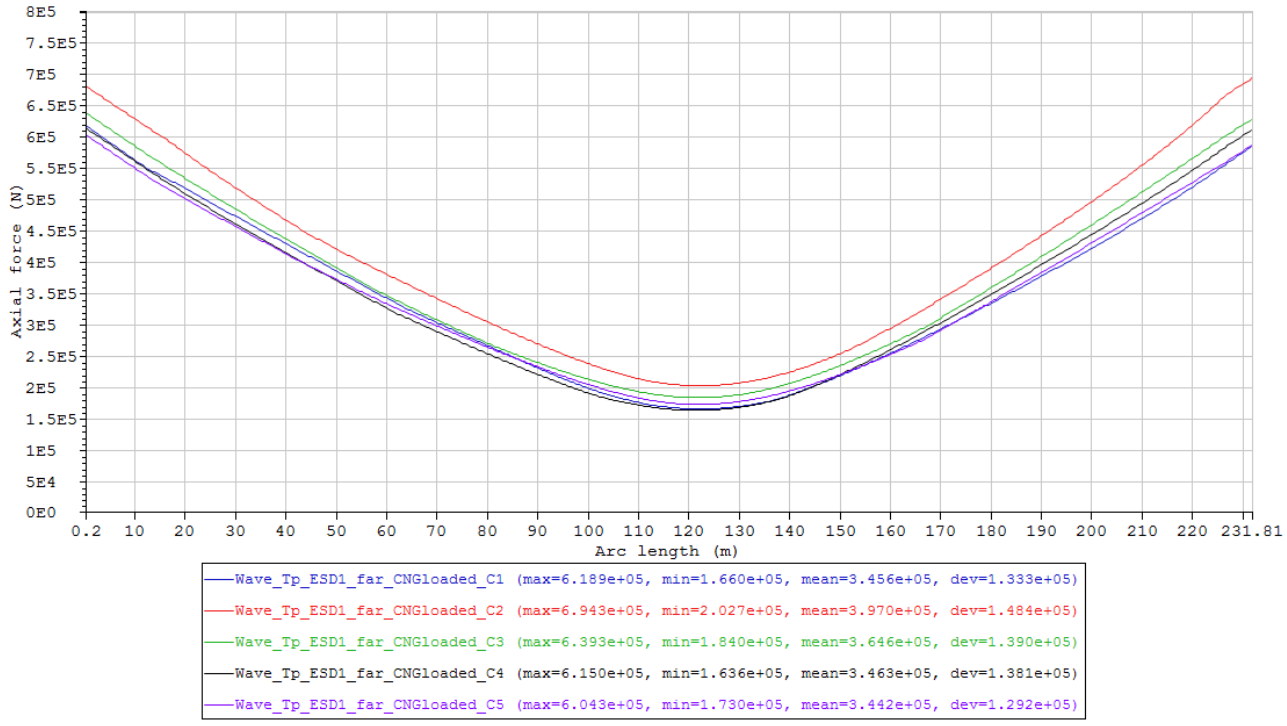

Figure 92 Maximum axial force envelope curves of the cases in Condition set – Wave_Tp_ESD1_far_CNGloaded (Table 23).

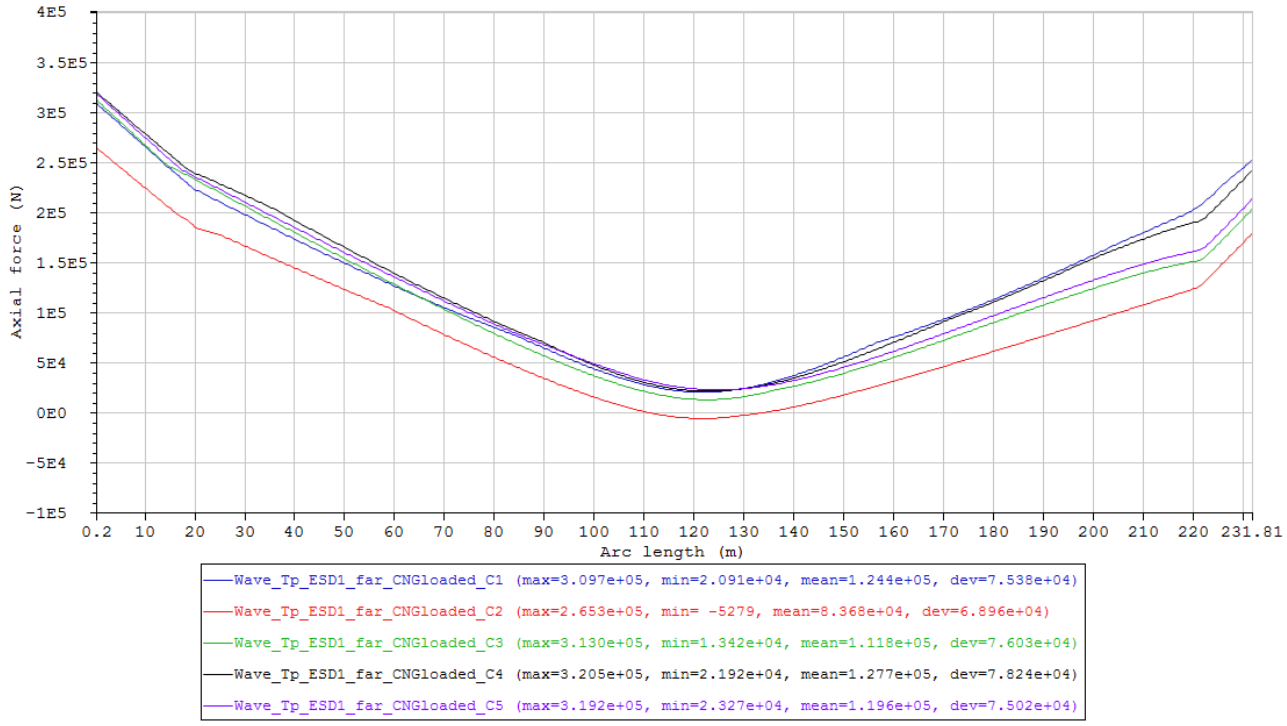

Figure 93 Minimum axial force envelope curves of the cases in Condition set – Wave_Tp_ESD1_far_CNGloaded (Table 23).

B. Wave drift forces from WAMIT

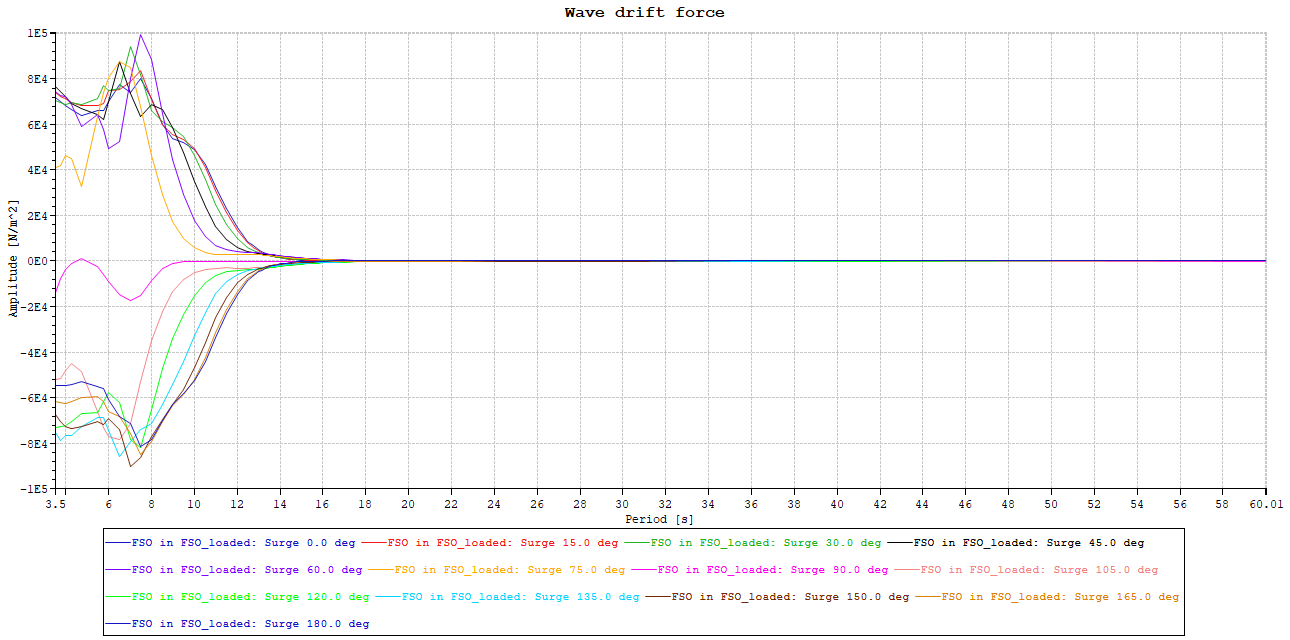

Figure 94 Surge wave drift force for FSO.

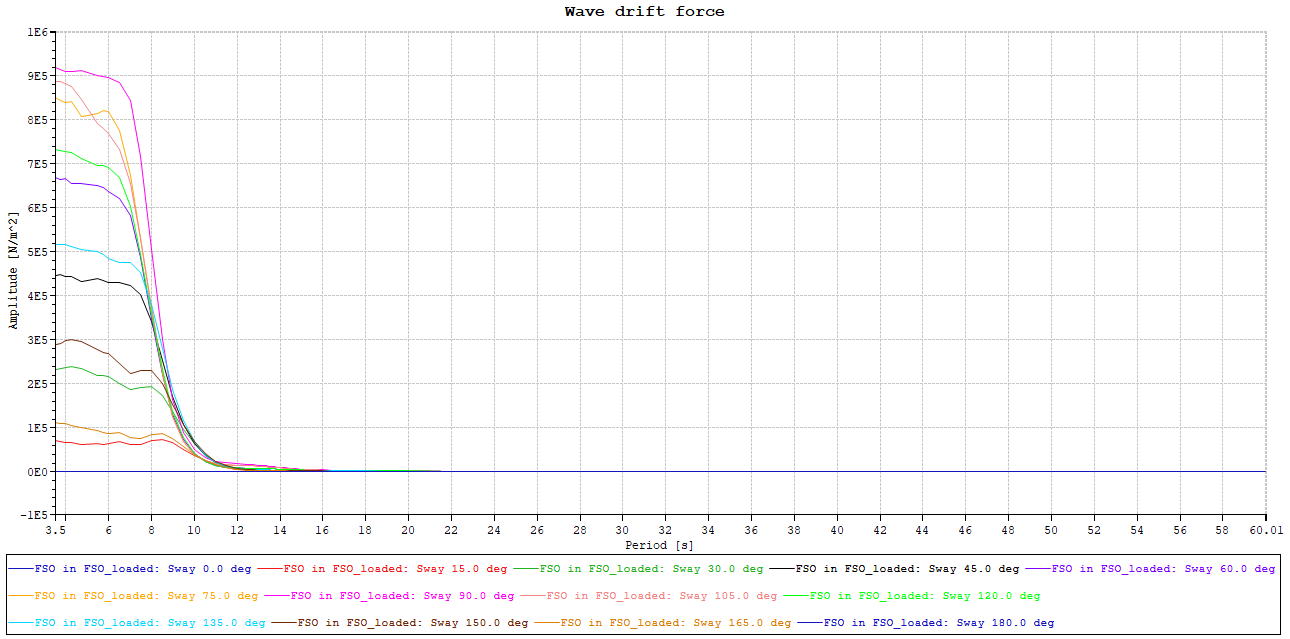

Figure 95 Sway wave drift force for FSO.

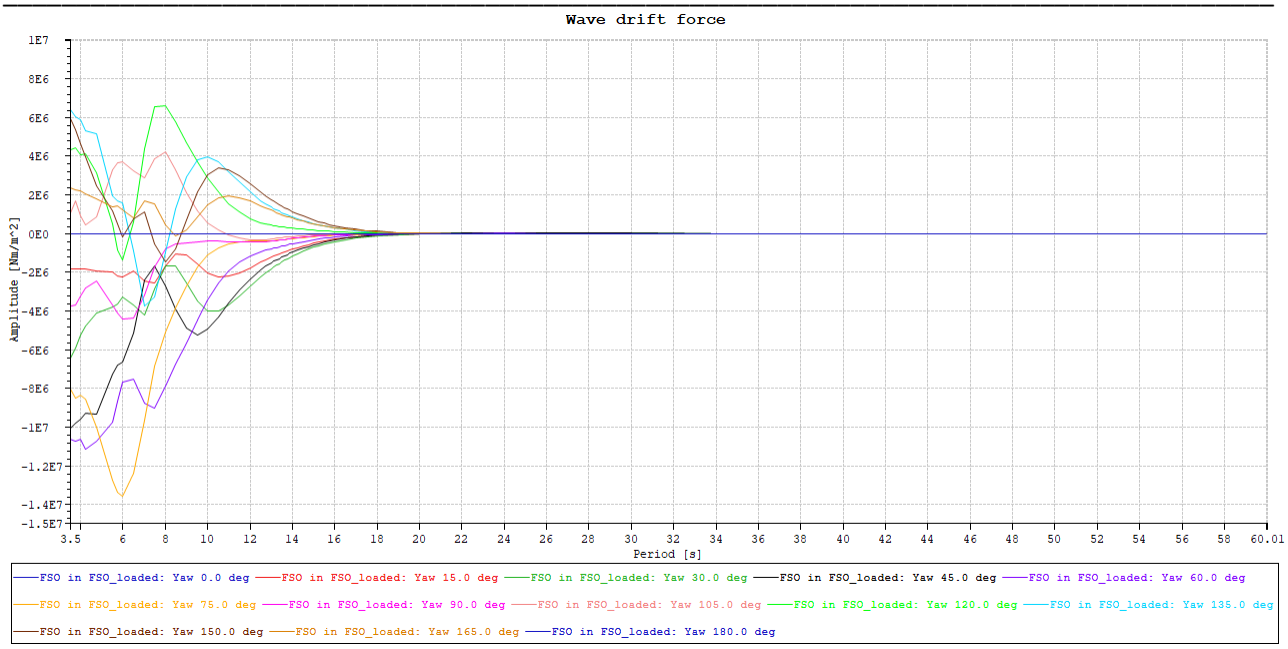

Figure 96 Yaw wave drift force for FSO.

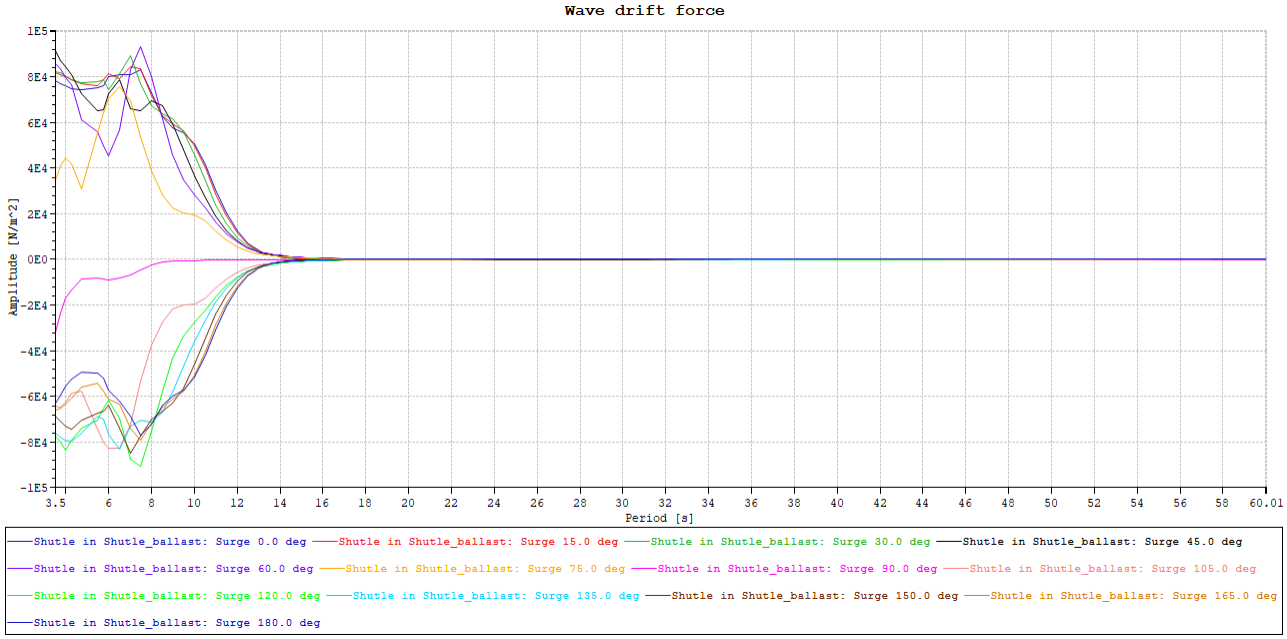

Figure 97 Surge wave drift force for GASVESSEL.

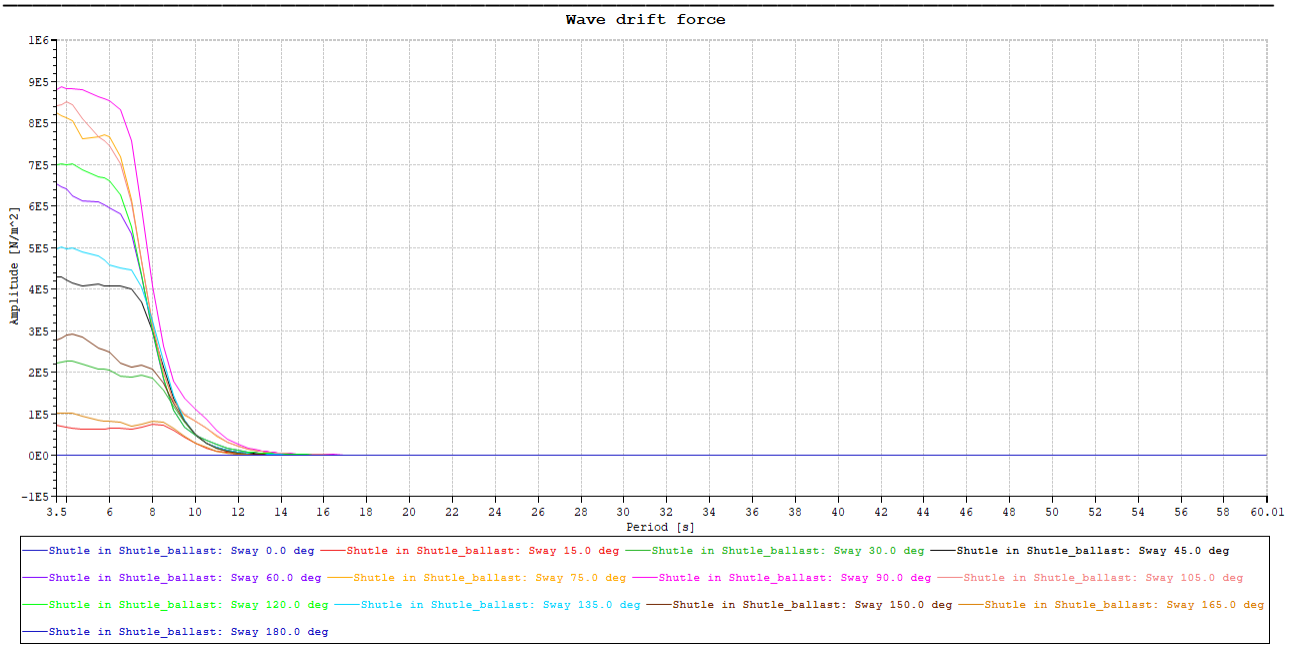

Figure 98 Sway wave drift force for GASVESSEL.

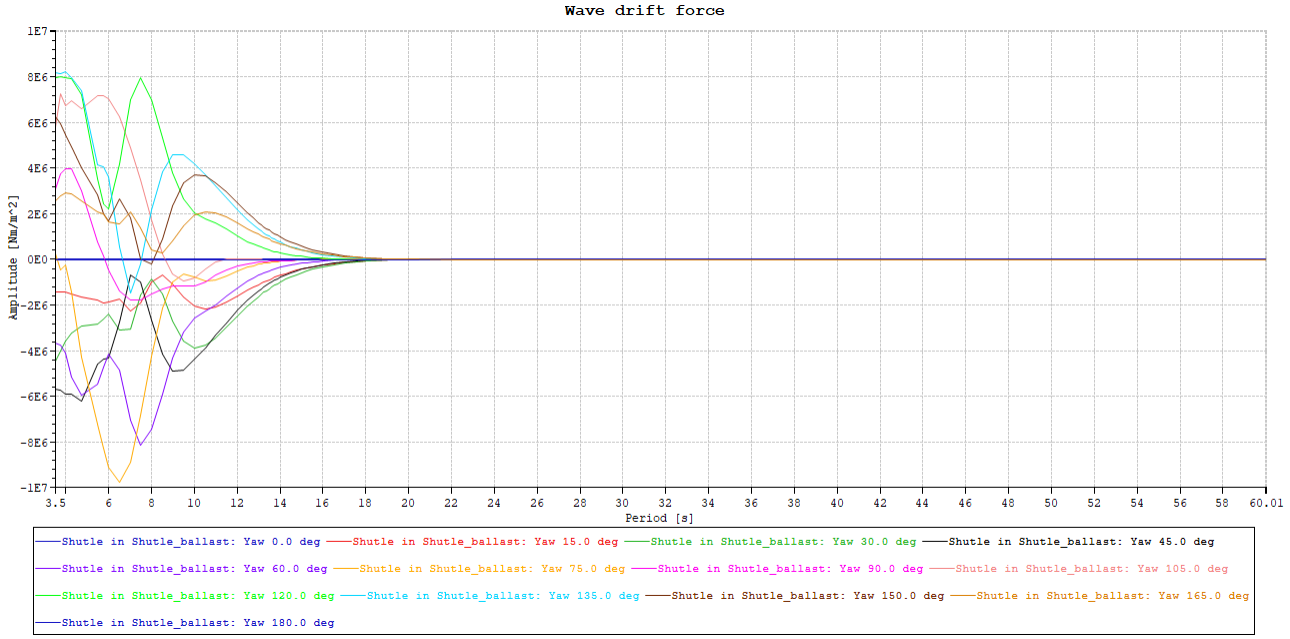

Figure 99 Yaw wave drift force for GASVESSEL.

C. Hose properties

The technical sheet of hose properties is attached as separate file.

D. ISOPE 2020-TPC-0704

The paper is attached as separate file.

TechnipFMC FLEXI FRANCE	*STRUCTURE 2.7 - TECHNICAL DATA SHEET* **REFERENCE FROM 355.20224 REV. 0** IN DATABASE SINCE 15/05/2019	Page : 1 / 1 Job n° : Name : GRMILNE Date : 15/05/2019

INTERNAL DIAMETER	14.00"	SOUR SERVICE
DESIGN PRESSURE	3480 psi	240 bars
DESIGN TEMPERATURE	70 °C	
FACTORY TEST PRESSURE	5221 psi	360 bars
FTP/DP 1.50		

14in Gas Dynamic Topside Jumper

N°	LAYER DESCRIPTION	UTS (MPa)	MYS (MPa)	Mass (Kg/m)	I.D. (mm)	Th. (mm)	SDP (MPa)
1	INTERLOCKED CARCASS 60.0 x 1.5 x 7.5 AISI 316L (FE 02)	570	-	41.46	355.60	7.50	
2	PRESSURE SHEATH CROSSFLEX (TP 10)			13.29	370.60	10.60	
3	ZETA WIRE 8.0 FI 09	850	750	66.64	391.80	8.00	427
4	SPIRAL FI 09 2 Flat wires: 15.3 x 4	850	750	34.52	407.80	4.00	415
5	ANTI-WEAR TAPE 100.0 x 1.5 ORGALLOY (BF 01)			1.83	415.80	1.50	
6	FIRST ARMOUR LAY. FI 09 71 Flat wires: 15.3 x 4 at 30 deg.	850	750	37.31	418.80	4.00	404
7	ANTI-WEAR TAPE 100.0 x 1.5 ORGALLOY (BF 01)			1.87	426.80	1.50	
8	SECOND ARMOUR LAY FI 09 73 Flat wires: 15.3 x 4 at -30 deg.	850	750	38.36	429.80	4.00	373
9	HIGH STRENGTH TAPE G2/PIPELON/KV230/KV230/ESTER/ESTER			2.29	437.80	2.75	
10	EXTERNAL SHEATH HD-FLEX (TP26+TP28) Yellow			16.32	443.30	12.00	

THEORETICAL CHARACTERISTICS	IMPERIAL	METRIC
DIAMETER inside	14.00 in	355.60 mm
DIAMETER outside	18.40 in	467.30 mm
VOLUME internal	1.104 cf/ft	102.59 l/m
VOLUME external	1.846 cf/ft	171.51 l/m
WEIGHT in air empty	170.61 lbf/ft	253.90 kgf/m
WEIGHT in air full of seawater	241.27 lbf/ft	359.05 kgf/m
WEIGHT in seawater empty	52.48 lbf/ft	78.11 kgf/m
WEIGHT in seawater full of seawater	123.14 lbf/ft	183.26 kgf/m
SPECIFIC GRAVITY in sea water empty	1.44	1.44
PRESSURE Nominal bursting	6164 psi	425 bars
HYDROSTATIC collapse pressure lay 2	594 psi	41 bars
DAMAGING PULL in straight line	1215124 lbf	5405.14 kN
MINIMUM BENDING RADIUS for STORAGE	10.21 ft	3.11 m
BENDING STIFFNESS at 20°C	966226 lbf.ft2	399.30 kN.m2
RELATIVE ELONGATION at design pressure	0.197 %	0.197 %
RELATIVE ELONGATION for 100 kN	0.009488 %	0.009488 %
THERMAL EXCHANGE COEFFICIENT at 20°C	6.30 Btu/hftF	10.91 W/m.K

Structure opened implementing parameter revision tag 148 (Current parameter revision tag 148)
Computed with STRUCTURE Version 2.7.0.4213 linked, as required, to following modules:

PEDStructureServer	2.7.0.4213	DataServer	2.6.0.3165	Therm Library	3.3.1.4216
collapselib.dll	2.7.3.4368				

ISOPE2020-TPC-0704

Feasibility Study of Loading/Unloading of Compressed Natural Gas Vessel in the Barents Sea

Decao Yin[a,*], Halvor Lie[a], Ivar Fylling[b], Frøydis Solaas[a], Jan Roger Hoff[a], Janne K. Ø. Gjøsteen[a]
a SINTEF Ocean, Trondheim, Norway
b Ivar Fylling Marin Teknikk, Trondheim, Norway

ABSTRACT

Offloading hoses/flexible pipes are used to transfer compressed natural gas (CNG) from an intermediate floating CNG storage unit - floating storage and offloading unit (FSO) to CNG vessel. The floating hoses are subjected to environmental loads that are mainly waves, current, and vessel motions from both the FSO and the CNG vessel.
As a part of European Commission Horizon 2020, GASVESSEL project develops offshore transport and distribution technologies for natural gas. In the present study, the feasibility of an offshore loading/unloading system of CNG transportation system in the Barents Sea is investigated.
Numerical simulations are performed by using the software RIFLEX under SIMA workbench. Critical responses such as curvature and axial forces are checked. For the new offloading hose, it is important to check the combined bending-tension loading capacity. The results show that the specified hoses/flexible pipes of the loading/unloading system has ample capacity for the considered operating conditions.

KEY WORDS: Compressed natural gas (CNG); Loading/Unloading; GASVESSEL;

Nomenclature

α	Utilization factor
$\ddot{r}$	Structural acceleration vector
$\dot{r}$	Structural velocity vector
κ	Curvature
ρ	Density
θ_c	Current direction
θ_h	Hose direction
θ_v	CNG vessel heading
θ_w	Wave propagation direction
B	Vessel breadth
b	Stiffness/load – parameter, $b = (EI/w)^{1/3}$
C_d	Drag coefficient
C_m	Added mass coefficient
D_h	Hose distance
EI	Bending stiffness of loading hose
H_s	Significant wave height
L_h	Hose length
L_{OA}	Length over all
L_{PP}	Length between perpendiculars
R	Radius of hose curvature
r	Non-dimensional radius
r	Structural displacement vector
R^D	Damping force vector
R^E	External force vector
R^I	Inertia force vector
R^S	Internal structural reaction force vector
R_0	Radius of hose curvature with zero tension
r_b	Non-dimensional radius of bending-dominated hose
R_c	Radius of catenary curve
r_c	Non-dimensional radius of catenary curve
T	Tension, support force, axial force, also called 'effective tension', not including effects of internal and external hydrostatic pressure
T_p	Peak wave period
U_c	Current velocity
U_z	Vessel heave velocity
v_f	Free fall speed
w	Weight/length in water
CNG	Compressed natural gas
CORDIS	Community Research and Development Information Service
ESD	Emergency shut-down

EU European Union
FE Finite element
FEM Finite element method
FPSO Floating production, storage and offloading unit
FSO Floating storage and offloading unit
GASVESSEL 1) EU Horizon 2020 GASVESSEL project. 2) Compressed natural gas vessel
JONSWAP Joint North Sea Wave Project
NG Natural gas
OLS Offshore Loading System
RAO Amplitude ratio of motion transfer functions

INTRODUCTION

Crude oil is by far European Union (EU)'s largest imported energy product (72 % of total EU energy imports in 2018), followed by natural gas in gaseous state (23 %) (Eurostat, 2019). To secure Europe's energy supply, the key is diversifying supply routes. This includes identifying and building new energy supply routes that unlock resources, to reduce Europe's dependence on a single supplier of natural gas and other energy resources (GASVESSEL, 2019) By proving the techno-economic feasibility of a novel CNG transport concept, the GASVESSEL project will open up new possibilities to exploit stranded, associated and flared gas where this is currently economically not viable and creates new cost-efficient gas transport solutions. The new offshore and onshore CNG system is enabled by a novel patented Pressure Vessel manufacturing technology and a new conceptual ship design including safe loading/unloading solution (CORDIS website, 2019).
The CNG transport concept of GASVESSEL studies possible new energy routes in Europe to three different oil and gas fields (Droushiotis, 2018):

- East Mediterranean gas fields – enable supply of remote areas such as the Greek and Italian islands and Cyprus
- Black Sea region – offer a flexible solution for early start-up of gas exploitation, before the planned pipeline will be finished
- Barents Sea offshore oil field – exploit gas associated to oil winning, which is currently re-injected in the oil fields

The present study focuses on the feasibility of the offshore loading/unloading system for CNG transport in the Barents Sea. For further development of the system more detailed analyses are recommended.

LOADING/UNLOADING SYSTEM

There exist several methods for offshore loading/unloading of oil/gas, as shown in Fig. 1. Side-by-side loading has been investigated by several early studies (Kim et al., 2006; Jeong et al., 2010; Moradi et al., 2015). Ship collision needs to be considered for such loading method. Kvitrud et al.(2012) summarized the position incidents during offshore loading with shuttle tankers on the Norwegian Continental Shelf from 2000 to 2011.
By considering the cost, effectiveness and the environmental loads, a tandem loading method is selected for the CNG vessel in the Barents Sea.
A typical tandem loading system is shown in Fig. 2, which include a FPSO/FSO, loading hose and a shuttle tanker.
Figure 3 illustrates the offshore loading of gas and transport to the gas unloading location using the GASVESSEL concept.

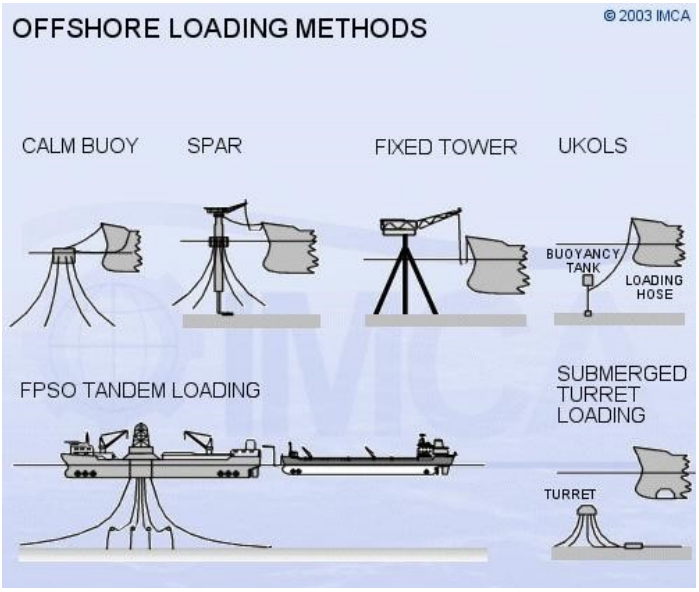

Fig. 1 Sketch of different offshore loading/unloading methods. (IMCA, 2003)

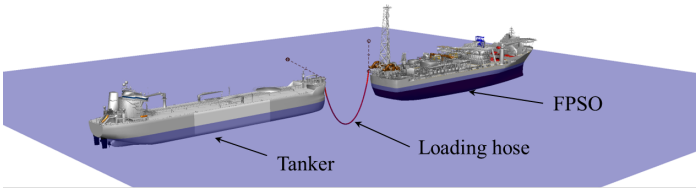

Fig. 2 A typical tandem offshore loading system. (Yin et al., 2017)

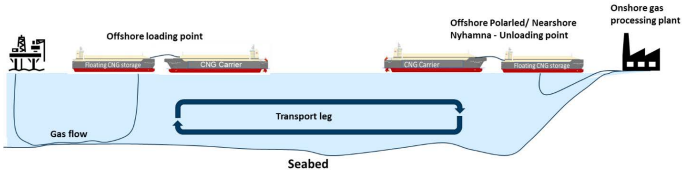

Fig. 3 Main value chain aspects of Barents Sea scenarios (Droushiotis, 2018).

Operational parameters

The operational sectors of the CNG vessel bow position are shown in Fig. 4, illustrating the emergency shut-down (ESD) zones for loading/unloading. ESD1 crossing indicates preparation for closing and disconnecting, while ESD2 indicates immediate disconnect. (Norwegian Oil and Gas Association, 2015)
Key operational parameters selected for this study are illustrated in Fig. 5:

- Distance between FSO stern and CNG vessel bow, D_h. Mean distance is 90 m, varied -25 m to + 45 m to cover the ESD2 limits.
- Heading of CNG vessel, θ_v.
- Loading hose direction, θ_h

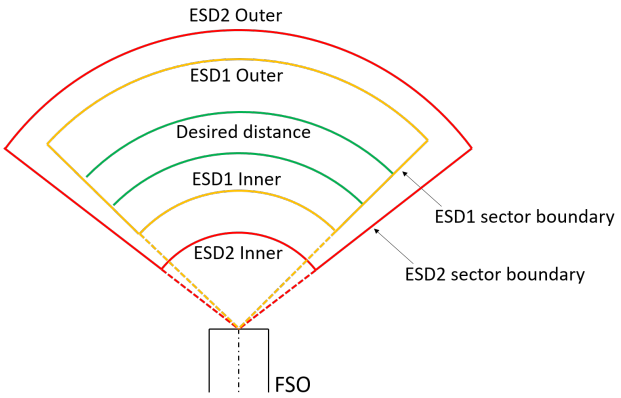

Fig. 4 Illustration of offloading sectors behind FSO.

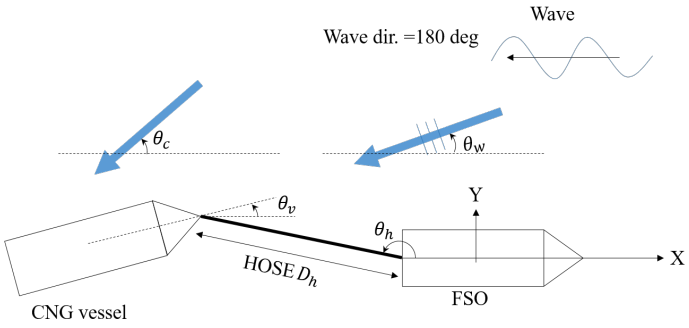

Fig. 5 Coordinate system and operational parameters of a tandem loading/unloading system.

Loading hose

The working pressure of 240 bar. In order to load CNG from FSO to CNG vessel efficiently, a minimum internal diameter of 14" is desired for the loading hose. Traditional loading hoses used form oil loading do not have the pressure capacity that is required in this study. Thus a un-bonded pipe which is typically used as flexible riser is studied. The properties of the loading hose is shown in Table 1. Free fall speed and acceleration are calculated, the free fall speed ($v_f = \sqrt{w/(\frac{1}{2}\rho C_d D)}$) through water is 2.63 m/s, free fall acceleration is 3.11 m/s^2 when the hose is filled with gas. In addition to pressure, tension and curvature capacities, there is concern about damage due to compressive loads. Compression may occur when weakly tensioned sections of the hose are subjected to vertical acceleration or vertical speed exceeding the free fall behaviour of the submerged hose section. Since the gas filled hose is lighter than typical oil loading hoses, free fall acceleration and speed will be smaller, and risk of compression correspondingly higher.

Vessels

For the Barents Sea the CNG vessel has maximum gross CNG capacity of 12×10^6 Nm^3. The main dimensions of the designed CNG vessel and FSO are presented in Table 2. A detail study of the FSO is not performed in the present study. Therefore modified version of the CNG vessel is used to define the FSO with a maximum gross storage capacity of CNG 15×10^6 Nm^3. The FSO has the same hull geometry as the CNG vessel except the draft, which is increased from 15.5 m to 22 m.

Table 1 Main dimensions of the loading hose and hydrodynamic parameters.

Property	Unit	Value
Outer diameter, 14"	m	0.467
Bending stiffness, EI	kNm^2	399.300
Density of sea water	t/m^3	1.025
Density of gas	t/m^3	0.190
Submerged weight, gas filled	kN/m	1.983
Drag coefficient, C_d	-	1.2
Added mass coefficient, C_m	-	1.0
Free fall speed, water filled	m/s	3.12
Free fall speed, gas filled	m/s	2.63
Free fall acceleration, water filled	m/s^2	4.39
Free fall acceleration, gas filled	m/s^2	3.11
With zero tension		
Radius of curvature, water filled	m	4.60
Radius of curvature, gas filled	m	5.16
Curvature utilization, $R_{storage}/R_{static}$	-	0.60
Damaging pull in straight line	kN	5405.14

Table 2 Main dimensions of the vessels (Navalprogetti, 2019).

Property	Unit	Value
Length over all, L_{OA}	m	205.0
Length between perpendiculars, L_{PP}	m	190.9
Max breath, B	m	36.0
Height of main deck, CNG vessel	m	15.5
Height of main deck, FSO	m	22
Connection point at FSO stern (above water line)	m	14.5
Connection point at CNG vessel bow (above water line)	m	8
Design draft	m	7.5
Load line summer draft above baseline	m	8.48
Capacity - NG @ 300 bar, 20 degree	Nm^3	12×10^6

There are three loading conditions for CNG vessel and FSO, as shown in Table 3, the draught at midship is presented in Fig. 4. The selected results presented in this paper are at the loading condition 1 - both FSO and CNG vessel are medium loaded.

NUMERICAL SIMULATION

Numerical simulation has been carried out to investigate the feasibility of the conceptual design of the tandem loading/unloading system between the CNG vessel and the FSO.

Table 3 Loading conditions of CNG vessel and FSO.

NO.	CNG vessel	FSO
1	Medium loaded	Medium loaded
2	Full loaded	Ballast
3	Ballast	Full loaded

Table 4 Midship draught of different loading conditions of CNG vessel and FSO.

NO.	CNG vessel (m)	FSO (m)
Ballast	6.47	6.97
Medium loaded	6.84	7.17
Full loaded	7.00	7.50

WAMIT calculation

First order wave force transfer functions, wave drift forces, added mass, potential damping and motion transfer functions for the vessel are calculated by use of the panel code WAMIT Version 7.062. The calculations have been carried out assuming infinite water depth for 13 wave directions between stern and head waves (0 - 180 degrees wave heading) and 54 wave periods from 3.5 to 60 seconds. The WAMIT panel model is shown in Fig. 6.

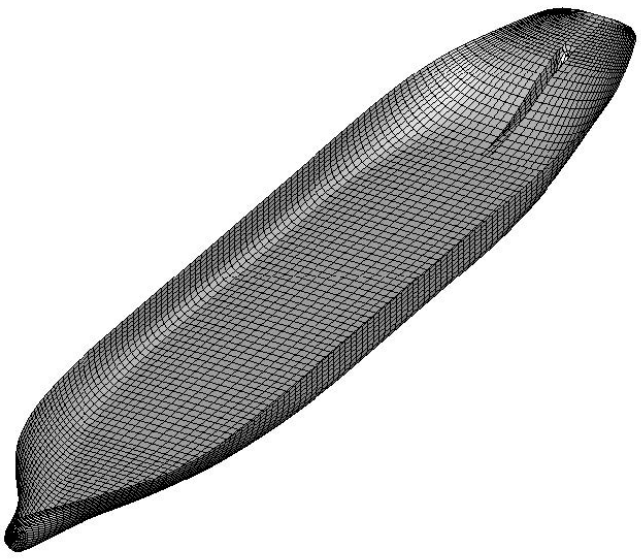

Fig. 6 Panel model for the CNG vessel with 5370 panels.

WAMIT can only include a linear damping matrix in addition to the potential damping calculated by the code itself. Applying a linear damping coefficient to describe the non-linear damping means that the damping coefficient and motion transfer functions obtained by use of WAMIT will depend on the wave amplitude/sea state. According to sea keeping model test performed by Krylov State Research Centre as a part of the GASVESSEL project, the roll damping of the vessel may be between 10% and 33%. For not being too non-conservative in the analysis, a roll damping equal to 15% is used in the simulations. This will be conservative for the largest sea-states, but non-conservative for small sea-states.

The calculated motion transfer functions for heave and pitch in head waves for the two hull variants and different loading conditions are given in Fig. 7 and Fig. 8, respectively. The calculated roll RAOs in beam waves are given in Fig. 9.

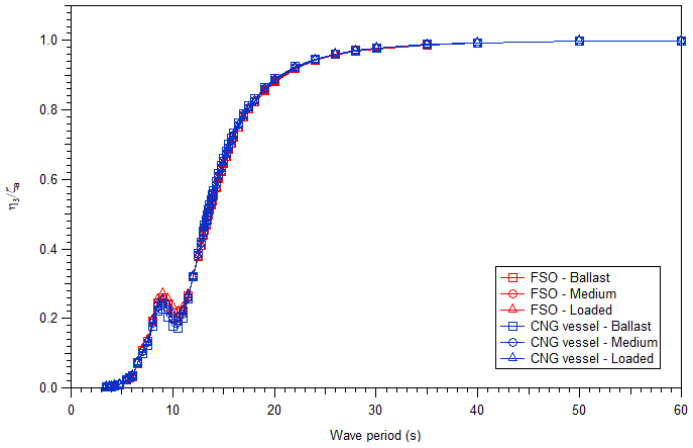

Fig. 7 Heave motion RAOs for the different hull variants and loading conditions in head waves ($\beta = 180$ deg).

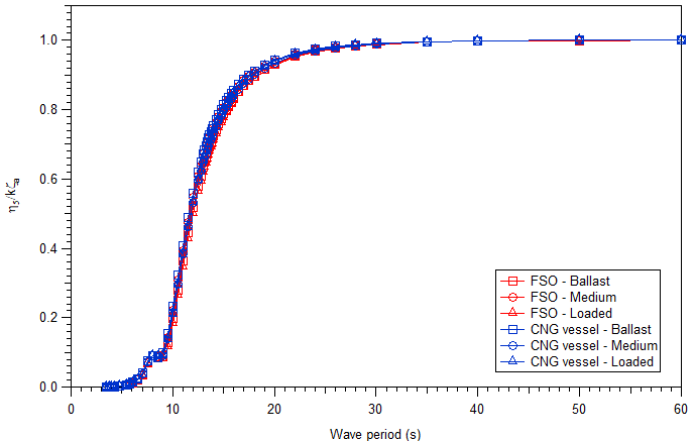

Fig. 8 Pitch motion RAOs for the different hull variants and loading conditions in head waves ($\beta = 180$ deg). The pitch RAO is given in rad/m.

In the present study of loading/unloading, the slender marine structure analysis tool - RIFLEX (SINTEF Ocean, 2019) is used. The SIMA (SINTEF Ocean, 2019) work bench is applied to establish the numerical model, run the RIFLEX calculation and post-process the results.

Numerical model

A RIFLEX analysis model has been prepared, which involves a finite element (FE) model of the hose and motion transfer functions of the two support vessels: CNG vessel and FSO. The general dynamic equilibrium of the time domain analysis of the offloading hose is:

$$R^I(r,\ddot{r},t) + R^D(r,\dot{r},t) + R^S(r,t) = R^E(r,\dot{r},t) \quad (1)$$

where R^I is inertia force vector, R^D is damping force vector, R^S is internal structural reaction force vector and R^E is external force

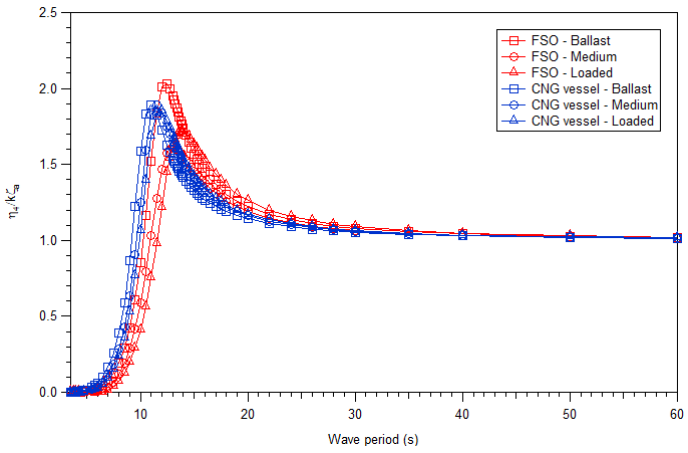

Fig. 9 Roll motion RAOs for the different hull variants and loading conditions in beam waves ($\beta = 90$ deg). The roll RAO is given in rad/m.

vector. $\ddot{r}$, $\dot{r}$ and r are structural displacement, velocity and acceleration vectors. More details could be found in the RIFLEX Theory Manual (SINTEF Ocean, 2019). For the hose a beam element model was applied, using mass, buoyancy and stiffness properties in accordance with the specified input document. The hose is connected to both vessels with pinned ends. It is free-to-rotate around local Y and Z axes, In X-rotation, which is local longitudinal axis of the beam, CNG vessel bow end is free and the FSO stern end is fixed. This model gives zero bending moment at the hose ends, zero torque, and the in-span curvature is obtained directly.

To ensure the provided loading hose is applicable to the GASVESSEL loading/unloading system, sensitivity studies have been performed on the hose distance, hose length and sea-states. The calculated curvature and axial force are compared with the specified capacity of the loading hose.

Static analysis

The static loads are governed by the hose weight, hose length, and the distance between the support points.

To evaluate the relative importance of bending stiffness and tension in controlling the hose shape, corresponding non-dimensional radii are defined (Yin et al., 2017).

A non-dimensional radius r_b that represents bending stiffness importance may be defined as:

$$r_b = R/b \tag{2}$$

where $b = (\frac{EI}{w})^{1/3}$ is stiffness/load – parameter with dimension 'length'; w is transverse load, submerged weight for horizontal sections; R is radius of curvature.

With zero bending stiffness, axial force as T, the hose shape would be a catenary curve, with a radius of $R_c = T/w$. A non-dimensional radius of the catenary is:

$$r_c = R_c/b = T/(wb) \tag{3}$$

r_c could also be taken as non-dimensional tension.

With zero tension the curvature radius is $R_0 = 0.88b$. If the minimum curvature radius is smaller than R_0, then the hose may be suspended without horizontal tension.

The loading/unloading hose is subject to combined tension-bending load, to check the capacity, a utilization factor α may be simplified to

$$\alpha^n = (\frac{T(t)}{T_{\kappa=0}})^n + (\frac{\kappa(t)}{\kappa_{T=0}})^n \tag{4}$$

$T_{\kappa=0}$ and $\kappa_{T=0}$ are the maximum tension force (curvature is zero) and maximum curvature (tension is zero), and taken as the largest values from hose capacity. α has a value less than 1.0. The inverse $1/\alpha$ may be taken as a load factor (safety factor) (Yin et al., 2017).

To illustrate the curvature and axial force distribution along the hose, results from hose distance of an initial study are presented in the following section. $L_h = 115\ m$, D_h varies from 50 m to 90 m with 10 m increment. The base environmental condition for sensitivity study is shown in Table 5 (Yin et al., 2017), the wave spectrum is JONSWAP double peaked spectrum, and the current profile is uniform. This environmental condition is considered to be harsh sea states in the Barents Sea.

Table 5 Base environmental condition for sensitivity study.

H_s (m)	T_p (s)	θ_w (deg)	U_c (m/s)	θ_c (deg)
6	13.5	210	0.89	225

The static X-Z configuration of different cases are shown in Fig. 10. It shows the larger the hose distance (D_h), the smaller the curvature at the mid point of the hose, while the less the maximum immersion depth of the loading hose apparently.

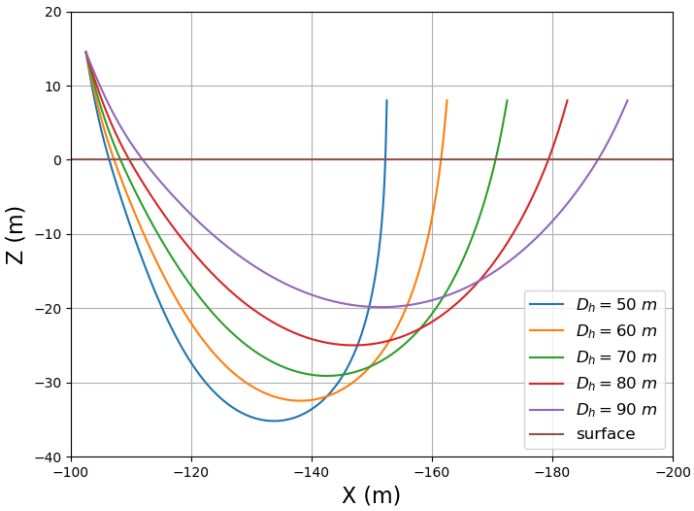

Fig. 10 Loading hose static profile, D_h varies from 50 m to 90 m. $L_h = 115\ m$. FSO at the left side, CNG vessel at the right side.

Figure 11 shows the static curvature along the hose, left side is the stern connection point of FSO, and the right side is the bow connection point of CNG vessel. It shows that along the hose, maximum static curvature occurs at the mid-point of the hose, in addition. Relative large curvature is seen near the surface at both sides when the hose penetrate the water surface. From Table 1, we know that gas filled radius of curvature 5.16 m, corresponding curvature is 0.194 m^{-1}. The static curvature are well within the capacity of the hose. Another observation is the shorter the hose distance, the larger curvature at the mid-point, refer to Fig. 10.

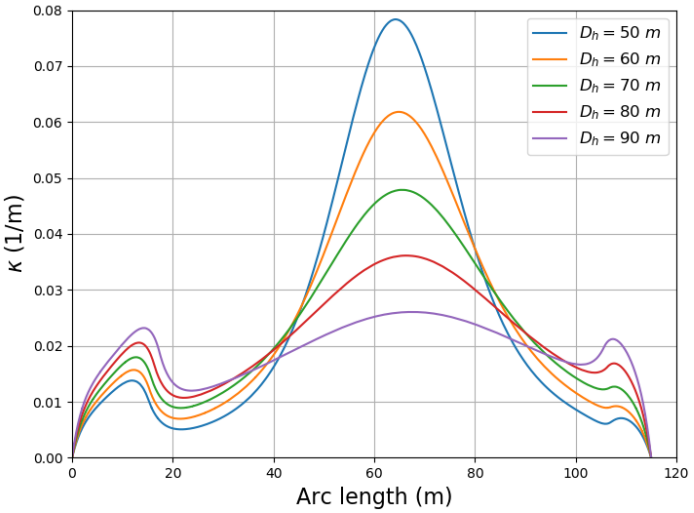

Fig. 11 Static curvature along the loading hose arc length, D_h varies from 50 m to 90 m. L_h = 115 m. FSO at the left side, CNG vessel at the right side.

Figure 12 shows the static tension along the hose, left side is the FSO stern connection point, and the right side is the CNG vessel bow connection point. The hose ends have large tension, and the end at FSO stern side has the largest value. Longer hose distance results larger tension at hose ends, but smaller tension at the sag bend. Static tension is well below the maximum tension capacity - 5405.14 kN for straight line.

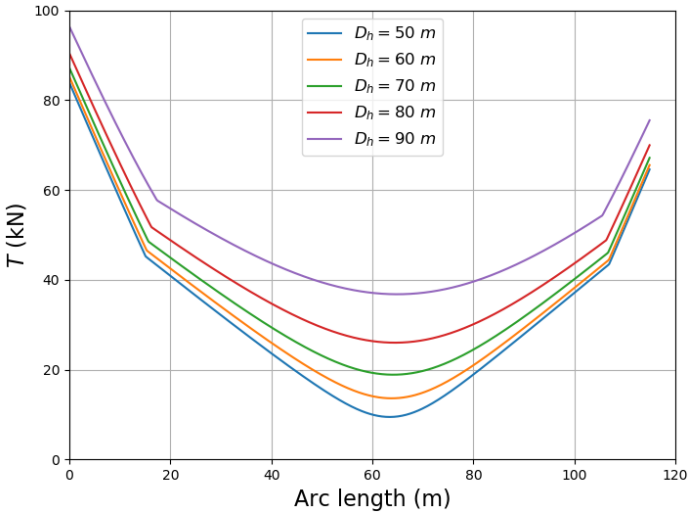

Fig. 12 Static tension along the loading hose arc length, D_h varies from 50 m to 90 m. L_h = 115 m. FSO at the left side, CNG vessel at the right side.

Dynamic analysis

A time domain numerical simulation of dynamic responses to irregular waves and consistent ship motions is carried out by means of the non-linear FEM software RIFLEX. Note that the slow drift motion is not included in the present study. Irregular wave time series are generated and applied as time-dependent loading on the vessels and on the hose. Selected dynamic responses results are stored and presented by means of the SIMA post processing module.

The time domain simulation duration is about 2.3 hours, which has been proved to be adequate for estimation of 3 h return period value from one seed number (Yin et al. 2017). The numerical simulation time step is 0.1 s. The present dynamic analysis comprises wave frequency dynamics only. Slowly varying motions, governed by the stationkeeping systems of the ships, wind gust and wave drift forces, will cause change of hose responses. These can be accounted for by changing the distance between the support points, a sensitivity analysis as shown in the following.

Sensitivity on hose distance

Refer to Table 1, gas filled minimum radius of curvature is 5.16 m for a gas filled pipe, corresponding curvature is 0.194 m^{-1}. From Fig. 13, we can see that the maximum dynamic curvature for the three shortest distances are within the limit (0.194 m^{-1}). For D_h = 80 m and D_h = 90 m, the maximum dynamic curvature on the CNG vessel side is above the limit, the location of the hose is near the wave zone.

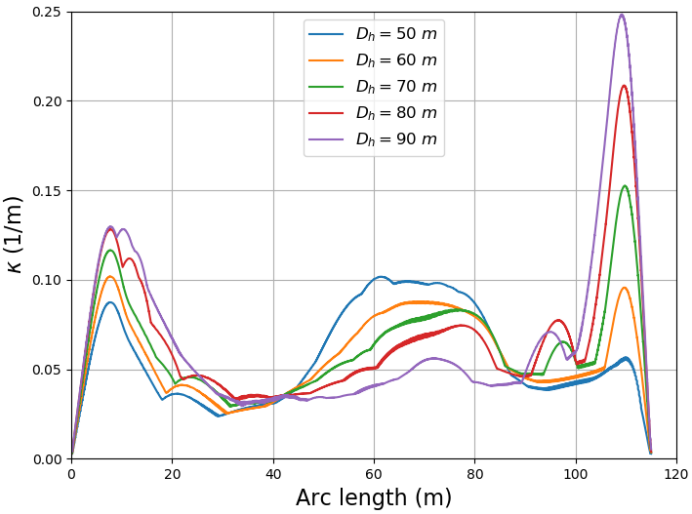

Fig. 13 Dynamic curvature envelope along the loading hose arc length, D_h varies from 50 m to 90 m. L_h = 115 m. FSO at the left side, CNG vessel at the right side.

Figure 14 shows the minimum and maximum dynamic axial force envelope curves. The maximum tension is about 330 kN (far below damaging pull in straight line 5405 kN shown in Table 1). The negative values in the upper figure indicate compression occurs. The hose at wave zone on the CNG vessel side has the largest compression force, varying from 30 kN to 40 kN. This should be checked with the capacity of the hose, however, such information is not available yet. We can see this value is a small percentage (0.74%) of the 'damaging pull' force.

The free fall acceleration and velocity of the hose section in water are important attributes related to hydrodynamic loading. If relative motions between support points and wave particle motions exceed these values, there will be compression in the hose section. In the gas filled condition the present hose has a free fall speed of 2.63 m/s and a free fall acceleration of 3.11 m/s^2.

A check on the heave motion of the CNG vessel bow has been performed, see Fig. 15. It shows that the heave velocity is between -4 m/s to 4 m/s, exceeding the free fall velocity of the gas filled hose is 2.63 m/s, see Table 1. This confirms that the compression is due to that the heave motion velocity is larger than

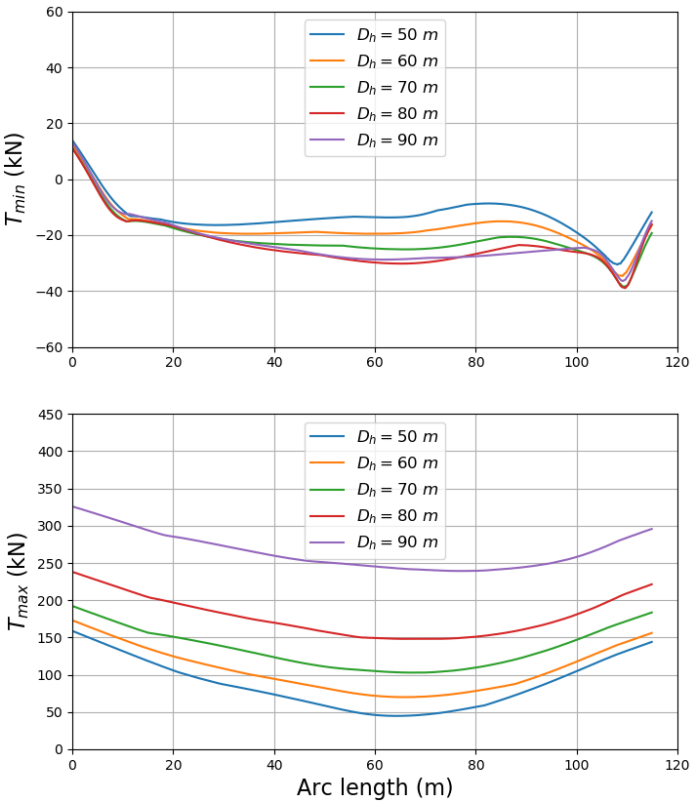

Fig. 14 Dynamic tension envelope curves (minimum and maximum) along the loading hose arc length, D_h varies from 50 m to 90 m. L_h = 115 m. FSO at the left side, CNG vessel at the right side.

the free fall velocity of the hose.

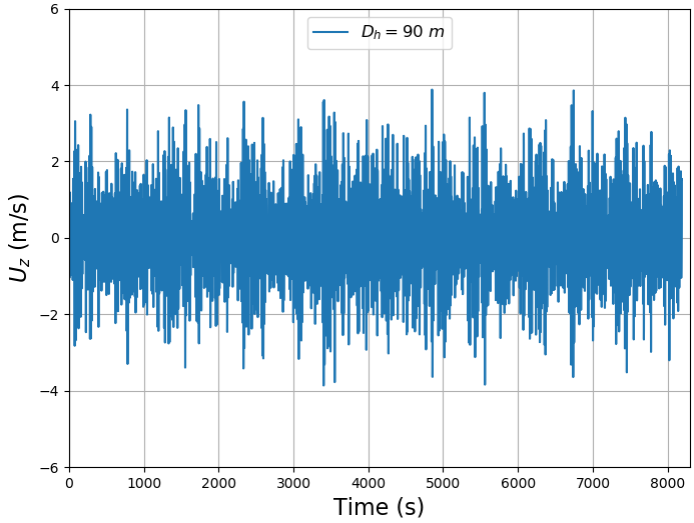

Fig. 15 Dynamic heave motion time series of CNG vessel bow, D_h = 90 m, L_h = 115 m.

Sensitivity on hose length

From Fig. 13, we can see that for the hose with length L_h = 115 m, when the hose distance D_h is 80 m and 90 m, the maximum dynamic curvature at the CNG vessel side exceeds the limit - 0.194 m^{-1}. However, a proper hose distance D_h is desired so that the loading/unloading operation is safe and efficient, at the same time, the gas filled hose can withstand the extreme dynamic load. Taking into account of the size of the FSO and CNG vessel, a hose distance D_h = 100 m is considered to be a proper value.

Based on the prior initial study, a sensitivity study on the hose length L_h is carried out in the present section, the hose distance D_h is kept as 100 m, and the hose length varies as 165 m, 182 m, 192 m, 202 m and 212 m. Figure 16 shows the dynamic curvature envelope curves. It shows that the hose end near the CNG vessel connection point has the maximum curvature, and all the maximum curvature values along the hose are within the capacity. As L_h increases, the maximum curvature value decreases. Fig. 17 shows the the minimum and maximum dynamic axial force envelope curves. The upper plot presents the minimum axial force envelope curves. On the FSO connection point, T_{min} increases with increasing L_h. Compression occurs mainly at the sag bend and near the CNG vessel connection point. The compression force at the sag bend becomes less significant as L_h increase, but less sensitive near the CNG vessel connection point. The maximum compression force is about 40 kN. The lower plot shows the maximum axial force. At both connection points, as L_h increases, T_{max} increases. T_{max} at the sag bend decreases with increasing L_h. A hose length L_h of 192 m is selected as sufficient for further study, as having acceptable curvature and axial force. Capacity of compressive loads must, however be ensured.

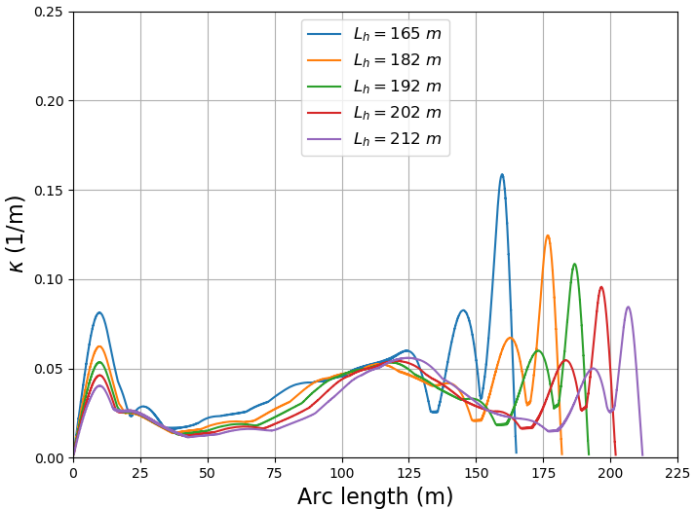

Fig. 16 Dynamic curvature envelope along the loading hose arc length, L_h varies from 165 m to 212 m. D_h = 100 m. FSO at the left side, CNG vessel at the right side.

Sensitivity on sea states

After sensitivity study on the hose distance D_h and hose length L_h, we decide to apply D_h = 100 m and L_h = 192 m in the further study. In this section, dynamic analysis under irregular wave and current condition are performed, with varying significant wave height H_s and wave period T_p. The key dynamic results are presented in Fig. 18 to Fig. 21.

The dynamic curvature envelope curves under varying H_s while keeping the other environmental conditions as presented in Table 5 are shown in Fig. 18. The hose sections near the wave zone and sag bend have maximum curvature, and the hose end near

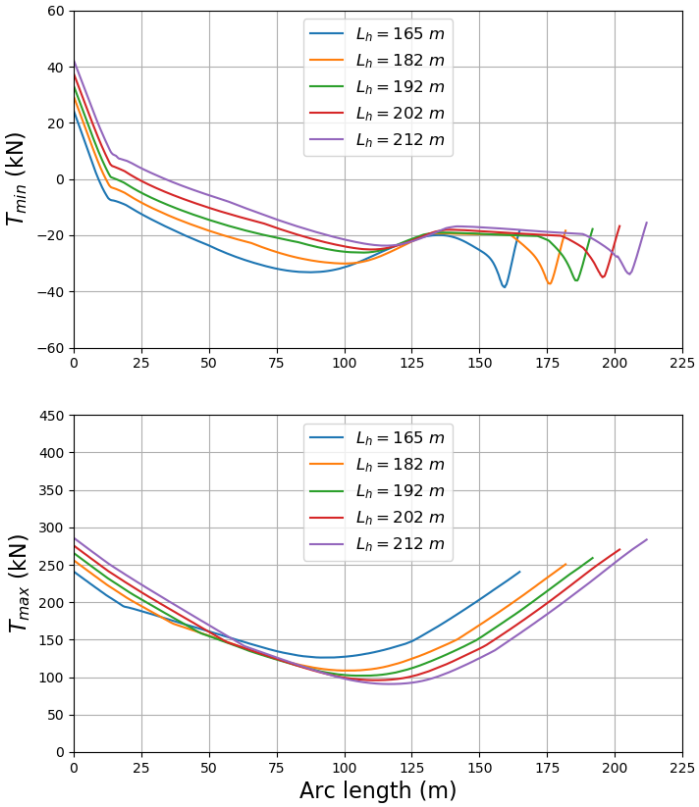

Fig. 17 Dynamic tension envelope curves (minimum and maximum) along the loading hose arc length, L_h varies from 165 m to 212 m. D_h = 100 m. FSO at the left side, CNG vessel at the right side.

the CNG vessel bow has larger curvature than the other end. As the wave height increases, the maximum curvature also increases, and the maximum values under all conditions are within the hose capacity.

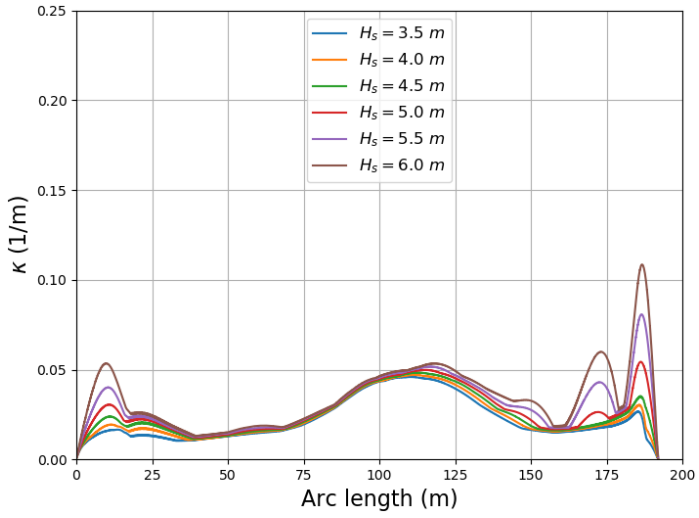

Fig. 18 Dynamic curvature envelope along the loading hose arc length. H_s varies from 3.5 m to 6.0 m, T_p = 13.6 s. L_h = 192 m, D_h = 100 m. FSO at the left side, CNG vessel at the right side.

Figure 19 presents the minimum and maximum dynamic axial force envelope curves. As shown in the figure, the magnitude of both minimum and maximum dynamic axial force increase with significant wave height H_s. The variation of axial force along the hose is similar to previous discussions. The maximum axial force is within the capacity for all significant wave heights H_s. The minimum axial force has negative values (compression) especially for the larger H_s cases, at the sag bend and near CNG vessel connection point.

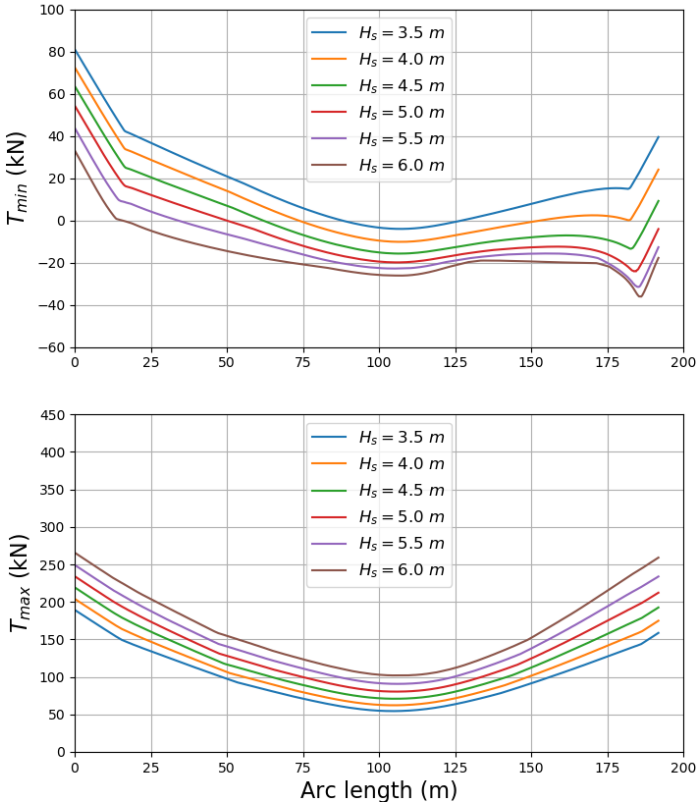

Fig. 19 Dynamic tension envelope curves (minimum and maximum) along the loading hose arc length. H_s varies from 3.5 m to 6.0 m. L_h = 192 m, D_h = 100 m. FSO at the left side, CNG vessel at the right side.

Then, the peak period T_p is varied as 8.0 s, 10.0 s, 13.6 s, 15.6 s and 17.6 s systematically, while the significant wave height H_s is kept as 6 m. The key results are presented in Fig. 20 and Fig. 21.

To interpret the presented results in these figures, we need to refer to Fig. 7, Fig. 8 and Fig. 9. Generally, the heave and pitch motion have more influence on the hose dynamics in waves. The roll motion has little influence since the connection points are assumed to be in the midship on both vessels. Variations of curvature and axial force envelope curves with different T_p are seen, and the magnitude of the maximum curvature and maximum axial force are within the hose capacity.

Challenges and possible solutions

Compared with oil-filled hose (Yin et al, 2017), the present gas-filled hose is lighter.This contributes to compression. Possible solutions could be either increasing the tension or the mass/length. Another challenge is the high internal pressure (240 bar) of internal gas. The hose studied in the present paper is an un-bonded

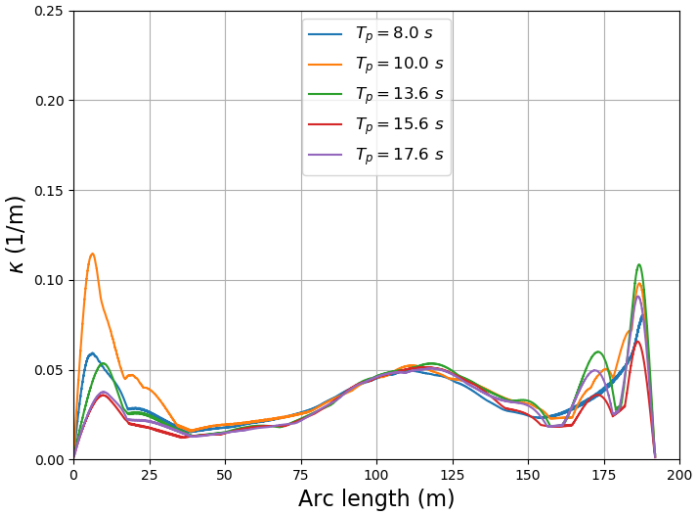

Fig. 20 Dynamic curvature envelope along the loading hose arc length. T_p varies from 8.0 s to 17.6 s, H_s = 6 m. L_h = 192 m, D_h = 100 m. FSO at the left side, CNG vessel at the right side.

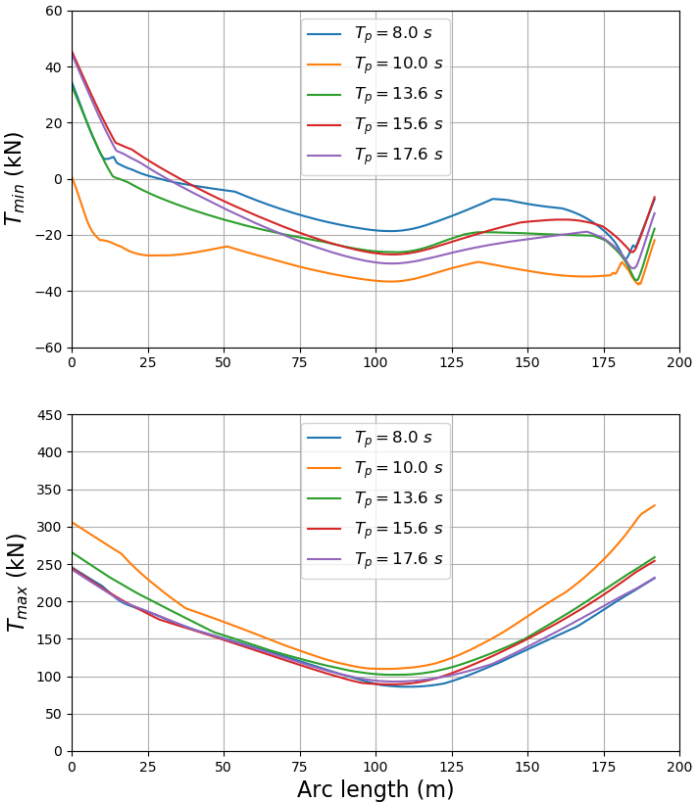

Fig. 21 Dynamic tension envelope curves (minimum and maximum) along the loading hose arc length. T_p varies from 8.0 s to 17.6 s, H_s = 6 m. L_h = 192 m, D_h = 100 m. FSO at the left side, CNG vessel at the right side.

flexible pipe, which has a relative large minimum radius of curvature, which means low curvature capacity. Another challenge not discussed in this paper, is that the Barents Sea has relative lower operation temperature, which need to be considered when designing the offshore loading/offloading system.

SUMMARY & CONCLUSION

As a task of the European Commission Horizon 2020 - GASVESSEL project, the paper presents a feasibility study of a hose during loading/unloading of compressed natural gas. The study includes a moored FSO, a CNG vessel and the hose. A non-linear FEM model for calculating dynamic responses has been prepared by means of RIFLEX under SIMA workbench. The environmental loads include irregular waves and currents. Irregular motions of the end supports are pre-generated from the wave pattern using motion transfer functions of the two vessels.
Sensitivity studies have been performed on various hose distance, hose length, significant wave height and peak wave period. Both tension and curvatures are well within the nominal capacities of the hose for the range of operational and environmental parameters covered in this study. Compression is observed at the sag bend and the wave zone near the CNG vessel connection point, which needs to be considered.

FUTURE WORK

An offshore loading/unloading system includes several parameters. Detail sensitivity study on other parameters needs to be carried out in order to have a detail design of the loading system, for example, vessel headings, wave and current directions.
Accidental limit state analysis, ultimate limit state analysis and fatigue limit state analysis are suggested to be carried out, and critical responses of the hose need to be checked against with the capacity.
The behavior of the hose during connecting/disconnecting operation should also be studied.

ACKNOWLEDGEMENTS

The authors would like to thank the partners of European Commission Horizon 2020 - GASVESSEL project and TechnipFMC for their collaboration and discussion. Their contribution and comments on this study are highly appreciated.

REFERENCES

Droushiotis, N. (2018). "GASVESSEL Deliverable NO. D2.1 - Scenario Description and Characterization".

European Commission (2019). The Community Research and Development Information Service (CORDIS) website, Retrieved from https://cordis.europa.eu/project/rcn/210914/factsheet/en, Oct.

Eurostat (2019). "EU imports of energy products - recent developments", Retrieved from https://ec.europa.eu/eurostat, May.

GASVESSEL project website (2019). https://www.gasvessel.eu, Oct.

IMCA (2003). "Station keeping incidents reported for 2001".

Jeong, H., Kim, M., Lee J., Kim, B., Ha, M. (2010) "Offloading Operability Analysis of Side-by-Side Moored LNG FPSO", The Ninth ISOPE Pacific/Asia Offshore Mechanics Symposium, Busan, Korea.

Kim, M.H., Kumar, B., Chae J.W. (2006) "Performance Evaluation of Loading/Offloading From Floating Quay to Super Container Ship", The Proceedings of The Sixteenth (2006) International Ocean and Polar Engineering Conference, California, USA.

Kvitrud, A., Kleppestø, H., Skilbrei, O.R. (2012) "Position Incidents During Offshore Loading With Shuttle Tankers On the Norwegian Continental Shelf 2000-2011", The Proceedings of The Twenty-second (2012) International Ocean and Polar Engineering Conference, Rhodes, Greece.

Moradi, N., Zhou, T., Cheng L. (2015) "A two-dimensional numerical study of resonant waves between two adjacent barges with different drafts", The Proceedings of The Twenty-fifth (2015) International Ocean and Polar Engineering Conference, Colorado, USA.

Navalprogetti (2019). "Drawing: WP5-D5.1-RV0-833-0-XXX-A01 B-Ship General Arrangement IN PROGRESS.dwg", Trieste, Italy.

Norwegian Oil and Gas Association (2015). "140-Norwegian Oil and Gas recommended guidelines for Offshore Loading Shuttle Tankers", Stavanger, Norway, May.

SINTEF Ocean (2019). "RIFLEX 4.16.0 Theory Manual", Trondheim, Norway.

SINTEF Ocean (2019). "SIMA 3.7 User's Guide", Trondheim, Norway.

WAMIT, Inc. (2019). "WAMIT User Manual", MA, USA.

Yin, D., Fylling, I., Lie, H., Baarholm, R.J. & Kendon, T.E. (2017) "On the design considerations of new offloading hose applied on a turret moored FPSO", Proceedings of the ASME 2017 36th International Conference on Ocean, Offshore and Arctic Engineering, Trondheim, Norway.